THACYANA TEIXEIRA DE CARVALHO

MECANISMOS ENVOLVIDOS NA HIPERALGESIA MECÂNICA INDUZIDA PELO FATOR ESTIMULADOR DE COLÔNIAS DE GRANULÓCITOS (G-CSF) EM CAMUNDONGOS E PARTICIPAÇÃO DA IL-33 EM MODELO DE DOENÇA DE KAWASAKI

Londrina
2018

THACYANA TEIXEIRA DE CARVALHO

MECANISMOS ENVOLVIDOS NA HIPERALGESIA MECÂNICA INDUZIDA PELO FATOR ESTIMULADOR DE COLÔNIAS DE GRANULÓCITOS (G-CSF) EM CAMUNDONGOS E PARTICIPAÇÃO DA IL-33 EM MODELO DE DOENÇA DE KAWASAKI

Tese apresentada ao Programa de Pós-Graduação em Patologia Experimental da Universidade Estadual de Londrina, como requisito parcial à obtenção do título de Doutora em Patologia Experimental.

Orientador: Prof. Dr. Waldiceu Aparecido Verri Júnior

Londrina
2018

Ficha de identificação da obra elaborada pelo autor, através do Programa de Geração Automática do Sistema de Bibliotecas da UEL

Carvalho, Thacyana Teixeira de .
Mecanismos envolvidos na hiperalgesia mecânica induzida pelo Fator Estimulador de Colônias de Granulócitos (G-CSF) em camundongos e participação da IL-33 em modelo de Doença de Kawasaki / Thacyana Teixeira de Carvalho. - Londrina, 2018.
100 f. : il.

Orientador: Waldiceu Aparecido Verri Júnior.
Tese (Doutorado em Patologia Experimental) - Universidade Estadual de Londrina, Centro de Ciências Biológicas, Programa de Pós-Graduação em Patologia Experimental, 2018.
Inclui bibliografia.

1. Hiperalgesia - Tese. 2. G-CSF - Tese. 3. Citocinas - Tese. 4. Doença de Kawasaki - Tese. I. Verri Júnior, Waldiceu Aparecido. II. Universidade Estadual de Londrina. Centro de Ciências Biológicas. Programa de Pós-Graduação em Patologia Experimental. III. Título.

THACYANA TEIXEIRA DE CARVALHO

MECANISMOS ENVOLVIDOS NA HIPERALGESIA MECÂNICA INDUZIDA PELO FATOR ESTIMULADOR DE COLÔNIAS DE GRANULÓCITOS (G-CSF) EM CAMUNDONGOS E PARTICIPAÇÃO DA IL-33 EM MODELO DE DOENÇA DE KAWASAKI

Tese apresentada ao Programa de Pós-Graduação em Patologia Experimental da Universidade Estadual de Londrina, como requisito parcial à obtenção do título de Doutora em Patologia Experimental.

BANCA EXAMINADORA

_____

Orientador: Prof. Dr. Waldiceu Aparecido Verri Júnior
Universidade Estadual de Londrina – UEL

_____

Profa. Dra. Cássia Calixto de Campos
Universidade Norte do Paraná – UNOPAR

_____

Profa. Dra.Graziela Scalianti Ceravolo
Universidade Estadual de Londrina – UEL

_____

Prof. Dr. Sérgio Marques Borghi
Universidade Norte do Paraná – UNOPAR

_____

Prof. Dr. Wander Rogério Pavanelli
Universidade Estadual de Londrina – UEL

Londrina, 26 de Julho de 2018.

Dedico este trabalho à minha família que
tanto me apoiou durante esta longa jornada.

AGRADECIMENTOS

Agradeço imensamente aos meus pais José e Elisa por acreditarem e investirem em mim, sempre cobrando empenho e dedicação e dando um suporte sem tamanho, principalmente no período que passei no exterior, obrigada mãe e pai, amo muito vocês!

À minha irmã Leilane e meu cunhado André por seu incentivo durante o doutorado e mais ainda enquanto eu estava fora de casa, vocês foram essenciais para que eu fosse nessa jornada com tranquilidade!

Ao meu namorado e amigo Pedro, agradeço imensamente por sempre estar me incentivando, apoiando e ouvindo. Mesmo sabendo que enfrentaríamos um tempão longe um do outro, me encorajou e compartilhou da minha vontade de ir para fora do país para o doutorado sanduíche, além de me ajudar a vencer este período afastada de todas as pessoas importantes em minha vida. Muito obrigada pela força e companheirismo incomensuráveis!

Às minhas amigas e companheiras de experimentos Camila, Cássia, Marília e Sandra... seu companheirismo, incentivo e amizade sempre me ajudaram a persistir mesmo nos momentos mais difíceis. Agradeço também ao apoio do Sérgio por me ajudar a continuar tocando este projeto em frente. Sem o auxílio de vocês este trabalho não seria possível!

Ao Prof. Dr. Waldiceu Ap. Verri Junior pela orientação, apoio e incentivo para que eu busque atingir níveis cada vez mais altos. Agradeço ainda pelo enorme esforço investido para que eu conquistasse a bolsa de doutorado sanduíche, mesmo com todas as adversidades que enfrentamos.

Agradeço aos colegas e a técnica Rosana, do laboratório de dor e inflamação, por todo o auxílio nas atividades diárias do laboratório, juntos nós podemos e crescemos muito mais.

Ao Prof. Dr. Moshe Arditi por ter me aceito e recebido em seu laboratório e também pela orientação e apoio no decorrer do projeto desenvolvido, nunca me esquecerei dos incontáveis “Short meetings”.

À Dra. Magali Noval Rivas pela supervisão, orientação e amizade durante o período que estive trabalhando no laboratório do Dr. Arditi, muito obrigada pela confiança e por tudo o que você me ensinou e que levarei para a vida!

Agradeço à todos os membros do laboratório do Dr. Arditi pelo companheirismo e ensinamentos que recebi durante o período do doutorado sanduíche.

Aos membros da banca de qualificação, Profa. Dra. Andressa de Freitas Mendes Dionísio e Prof. Dr. Wander Rogério Pavanelli, pela atenção e apontamentos realizados em meu trabalho.

Ao financiamento do projeto pelo Fundo de Apoio ao Ensino Pesquisa e Extensão/Universidade Estadual de Londrina [FAEPE/UEL 01/2009], Conselho Nacional de Pesquisa (CNPq) e Fundação Araucária, e à Coordenadoria de aperfeiçoamento de Pessoal de Nível Superior (CAPES) pela bolsa estudantil fornecida no país e pela bolsa do Programa de Doutorado Sanduíche no Exterior [PDSE/CAPES – Processo: 88881.133324/2016-01].

“Success is the ability to go from one failure to another with no loss of enthusiasm”
Winston Churchill

CARVALHO, Thacyana Teixeira de. **Mecanismos envolvidos na hiperalgesia mecânica induzida pelo fator estimulador de colônias de granulócitos (G-CSF) em camundongos e participação da IL-33 em modelo de Doença de Kawasaki.** 2018. 100 f. Tese (Doutorado em Patologia Experimental) – Universidade Estadual de Londrina, Londrina, 2018.

RESUMO

O fator estimulador de colônias de granulócitos (G-CSF) é a abordagem terapêutica atual para aumentar a contagem de neutrófilos periféricos pós-quimioterapia. A dor é o efeito adverso mais relevante da terapia com G-CSF. Contudo, os mecanismos envolvidos nesta hiperalgesia ainda não foram completamente elucidados. Este estudo investigou a participação das citocinas TNF-α, IL-1β e IL-10, do NFκB e da via Nrf2/HO-1 na hiperalgesia induzida pelo G-CSF em camundongos. O G-CSF induziu significativa hiperalgesia mecânica nos camundongos que foi reduzida pelo tratamento com etanercepte, IL-1ra, talidomida, pentoxifilina e rutina, também reduzida em camundongos deficientes para o receptor do TNF-α (TNFRI). Camundongos deficientes na citocina IL-10 apresentaram maior hiperalgesia após estímulo com G-CSF. Além disso, o tratamento com talidomida e pentoxifilina inibiu a produção de TNFα, IL-1β e IL-10 induzido pelo G-CSF no tecido plantar; o tratamento com rutina inibiu a produção de TNFα e IL-1β e aumentou a produção de IL-10. O G-CSF induziu a ativação de NFκB e reduziu a expressão do RNAm de Nrf2. O tratamento com rutina inibiu a ativação de NFκB e aumentou a expressão do RNAm de Nrf2 e HO-1. O tratamento combinado da morfina ou indometacina com talidomida, pentoxifilina ou rutina, em doses que são ineficazes *per se*, inibiu a hiperalgesia induzida pelo G-CSF. E ainda, o tratamento com estas drogas não afetou a mobilização de neutrófilos para o sangue periférico induzido pelo G-CSF. Os presentes resultados indicam que a dor induzida pelo G-CSF pode se dar por mediar a produção periférica de citocinas pró-nociceptivas, TNF-α e IL-1β, e sub-regular a citocina anti-nociceptiva IL-10, ativando o fator de transcrição NFκB e inibindo o Nrf2. Além disso, o tratamento com drogas que inibem citocinas ou flavonoides, como a rutina, são abordagens promissoras para o tratamento da dor induzida pelo G-CSF sem interferir no efeito terapêutico de mobilização de neutrófilos para o sangue periférico. A doença de Kawasaki (KD) é uma doença inflamatória multissistêmica que afeta crianças menores de 5 anos de idade e leva a formação de aneurismas nas artérias coronárias e aorta abdominal (AA), sendo a principal causa de vasculite em países desenvolvidos. A IL-33 é uma citocina membro da família da IL-1 que foi demonstrada estar aumentada no soro de pacientes com KD mesmo após tratamento, porém não são conhecidos os mecanismos envolvidos na participação da IL-33 nesta doença. Neste estudo, o papel da IL-33 no modelo de vasculite induzida pelo Extrato da Parede Celular de *Lactobacillus casei* (LCWE) foi avaliado em camundongos. Foi demonstrado que o gene da *il33* estava aumentado no coração e na AA dos camundongos estimulados com LCWE. A neutralização da IL-33 com anticorpo anti-IL-33, reduziu a formação das lesões na artéria coronária e dos aneurismas na AA induzidos pelo LCWE. A expressão de IL-33 estava aumentada na AA e as células produtoras desta citocina neste modelo não são os macrófagos. Não houve diferença na produção e na expressão do receptor de IL-33 (ST2) no soro e na AA, respectivamente. Os resultados obtidos neste estudo demonstraram que a IL-33 tem um papel importante no desenvolvimento das lesões induzidas pelo LCWE, no entanto, mais estudos são necessários para elucidar os mecanismos e células envolvidos neste processo.

Palavras-chave: G-CSF. Hiperalgesia. TNFα. IL-1β. IL-33. Doença de Kawasaki.

CARVALHO, Thacyana T. **Mechanisms involved in granulocyte colony stimulating factor (G-CSF)-induced mechanical hyperalgesia in mice and participation of the IL-33 in a model of Kawasaki Disease.** 2018. 100 p. Thesis (Doctorade in Experimental Pathology) – Universidade Estadual de Londrina, Londrina, 2018.

ABSTRACT

Granulocyte-colony stimulating factor (G-CSF) is the current therapeutic approach to increase peripheral neutrophil counts after chemotherapy. Pain is the most relevant side effect of G-CSF therapy. However, the mechanisms involved in this hyperalgesia have not yet been fully elucidated. In this study, the participation of the cytokines TNF-α, IL-1β and IL-10, NFκB, and the Nrf2/HO-1 pathway in G-CSF-induced hyperalgesia in mice was investigated. G-CSF induced significative mechanical hyperalgesia in mice that was reduced by treatment with etanercept, IL-1ra, thalidomide, pentoxifylline and rutin, also reduced in TNF-α (TNFRI) receptor deficient mice. IL-10 deficient mice showed higher hyperalgesia after G-CSF stimulation. Furthermore, treatment with thalidomide and pentoxifylline inhibited G-CSF-induced production of TNFα, IL-1β and IL-10 in the plantar tissue; treatment with rutin inhibited the production of TNFα and IL-1β and increased IL-10 production. G-CSF induced NFκB activation and reduced the expression of Nrf2 mRNA. Treatment with rutin inhibited NFκB activation and increased expression of Nrf2 and HO-1 mRNA. Combined treatment of morphine or indomethacin with thalidomide, pentoxifylline or rutin, at doses that are ineffective *per se*, inhibited G-CSF-induced hyperalgesia. In addition, treatment with these drugs did not affect the G-CSF-induced mobilization of neutrophils into the peripheral blood. The present results indicate that G-CSF-induced pain can occur by mediating the peripheral production of pro-nociceptive cytokines, TNF-α and IL-1β, and downregulation of the anti-nociceptive cytokine IL-10, the transcription factor NFκB activation and Nrf2 inhibition. Further, treatment with cytokine-inhibiting or flavonoid drugs, such as rutin, are promising approaches for the treatment of G-CSF-induced pain without interfering with the therapeutic effect of mobilization of neutrophils into the peripheral blood. Kawasaki disease (KD) is a multisystem inflammatory disease that affects children under 5 years of age and leads to coronary arteries and abdominal aorta (AA) aneurysms development, being the main cause of vasculitis in developed countries. IL-33 is a cytokine member of the IL-1 family that was shown to be increased in the serum of KD patients even after treatment, nevertheless, the mechanisms involved in the participation of IL-33 in this disease are not known. In this study, the role of IL-33 in the vasculitis model induced by the *Lactobacillus casei* cell-wall extract (LCWE) was evaluated in mice. It was demonstrated that the *il33* gene was increased in the heart and AA of the LCWE-stimulated mice. The neutralization of IL-33 with anti-IL-33 antibody reduced the LCWE-induced coronary artery lesions and AA aneurysms development. IL-33 expression was increased in the AA and the cells producing this cytokine are not macrophages in this model. There was no difference in the production and expression of IL-33 (ST2) receptor in serum and AA, respectively. The results obtained in this study demonstrated that IL-33 plays an important role in the LCWE-induced lesions development, however, more studies are needed to elucidate the mechanisms and cells involved in this process.

Keywords: G-CSF. Hyperalgesia. TNFα. IL-1β. IL-33. Kawasaki Disease.

LISTA DE ILUSTRAÇÕES

LISTA DE ABREVIATURAS E SIGLAS

AA	Ácido araquidônico
AP-1	Proteína de ativação 1
ARE	Elemento responsivo a antioxidante
ASC	Proteína *speck-like* associada à apoptose com domínio de recrutamento de caspase
CLRs	Receptores de lectina tipo C
COX	Cicloxigenase
DAMPs	Padrões moleculares associados a danos
ERNs	Espécies reativas de nitrogênio
EROs	Espécies reativas de oxigênio
G-CSF	Fator estimulador de colônias de granulócitos
GMPc	Guanosina monofosfato cíclico
GPx	Glutationa peroxidase
GRD	Gânglio da raiz dorsal
HO-1	Hemeoxigenase-1
IASP	Associação internacional para o estudo da dor
IFN-γ	Interferon gamma
IκB	Inibidores do kappa B
IL	Interleucina
IL-1RAcP	Proteína acessória do IL-1R
i.p.	Intraperitoneal
i.pl.	Intraplantar
IVIG	Imunoglobulina intravenosa
KD	Doença de Kawasaki
LCWE	Extrato da Parede Celular de *Lactobacillus casei*
LPS	Lipopolissacarídeo
MAP	Proteínas ativadas por mitógeno
MMPs	Metaloproteinases de matrix
NETs	Armadilhas extracelulares de neutrófilos
NFκB	Fator nuclear kappa B
NK	*Natural killer*

NLRs	Receptores semelhantes a NOD
NO	Óxido nítrico
NOS	Óxido nítrico sintase
iNOS	Óxido nítrico sintase induzível
Nrf2	Fator nuclear eritroide-2 relacionado ao fator 2
PAF	Fator de ativação das plaquetas
PAMPs	Padrões moleculares associados a patógenos
PGE_2	Prostaglandina E 2
PKC	Proteína quinase C
PRRs	Receptores de reconhecimento de padrão
RLRs	Receptores tipo RIG
SNC	Sistema nervoso central
STAT	Transdutor de sinal de transcrição
TLRs	Receptores semelhantes a Toll
TNFα	Fator de necrose tumoral alfa (α)
TNF-RI	Receptor do fator de necrose tumoral alfa tipo I
TNF-RII	Receptor do fator de necrose tumoral alfa tipo II
TRAF	Fatores associados ao receptor de TNF

SUMÁRIO

1 INTRODUÇÃO

1.1 INFLAMAÇÃO

A inflamação é uma resposta do organismo a infecções e tecidos lesados. Esta resposta ocorre por meio do recrutamento de células e moléculas de defesa para o local da injúria, sendo que o objetivo final é a eliminação do agente nocivo. Apesar de ser lesiva ao organismo, a resposta inflamatória é essencial para a proteção e sobrevivência, tendo por finalidade não somente livrar o organismo da causa inicial da lesão celular e tecidual (p.ex., microrganismos, toxinas), mas também eliminar as respectivas consequências da resposta gerada para este fim (p.ex., células necróticas) (KUMAR; ABBAS; ASTER, 2016).

A resposta inflamatória ocorre em uma sequência de eventos: reconhecimento do agente agressor pelas células residentes; ativação destas células e produção de mediadores químicos que levam ao recrutamento de leucócitos e proteínas do plasma da circulação para o foco inflamatório; ativação destas células e atuação das proteínas plasmáticas para destruir e eliminar o agente nocivo; controle da resposta inflamatória e resolução da inflamação; reparo tecidual (KUMAR; ABBAS; ASTER, 2016).

A primeira barreira contra infecções é formada pelas células e componentes da imunidade inata, tais como, barreiras físicas (p.ex., células epiteliais) e químicas (p.ex., substâncias químicas produzidas nas superfícies epiteliais que têm propriedade antimicrobiana); células fagocitárias (p.ex., neutrófilos, macrófagos), células dendríticas e células assassinas naturais (*natural killer* – NK); proteínas do sangue (p.ex., proteínas do sistema complemento); citocinas (ABBAS; LICHTMAN; PILLAI, 2011). O início da resposta inflamatória ocorre quando as células residentes reconhecem o antígeno (substâncias estranhas que induzem respostas imunes específicas ou que são reconhecidas pelos linfócitos ou anticorpos) (ABBAS; LICHTMAN; PILLAI, 2011). Os estímulos que podem deflagrar uma resposta inflamatória aguda são, por exemplo: infecções (bacteriana, virótica, fúngica, parasitária); necrose tecidual; corpos estranhos (lascas de madeira, sujeira, suturas); reações imunes (reações de hipersensibilidade) (KUMAR; ABBAS; ASTER, 2016). O reconhecimento do antígeno se dá pelos seus receptores de membrana específicos, os receptores de reconhecimento de padrão (PRRs) (ABBAS; LICHTMAN; PILLAI, 2011). Os receptores mais específicos pertencem à família dos receptores Receptores semelhantes a *Toll* (TLRs), outro grupo de receptores é o dos receptores semelhantes a NOD (NLRs), outros receptores são: receptores de lectina tipo C (C-typer lectin receptors – CLRs); receptores tipo

RIG (RIG-*like* receptors – RLRs); receptores acoplados à proteína G; receptores *scavenger* (ABBAS; LICHTMAN; PILLAI, 2011, KUMAR; ABBAS; ASTER, 2016). Estes receptores encontram-se expressos em diferentes tipos de células da imunidade inata e estão localizados em todos os compartimentos celulares nos quais microrganismos estão presentes: receptores de membrana citoplasmática; receptores endossomais; receptores citoplasmáticos (KUMAR; ABBAS; ASTER, 2016). Desta forma, as células que participam da imunidade inata são capazes de reconhecer diversas moléculas que são componentes compartilhados entre microrganismos. Estes componentes são conhecidos como os padrões moleculares associados a patógenos (PAMPs) e/ou padrões moleculares associados a danos (DAMPs) (ABBAS; LICHTMAN; PILLAI, 2011). A partir da interação entre receptor e antígeno dá-se início uma série de eventos vasculares e celulares que visam à eliminação do agente agressor e a restauração da homeostase, com danos mínimos ao organismo (KUMAR; ABBAS; ASTER, 2016).

Quando o agente lesivo é reconhecido, as células que residem no local são ativadas para eliminá-lo. A ativação destas células promove a produção de mediadores químicos, dentre eles, citocinas pró-inflamatórias, como o fator de necrose tumoral alfa (TNFα) e a interleucina (IL)-1β, e quimiocinas (p.ex., IL-8/CXCL8 – quimioatraente de neutrófilos), levando ao aumento na produção de diversos outros mediadores inflamatórios (aminas vasoativas, proteínas plasmáticas, metabólitos do ácido araquidônico, fator de ativação das plaquetas (PAF), óxido nítrico (NO), entre outros) e o aumento no calibre vascular com aumento no fluxo sanguíneo e na permeabilidade vascular. Uma das primeiras manifestações da inflamação aguda é a vasodilatação, promovida, principalmente pela ação da histamina sobre a musculatura lisa vascular e que causa a vermelhidão e o calor no local da inflamação (KUMAR; ABBAS; ASTER, 2016). Em sequência, o aumento da permeabilidade vascular promove o extravasamento de fluído rico em proteínas plasmáticas e o aumento no influxo de leucócitos para o tecido. No local da lesão, os leucócitos reconhecem o agente nocivo por meio dos PRRs o que promove sua ativação para fagocitose e produção de proteínas, como citocinas, espécies reativas de oxigênio (EROs) e espécies reativas de nitrogênio (ERNs – principalmente derivados do NO), além da liberação de enzimas e outras proteínas lisossômicas pelos granulócitos (p. ex., neutrófilos, monócitos) e de armadilhas extracelulares de neutrófilos (NETs) para a destruição intracelular dos microrganismos e resíduos fagocitados. Após a remoção dos agentes lesivos a inflamação diminui devido ao fato do curto tempo de meia-vida e rápida degradação dos mediadores inflamatórios, além dos neutrófilos também possuírem meia-vida curta nos tecidos. Ademais, durante o desenvolvimento da

resposta inflamatória, o próprio processo inicia uma gama de sinais de alerta que atuam para o controle e cessação da inflamação (Figura 1). Estes mecanismos se dão, dentre outros, por meio dos metabólitos do ácido araquidônico (AA) e citocinas anti-inflamatórias (p.ex., IL-10) que atuam de forma a restaurar o organismo à homeostase (KUMAR; ABBAS; ASTER, 2016).

Figura 1: Sequência de eventos em uma resposta inflamatória.

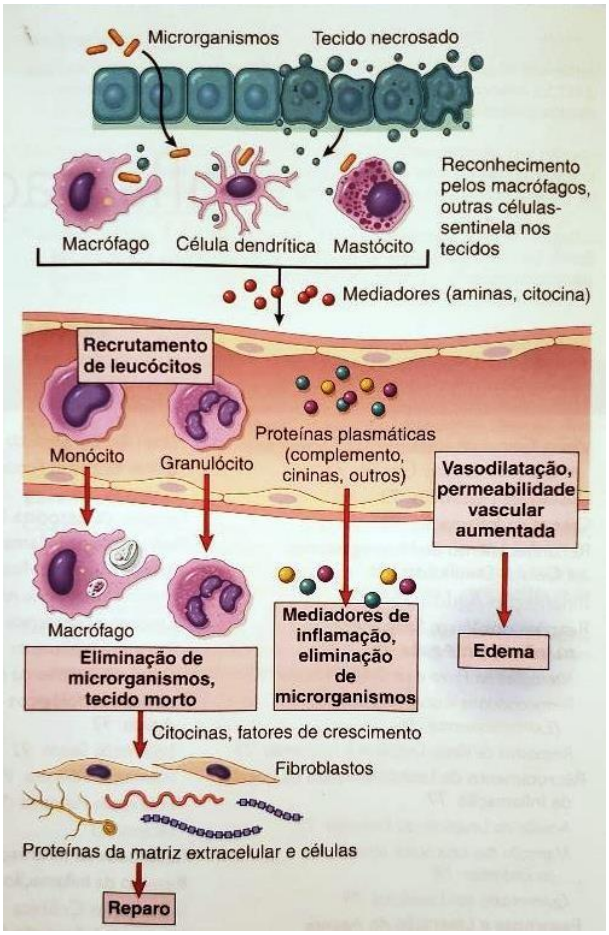

Fonte: KUMAR; ABBAS; ASTER (2016, p. 72).

1.2 Fatores de Transcrição

1.2.1 Fator Nuclear κB (NFκB)

A família do fator nuclear κB (NFκB) tem muitos membros, incluindo RELA (p65), NF-κB1 (p50; p105), NF-κB2 (p52; p100), c-REL e RELB. Cada membro da família do NFκB, exceto RELB, pode formar dímeros, tanto homodímeros, quanto heterodímeros uns com os outros, porém a forma mais ativada de NFκB é o heterodímero da subunidade p65

associada com as subunidades p50 ou p52 (revisado por LI & VERMA, 2002). As proteínas que formam o NFκB existem no citoplasma em uma forma inativa devido à sua associação com proteínas IκB (Inibidores do kappa B). Estas protéinas impedem a exposição das sequências de localização nuclear nas subunidades do NFκB impedindo, dessa forma, a entrada do NFκB no núcleo. Uma vez que um estímulo é reconhecido pelos PRRs das células, uma cascata de sinais intracelulares é ativada e resulta na fosforilação do IκB, levando este inibidor a ubiquitinação e degradação proteossômica (ABBAS; LICHTMAN; PILLAI, 2011; revisado por LI & VERMA, 2002).

A ativação do NFκB se dá em resposta à diversos estímulos como, por exemplo, patógenos, sinais de estresse e citocinas pró-inflamatórias (p. ex., TNFα e IL-1β). Após o reconhecimento destes sinais, o NFκB consegue migrar ao núcleo e ligar-se a regiões promotoras de diversos genes-alvo, regulando assim a transcrição de genes pró-inflamatórios. O NFκB regula a transcrição de citocinas pró-inflamatórias, quimiocinas, moléculas de adesão, metaloproteinases de matrix (MMPs), cicloxigenase 2 (COX-2) e óxido nítrico sintase induzível (iNOS) (revisado por LI & VERMA, 2002).

1.2.2 Fator nuclear eritroide-2 relacionado ao fator 2 (Nrf2)

O fator nuclear eritroide-2 relacionado ao fator 2 (Nrf2) é um fator de transcrição regulado pelo estado redox que é envolvido com na regulação dos sistemas de defesa antioxidante. A ativação do Nrf2 é um importante mecanismo da resposta inata do corpo contra o aumento do estresse oxidativo. O Nrf2 é responsável pela regulação da expressão de genes de enzimas de detoxificação de fase II e de proteínas por meio de uma sequência potenciadora conhecida como elemento responsivo a antioxidante (ARE) (LISK et al., 2013).

A chave reguladora na indução coordenada de diversos genes citoprotetores é a transcrição do Nrf2. Além disso, a ARE é o elemento promotor comum à quase todas as enzimas antioxidantes, como peroxiredoxinas, tioredoxinas, catalase, glutationa peroxidase (GPx) e a hemeoxigenase-1 (HO-1) (LOU et al., 2014; LISK et al., 2013).

Nrf2 é mantido inativo pela sua associação com a proteína ligadora Keap1 no compartimento citosólico e, na presença de estresse oxidativo, Keap1 libera o Nrf2 que, por sua vez se desloca para o núcleo da célula e ativa a transcrição de genes dirigidos por ARE (LISK et al., 2013).

1.3 CITOCINAS

1.3.1 Fator de necrose tumoral alfa (TNFα)

O fator de necrose tumoral (TNF) α é uma das citocinas pró-inflamatórias mais importantes do sistema imune. Ele é produzido por macrófagos e células dendríticas, entre outros tipos celulares em resposta ao reconhecimento de PAMPs e DAMPs pelos PRRs e consequente ativação do NFκB (ABBAS; LICHTMAN; PILLAI, 2011).

O TNFα pode exercer sua ação por se ligar a um de seus receptores, tipo I (TNF-RI) ou tipo II (TNF-RII), que são encontrados na maioria das células. A ligação do TNF a um de seus receptores leva ao recrutamento das proteínas denominadas fatores associados ao receptor de TNF (TRAF). Uma vez ativados, os TRAF ativam fatores de transcrição, como o NFκB e a proteína de ativação 1 (AP-1) (ABBAS; LICHTMAN; PILLAI, 2011).

1.3.2 Interleucina-1 beta (IL-1β)

A interleucina (IL)-1β é produzida por muitos tipos celulares, como neutrófilos, células epiteliais e céllulas endoteliais. Sua ativação depende de dois sinais distintos, um que ativa a transcrição gênica do precursor pró-IL-1β e, um segundo sinal que ativa o inflamassoma, responsável por clivar proteoliticamente o precursor, gerando a IL-1β madura (Figura 2). A transcrição gênica ocorre via sinalização por meio de TLRs ou NOD, que ativam NFκB, enquanto a clivagem é mediada pelo inflamassoma NLRP3 (também conhecido com NALP3 ou criopirina (ABBAS; LICHTMAN; PILLAI, 2011).

Figura 2: Ativação do inflamassoma NLRP3.

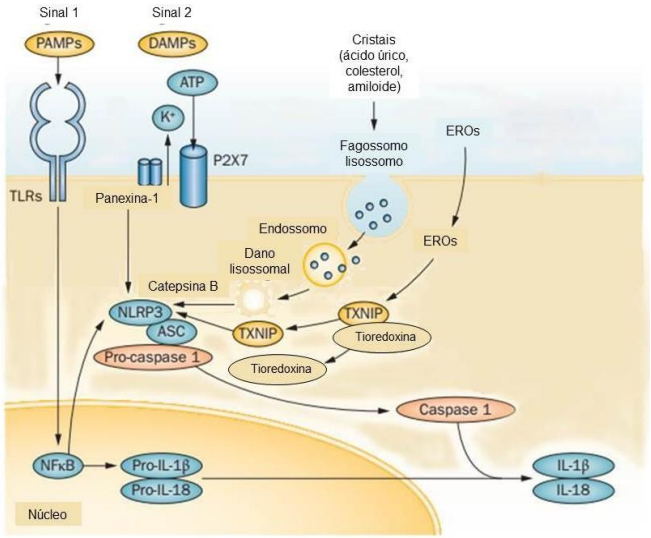

Fonte: Modificado de SZABO & PETRASEK (2015).

Os efeitos biológicos de IL-1β ocorrem pela sua ligação com o receptor de membrana chamado receptor de IL-1 do tipo I. Este receptor é expresso por vários tipos celulares, entre os quais: células endoteliais e leucócitos. A ligação entre IL-1β e seu receptor desencadeia uma sequências de eventos de sinalização que resultam na ativação dos fatores de transcrição NFκB e AP-1 (ABBAS; LICHTMAN; PILLAI, 2011).

1.3.3 Interleucina (IL)-33

A interleucina (IL)-33 é uma citocina membro da família da IL-1 e apresenta estrutura relacionada com a IL-18 e a IL-1β (SCHMITZ et al., 2005). As citocinas IL-18 e a IL-1β tornam-se biologicamente ativas após clivagem pela caspase-1, uma cisteína protease que é sintetizada como uma forma inativa, a pró-caspase-1 (GUO, CALLAWAY & TING, 2015). Então, quando um estímulo ativa o complexo do inflamassoma, a pró-caspase-1 se torna ativa e pode exercer seu papel (GUO, CALLAWAY & TING, 2015). Diferente da IL-18 e a IL-1β, a IL-33 torna-se funcionalmente inativada quando clivada pela caspase-1 (CAYROL & GIRARD, 2009). Nesse sentido, MADOURI e cols. (2015) observaram um aumento na liberação de IL-33 em modelo de inflamação alérgica de vias aéreas em camundongos deficientes para caspase-1/11, proteína *speck-like* associada à apoptose com domínio de recrutamento de caspase (ASC) e NLRP3. Por outro lado, a IL-33 induz a produção de IL-1β em modelos de inflamação e neuropatia (VERRI et al., 2008; ZARPELON et al., 2013; 2016).

A atividade da IL-33 se dá através da ligação com o receptor ST2 (SCHMITZ et al., 2005), membro da família da IL-1, que forma um complexo com a proteína acessória do IL-1R, a IL-1RAcP (CHACKERIAN et al., 2007). O gene *ST*2 pode codificar duas formas do receptor: o receptor de membrana (ST2L) que é responsável pela sinalização da IL-33 e o receptor solúvel (ST2s) que funciona como um receptor sequestrador de IL-33 (Figura 3) (SCHMITZ et al., 2005; TRAJKOVIC, SWEET & XU, 2004). A ligação da IL-33 com o complexo ST2/IL-1RAcP leva a transdução de sinal ativando a via das proteínas quinase ativadas por mitógeno (MAP) e o fator de transcrição nuclear NFκB (SCHMITZ et al., 2005; ZARPELON et al., 2016). Sabe-se que o receptor ST2 é expresso em vários tipos celulares, tais como células Th2 (XU et al., 1998), mastócitos (ALI et al., 2007, ALLAKHVERDI et l., 2007), cardiomiócitos (WEINBERG et al., 2002), entre outros.

Figura 3: Sinalização da IL-33.

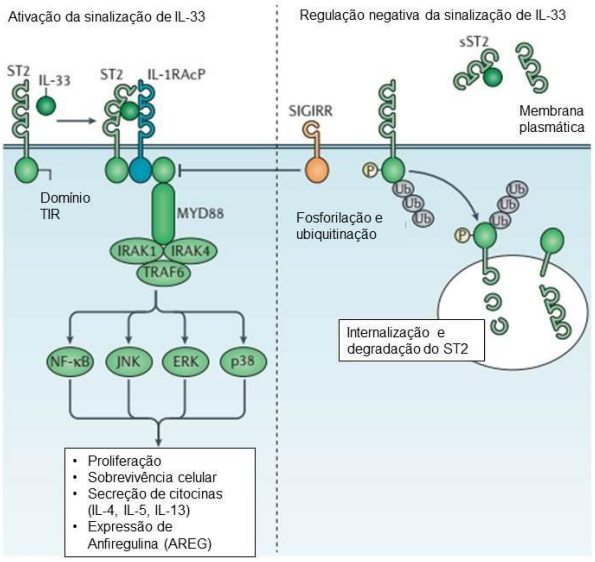

Fonte: Modificado de LIEW, GIRARD & TURNQUIST (2016).

1.3.4 Interleucina (IL)-10

A interleucina (IL)-10 é uma potente citocina anti-inflamatória envolvida no controle de patologias inflamatórias e autoimunes. A IL-10 faz perte de uma família de citocinas heterodiméricas e seu receptor pertence à família de receptores de citocinas do tipo II (semelhante ao receptor de interferons), que se associam a quinases JAK1 e TYK2 das família Janus e ativam o Transdutor de sinal de transcrição-3 (STAT3). A IL-10 é produzida por muitas células do sistema imune, incluindo macrófagos ativados, células dendríticas, células T

reguladoras e células T_H1 e T_H2 (ABBAS; LICHTMAN; PILLAI, 2011).

Algumas das funções da IL-10 são: inibir a produção de IL-12 por macrófagos ativados e células dendríticas, inibindo assim a produção de interferon gamma (IFN-γ); inibir a expressão de coestimuladores e moléculas do MHC de classe II em células dendríticas e macrófagos, inibindo dessa forma a ativação de células T (ABBAS; LICHTMAN; PILLAI, 2011). Nesse sentido, foi demonstrado que a deficiência ou expressão aberrante de IL-10 pode aumentar a resposta inflamatória à infeções, mas também pode levar ao desenvolvimento de doenças inflamatórias intestinais e doenças autoimunes (SELLON et al., 1998; O'GARRA et al., 2008; GAZZINELLI, 1996).

1.3.5 Fator Estimulador de Colônias de Granulócitos (G-CSF)

Fatores estimuladores de colônia são glicoproteínas que atuam em células hematopoiéticas estimulando a proliferação, diferenciação e ativação funcional da célula final (Figura 4). O fator estimulador de colônias de granulócitos (G-CSF) é uma citocina produzida por diversos tipos celulares, incluindo células T ativadas, macrófagos e células endoteliais. Essa característica é fundamental para o controle de infecções e outras doenças inflamatórias que cursam com alto consumo de granulócitos (ABBAS; LICHTMAN; PILLAI, 2011). Além disso, o G-CSF também atua na maturação e na atividade dos neutrófilos maduros, promovendo um aumento em sua atividade fagocítica, na quimiotaxia e na produção de superóxido. G-CSF se liga a um receptor de citocina do tipo I (G-CSFR). A ligação do G-CSF com seu receptor promove a ativação de cascatas de vias sinalização, como a via JAK-STAT, a via p21ras/MAPK e a via mediada por cAMP (revisado por HOGGATT & PELUS, 2014; revisado por WELTE, 2014).

Tendo em vista a importância do G-CSF, logo após a disponibilidade do G-CSF purificado na década de 1980, os primeiros estudos não clínicos *in vivo* foram realizados visando observar o aumento na população de células brancas no sangue de animais, testar a quimiotaxia de neutrófilos e a habilidade destas células em matar bactérias fagocitadas (WELTE et al., 1987). Em sequência, no final dos anos 1980 e início dos anos 1990, o desenvolvimento do G-CSF como um agente terapêutico foi benéfico para o tratamento de pacientes que receberam quimioterapia, dentre outros (revisado por WELTE, 2014).

Atualmente, o tratamento com G-CSF é indicado para pacientes com câncer recebendo quimioterapia mielossupressiva, pacientes com leucemia mieloide aguda recebendo indução ou quimioterapia de consolidação, pacientes com câncer recebendo transplante de medula

óssea, pacientes submetidos à coleta e terapia de células progenitoras de sangue periférico e pacientes com neutropenia crônica grave (NEUPOGEN® [Filgrastim] package insert, 2013). O tratamento com G-CSF é considerado ser seguro e eficaz em acelerar a recuperação na contagem de neutrófilos, contudo, o principal efeito adverso da terapia com G-CSF é a dor óssea ou músculo-esquelética (NEUPOGEN® [Filgrastim] package insert, 2013).

Figura 4: Hematopoiese.

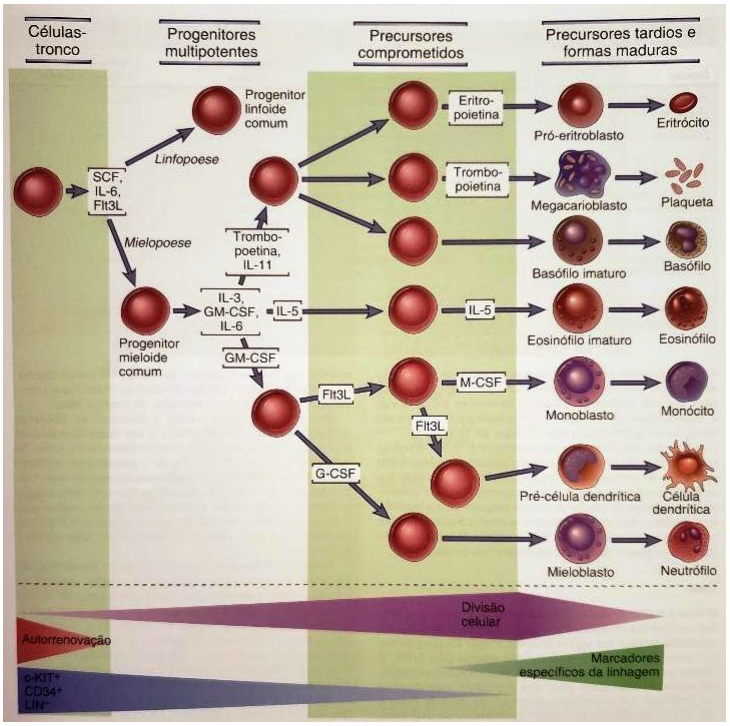

Fonte: ABBAS; LICHTMAN; PILLAI (2011, p. 27)

1.4 DOR INFLAMATÓRIA

A dor é uma resposta do organismo a estímulos físicos e químicos nocivos que visa proteger o indivíduo, sendo, desta forma, extremamente importante para mostrar que a integridade do organismo está ameaçada ou que alguma disfunção está ocorrendo no organismo (FERREIRA et al., 2009). A dor é definida pela Associação Internacional para o Estudo de Dor (IASP) como uma "experiência sensorial e emocional desagradável associada a dano tecidual real ou potencial, ou descrita em termos de tal dano" (IASP, 2012).

A dor inflamatória é resultado da interação entre o tecido lesado e os neurônios sensoriais nociceptivos periféricos, com a participação de mediadores inflamatórios. A dor inflamatória aguda resulta da ação de um estímulo desencadeante (mecânico, químico ou térmico) ou de um mediador, que ativa esses neurônios periféricos sensibilizados. Por outro

lado, a hiperalgesia inflamatória é o resultado de modificações funcionais nos neurônios aferentes primários nociceptivos, modificações estas que ocorrem por meio de uma ação metabotrópica em todo o neurônio facilitando sua ativação (HARDY; WOLFF; GOODELL, 1950, revisado por FERREIRA et al., 2009).

Os neurônios nociceptivos são responsáveis por detectar e transmitir o estímulo derivado do dano ou injúria tecidual. Os neurônios nociceptivos primários (de primeira ordem) são integrantes do sistema nervoso somatossensorial cujas terminações nervosas possuem receptores de membrana especializados na detecção de estímulos de alto limiar ou alta intensidade de natureza mecânica, térmica ou química. Os nociceptores encontram-se amplamente distribuídos nos diferentes tecidos e suas fibras podem ser classificadas nos subtipos A-δ (mielinizadas, de transmissão rápida - cerca de 12 a 30 m/s) e C (não mielinizadas, de transmissão lenta - cerca de 0,5 a 2 m/s). Cada uma dessas fibras transmite um tipo de sinal doloroso (RANG; BEVAN; DRAY, 1991; revisado por FERREIRA et al., 2009).

O centro metabólico de cada célula neuronal é o gânglio da raiz dorsal (GRD), localizado em seu corpo celular. Um prolongamento axônico sai de cada GRD e se divide em dois troncos, um se dirige para os tecidos periféricos e o outro para a medula espinal (nervos espinais) ou para o tronco encefálico (nervos cranianos) (DEVOR, 1999; revisado por FERREIRA et al., 2009). Sabendo que as fibras sensoriais periféricas se dirigem para o sistema nervoso central (SNC), a informação sensorial percorre um longo caminho desde a estimulação periférica, passando pelo GRD e chegando até a medula espinal, só então ela vai para os centros superiores de processamento (Figura 5). No corno dorsal da medula espinal, os neurônios aferentes primários fazem sinapse com os neurônios secundários, por meio da liberação de neurotransmissores (como o glutamato, aminoácido excitatório, ou a substância P). Então, o neurônio nociceptivo secundário conduz a informação até o SNC supra-espinal, onde é analisada e interpretada como dor (revisado por FERREIRA et al., 2009).

Figura 5: Mecanismos da dor inflamatória.

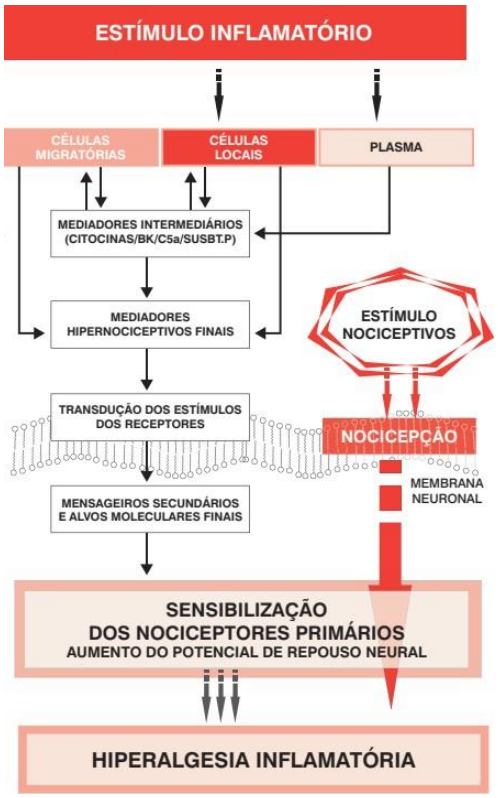

Fonte: FERREIRA et al. (2009, p. 267).

Quando a dor é estudada em modelos animais outras definições são necessárias para a compreensão do tema, como, por exemplo, o termo hiperalgesia, ou seja, o "aumento da dor a partir de um estímulo que normalmente provoca dor" (IASP, 2012).

1.5 FLAVONOIDES

Os flavonoides são um vasto grupo de aminoácidos aromáticos sintetizados em plantas como glicosídeos, formados pelos aminoácidos fenilalanina e malatonato. Os flavonoides podem ser encontrados em diversos tipos de alimentos, como por exemplo: frutas cítricas, berries e chás feitos com folhas de plantas, desta forma, seu consumo é diário, dependendo do tipo de dieta de cada um (GILDAWIE et al., 2018; VERRI et al., 2012). A síntese dos flavonoides se dá em plantas em resposta à uma infecção microbiana (KUMAR & PANDEY, 2013). A estrutura básica dos flavonoides é o núcleo flavona, o qual consiste em 15 átomos de carbono arranjados em três anéis (C6–C3–C6) (Figura 6), sendo dois anéis aromáticos e um anel pirano central (GILDAWIE et al., 2018; VERRI et al., 2012). A atividade dos flavonoides é dependente de sua estrutura. Neste sentido, as principais classes de flavonoides são flavonois, flavanois, flavonas, flavanonas, catequinas, antocianinas, isoflavona,

diidroflavonois e chalconas (YAO et al., 2004). A sua classificação é feita conforme o estado de oxidação do anel pirano (GILDAWIE et al., 2018).

Figura 6: Estrutura básica de um flavonoide.

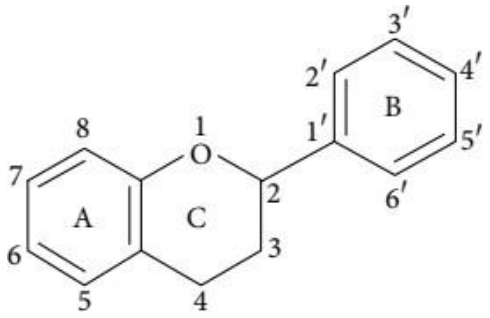

Fonte: KUMAR & PANDEY (2013).

Os efeitos biológicos dos flavonoides são principalmente atribuídos a sua atividade antioxidante. Tal efeito é relacionado a neutralização de EROs, tais como: ânions peróxido, ânion superóxido, radicais hidroxil e hidroperóxidos. Nesse sentido, a resposta inflamatória leva a ativação de NFκB que, por sua vez, leva a produção de mediadores pró-inflamatórios, como citocinas, quimiocinas, COX-2, iNOS e outros mediadores inflamatórios. Os flavonoides podem inibir a ativação do NFκB, agir como sequestradores de quimiocinas e até induzir a produção de citocinas anti-inflamatórias, assim, reduzindo a inflamação (VERRI et al., 2012).

1.5.1 Rutina

A rutina (3-[[6-*O*-(6-deoxi-α-$_{L}$-manopiranosil)-β-$_{D}$-glucopiranosil]oxi]-2-(3’,4’-diidroxifenil)-5,7-diidroxi-4H-1-benzopiran-4-ona) é um dos flavonoides mais comuns, naturalmente presentes em diversas plantas e frutos como, por exemplo, trigo-mourisco (também conhecido como serraceno), flor de maracujá, laranja, chá-da-índia, tomate, ruibarbo e damasco (revisado por HOSSEINZADEH & NASSIRI-ASL, 2014; UGUSMAN et al., 2014). A rutina é um flavonol que apresenta em sua estrutura um dissacarídeo (ramnose + glicose) ligados a posição 3 do anel pirano (PEDRIALI, 2005) (Figura 7).

Figura 7: Estrutura química da rutina.

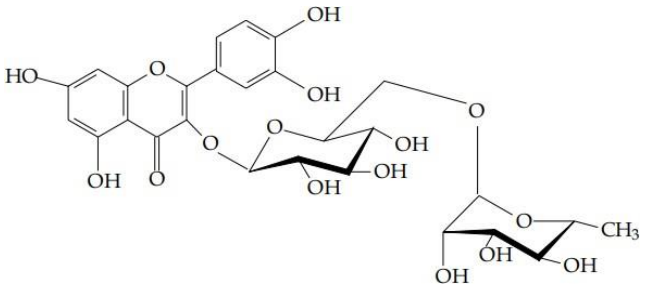

Fonte: PEDRIALI, C. A. (2005).

A rutina também é conhecida como vitamina P ou quercetina-3-*O*-rutinosídeo, sendo que ela é o glicosídeo principal que forma a quercetina (flavonol mais abundante em frutas e vegetais). A rutina quando metabolizada tem como um de seus metabólitos a quercetina (revisado por HOSSEINZADEH & NASSIRI-ASL, 2014).

Por ser um flavonoide, grande interesse nas propriedades farmacológicas da rutina tem sido demonstrado pela comunidade científica e pela indústria farmacêutica. A rutina mostrou ter efeito antidiabético (KAMALAKKANNAN & PRINCE, 2006; KAMALAKKANNAN & STANLEY MAINZEN PRINCE, 2006), antioxidante (KAMALAKKANNAN & STANLEY MAINZEN PRINCE, 2006), anti-inflamatório (KODA, T.; KURODA, Y.; IMAI, H., 2009; MASCARAQUE et al., 2014) e no tratamento da dor neuropática (TIAN et al., 2016) em diferentes modelos animais.

1.6 Modelo de Dor Induzida pelo Fator Estimulador de Colônias de Granulócitos (G-CSF)

O teste da pressão crescente na pata dos camundongos por meio do Analgesímetro digital (Insight®) é um método comparável ao teste dos filamentos de von Frey (VON FREY, 1896), no qual pode-se distinguir entre dois componentes da dor inflamatória: I) Sensibilização; e II) Ativação do nociceptor, tornando-o mais vantajoso do que o teste de contorções abdominais e o teste da formalina (CUNHA et al., 2004). O Analgesímetro digital registra o peso (em gramas) decorrente da pressão exercida pelo experimentador, com o transdutor de sinal acoplado a uma ponteira de polipropileno, na pata a ser avaliada até que o camundongo realize o movimento de retirada ou sacudida (*flinch*) da pata, assim, obtêm-se a intensidade de hiperalgesia do animal devido à administração de um estímulo nocivo (p. ex.: Carragenina, Prostaglandina E_2 (PGE_2), Lipopolissacarídeo (LPS)).

Foi padronizado em nosso laboratório um modelo animal de dor induzida pelo G-CSF (Figura X) por meio da avaliação da hiperalgesia mecânica utilizando o teste pressão crescente da pata (CARVALHO et al., 2011). A injeção intraplantar (i.pl.) de Granulokine® mostrou ser capaz de induzir hiperalgesia mecânica em camundongos, mas não hiperalgesia térmica ou edema plantar. Esse modelo torna-se importante para a realização de estudos acerca dos mecanismos envolvidos no desenvolvimento da dor induzida pelos fatores estimuladores de colônias de granulócitos (G-CSFs), para, dessa maneira, fornecer base para novos tratamentos que atuem diretamente no alvo da dor e que possuam menor (ou nenhuma) incidência de reações adversas ao medicamento.

1.7 MODELO DE VASCULITE INDUZIDA PELO EXTRATO DA PAREDE CELULAR DE *LACTOBACILLUS CASEI* (LCWE)

A doença de Kawasaki (KD) é uma doença inflamatória multissistêmica de causa desconhecida que resulta em uma síndrome febril aguda. Esta patologia ainda é responsável pelo aparecimento de lesões secundárias em artérias coronárias sendo a principal causa de vasculite nos Estados Unidos (GUPTA-MALHOTRA et al., 2009; SCHULTE et al., 2009) ocorrendo predominantemente em crianças com menos de 5 anos de idade (CHEN et al., 2012). A formação de aneurisma de artéria coronária ocorre em aproximadamente 25% das crianças com KD não tratadas (NEWBURGER et al., 1986; CHEN et al., 2012) e pode levar a doença cardíaca isquêmica, infarto do miocárdio e, até mesmo, a morte (SCHULTE et al., 2009). Apesar dos esforços para reduzir a inflamação, entre 11 a 23% dos pacientes podem apresentar resistência ao tratamento com imunoglobulina intravenosa (IVIG - terapia atual), tornando-os uma população de alto risco para o desenvolvimento de problemas cardíacos (WALLACE et al., 2000). Tem sido sugerido que a ocorrência de KD na infância pode estar relacionada com o desenvolvimento de aterosclerose precoce e doenças cardiovasculares na vida adulta (GUPTA-MALHOTRA et al., 2009; CHEN et al., 2012). A administração em camundongos, por via intraperitoneal (i.p.), de um extrato da parede celular de *Lactobacillus casei* (LCWE) induz arterite local com alterações histopatológicas semelhantes às lesões nas artérias coronárias encontradas na KD em humanos, sendo considerado um modelo animal para estudos acerca dos mecanismos desta doença (LEHMAN et al., 1985; ROSENKRANZ et al., 2005; SCHULTE et al., 2009) para, dessa maneira, fornecer base para novos tratamentos que sejam mais eficazes em abolir o estado febril prolongado e reduzir o risco de complicações vasculares durante a vida adulta.

Foi padronizado no laboratório do Dr. Moshe Arditi no Centro Médico Cedars-Sinai em Los Angeles, Califórnia, EUA, um modelo animal de vasculite induzida pelo Extrato da Parede Celular de *Lactobacillus casei* (LCWE) que se assemelha muito aos achados em pacientes que desenvolvem a doença de Kawasaki.

2 OBJETIVOS

2.1 OBJETIVO GERAL

Avaliar os mecanismos pelos quais o Fator Estimulador de Colônias de Granulócitos (G-CSF) induz hiperalgesia mecânica em camundongos e possíveis abordagens terapêuticas para o tratamento da dor induzida pelo G-CSF e avaliar o papel da Interleucina (IL)-33 na vasculite induzida pelo Extrato da Parede Celular de *Lactobacillus casei* (LCWE) em camundongos.

2.2 OBJETIVOS ESPECÍFICOS

Avaliar:

- A participação das citocinas TNFα, IL-1β e IL-10 hiperalgesia mecânica induzida pela administração intraplantar (i.pl.) do Fator Estimulador de Colônias de Granulócitos (G-CSF);
- O efeito da hiperalgesia mecânica induzida pelo G-CSF em animais tratados com: etanercepte (receptor solúvel de TNF, TNFRII), anakinra (IL-1ra; antagonista do receptor de IL-1), talidomida, pentoxifilina ou rutina reduz a hiperalgesia mecânica induzida pelo G-CSF; e em camundongos deficientes: no receptor I de TNF ($TNFRI^{-/-}$) ou na citocina anti-inflamatória IL-10 ($IL\text{-}10^{-/-}$);
- Se o tratamento com talidomida, pentoxifilina ou rutina interfere na produção das citocinas TNFα, IL-1β e IL-10;
- O efeito do tratamento com rutina na: ativação da via de sinalização do NO−cGMP−PKG−K_{ATP}, ativação do fator de transcrição nuclear NFκB, expressão de Nrf2 e HO-1;
- O efeito do tratamento com etanercepte, anakinra, talidomida, pentoxifilina, morfina, indometacina e rutina na contagem de leucócitos no sangue periférico após administração do G-CSF;
- O perfil de expressão da IL-33 por sequenciamento de RNA no coração e aorta de camundongos 14 dias após a indução da vasculite pela injeção i.p. do Extrato da Parede Celular de *Lactobacillus casei* (LCWE);
- A produção de IL-33 e ST2 no soro de camundongos 14 dias após a injeção de LCWE;
- O efeito da neutralização da IL-33 na artéria coronária e no aneurisma da aorta abdominal após 14 dias do estímulo com LCWE;
- A expressão da IL-33 e do ST2 na aorta abdominal após 14 dias do estímulo com LCWE e

se os macrófagos recrutados para a aorta abdominal são a fonte de IL-33 após o estímulo com LCWE.

3 ARTIGOS

Este é um trabalho realizado no Laboratório de Dor e Inflamação, formado pelos artigos científicos: “Granulocyte-colony stimulating factor (G-CSF)-induced mechanical hyperalgesia in mice: Role for peripheral TNFα, IL-1β and IL-10”, de autoria de: Thacyana T. Carvalho, Sergio M. Borghi, Felipe A. Pinho-Ribeiro, Sandra S. Mizokami, Thiago M. Cunha, Sergio H. Ferreira, Fernando Q. Cunha, Rubia Casagrande e Waldiceu A. Verri Jr., publicado no periódico *European Journal of Pharmacology*; e “The granulopoietic cytokine granulocyte-colony stimulating factor (G-CSF) induces pain: analgesia by rutin”, de autoria de: Thacyana T. Carvalho, Sandra S. Mizokami, Camila R. Ferraz, Marília F. Manchope, Sergio M. Borghi, Victor Fattori, Cassia Calixto-Campos, Doumit Camilios-Neto, Rubia Casagrande e Waldiceu A. Verri Jr., submetido e sob revisão pelo periódico *Inflammopharmacology.*

O terceiro artigo científico que compõe esta tese é: “Role of IL-33 in LCWE-induced Kawasaki Disease Vasculitis and Aneurysms”, de autoria de: Thacyana T. Carvalho; Masanori Abe; Michael K. Franklin; Waldiceu A. Verri; Moshe Arditi e Magali Noval Rivas. Este artigo é resultado das pesquisas realizadas durante junho/2017 à maio/2018 no laboratório do Dr. Moshe Arditi, Cedars-Sinai Medical Center, Los Angeles, CA, EUA. As formatações deste artigo seguem as normas do periódico *Arteriosclerosis, Thrombosis, and Vascular Biology*.

3.1 ARTIGO PUBLICADO NO PERIÓDICO EUROPEAN JOURNAL OF PHARMACOLOGY

Granulocyte-Colony Stimulating Factor (G-CSF)-induced mechanical hyperalgesia in mice: role for peripheral TNFα, IL-1β and IL-10

Thacyana T. Carvalho[a], Sergio M. Borghi[a], Felipe A. Pinho-Ribeiro[a], Sandra S. Mizokami[a], Thiago M. Cunha[b], Sergio H. Ferreira[b], Fernando Q. Cunha[b], Rubia Casagrande[c], Waldiceu A. Verri, Jr.[a*]

[a]Departament of Pathology, Center of Biological Science, University State of Londrina, Rod. Celso Garcia Cid KM480 PR445, CEP 86051-990, Cx Postal 6001, Londrina, Paraná, Brazil.
[b]Department of Pharmacology, Ribeirao Preto Medical School, University of Sao Paulo, Sao Paulo, Avenida Bandeirantes, 3900, CEP 14049-900 – Ribeirao Preto, Sao Paulo, Brazil.

[c]Department of Pharmaceutical Sciences, University Hospital (Health Science Centre), Londrina State University, Avenida Robert Koch, 60, Hospital Universitário, 86038- 350, Londrina, Paraná, Brazil.

*Corresponding Author: Prof. Dr. Waldiceu A. Verri Jr. Present Address: Departamento de Patologia, Universidade Estadual de Londrina, Rod. Celso Garcia Cid Km 480 Pr 445, CEP 86.051-990, Cx Postal 6001, Londrina, Paraná, Brazil. Tel.: +55 43 3371- 4979; Fax: +55 43 3371-4387; E-mail: waverri@uel.br; waldiceujr@yahoo.com.br

Abstract

Granulocyte-colony stimulating factor (G-CSF) is a therapeutic approach to increase peripheral neutrophil counts after anti-tumor therapies. Pain is the major side effect of G-CSF. Intraplantar administration of G-CSF in mice induces mechanical hyperalgesia. However, the peripheral mechanisms involved in this effect were not elucidated. Therefore, the participation of pronociceptive cytokines tumor necrosis factor (TNF) alpha (TNFα), interleukin (IL)-1 beta (IL-1β) and antinociceptive cytokine IL-10 in G- CSF-induced mechanical hyperalgesia in mice were investigated. G-CSF-induced mechanical hyperalgesia was inhibited by systemic and local treatment with etanercept and IL-1 receptor antagonist (IL-1ra) or TNF receptor 1 (TNFR1) deficiency and increased in IL-10 deficient mice. In agreement, G-CSF injection induced significant TNFα, IL-1β and IL-10 production in paw tissue. G-CSF-induced hyperalgesia was dose-dependently inhibited by thalidomide (5–45 mg/kg) and pentoxifylline (0.5 – 13.5 mg/kg), and treatment with these drugs inhibited G-CSF-induced TNFα, IL-1β and IL-10 production. The combined treatment with pentoxifylline or thalidomide with morphine, at doses that are ineffective as single treatment, diminished G-CSF-induced hyperalgesia through inhibiting cytokine production. Indomethacin also reduces G-CSF hyperalgesia alone or combined with pentoxifylline or thalidomide. Thus, G-CSF- induced hyperalgesia might be mediate by peripheral production of pronociceptive cytokines TNFα and IL-1β and down-regulated by IL-10. Systemic IL-1ra reduced G- CSF-induced increase of peripheral neutrophil counts. However, local treatment with morphine, IL-1ra or etanercept, and systemic treatment with indomethacin, etanercept, thalidomide and pentoxifylline did not alter G-CSF-induced mobilization of neutrophils. Therefore, this study advances in the

understanding of G-CSF-induced hyperalgesia and suggests therapeutic approaches for its control.

Keywords: G-CSF; pain; cytokine; thalidomide; pentoxifylline; morphine

1. Introduction

Commercial forms of granulocyte-colony stimulatory factor (G-CSF) such as filgrastim and biosimilars are clinically used to induce granulopoiesis in conditions such as myelosuppressive chemotherapy, acute myeloid leukemia and severe chronic neutropenia (Battiwalla & McCarthy, 2009; Dale et al., 1993; Filgrastim package insert; Santjohanser et al., 2013). The main side effect of G-CSF therapy is pain as reported by healthy volunteers and cancer patients (Battiwalla & McCarthy, 2009; Filgrastim package insert). Corroborating the hyperalgesic role of G-CSF, nociceptive neurons express G- CSF receptor and targeting this receptor inhibits pancreatic carcinoma-induced hyperalgesia (Schweizerhof et al., 2009). Carrageenan-induced facial inflammatory pain was also related to increased G-CSF mRNA expression (Poh et al., 2011). The intraplantar (i.pl.) administration of G-CSF induces mechanical hyperalgesia by a mechanism dependent on spinal activation of mitogen activated protein (MAP) kinases and phosphatidilinositil 3-kinase (PI_3K) (Carvalho et al., 2011) and G-CSF activates these kinases in cancer pain (Schweizerhof et al., 2009). Cytokines such as tumor necrosis factor alpha (TNFα) and interleukin (IL)-1 beta (IL-1β) activate these kinases in models of inflammatory and neuropathic pain (Obata et al., 2004; Pezet et al., 2008; Svensson et al., 2003; Xu et al., 2007). The hyperalgesia induced by peripheral administration of TNFα and IL-1β depends on prostaglandin production (Verri et al., 2006). On the other hand, IL-10 is known by its anti-hyperalgesic effects attributed to inhibition of TNFα and IL-1β production and action (Poole et al., 1995; Verri et al., 2006). IL-10 inhibits carrageenan-, TNFα- and IL-1β-induced mechanical hyperalgesia in rats (Verri et al., 2006). In other systems, G-CSF induces TNFα, IL-1β and IL-10 production (Bien et al., 2013; Schmidt et al., 1999). However, the role of TNFα, IL-1β and IL-10 in G-CSF-induced mechanical hyperalgesia is unknown. Biological therapies targeting cytokines are recognized as important anti- inflammatory approaches (Murdaca et al., 2014; Niu et al., 2011; Verri et al., 2006). Additionally, cytokines can be target by non-biological approaches. For instance, thalidomide and pentoxifylline are the chosen options for the treatment of several clinical conditions such as erythema nodosum leprosum and multiple myeloma since they inhibit TNFα production (Breitkreutz & Anderson, 2008; Majumder et al., 2012; Putinatti et al., 2014). Thus, they could be considered as interesting pharmacological approaches for the treatment of cytokine-dependent inflammatory pain diseases in clinical practice. Opioids are used to treat G-CSF-induced pain in humans (Filgrastim package insert). G-CSF-induced mechanical hyperalgesia in mice is also amenable by morphine treatment (Carvalho et al., 2011). However, prolonged treatment with opioids induces dependence because of opioid receptors desensitization leading to increasing doses of morphine. The side effects of morphine include nausea, constipation, somnolence/sedation, and respiratory failure, which increase with the dose increment (Devulder et al., 2009). Interestingly, synergy of thalidomide and pentoxifylline with morphine has been reported and could account to reduce the dose of morphine (Lee et al., 2013; Lu et al., 2004; Mika et al., 2009). Taking into account the above evidence, the role of TNFα, IL-1β and IL-10 in G-CSF-induced mechanical hyperalgesia was evaluated using biological therapies, knockout mice, thalidomide, pentoxifylline and indomethacin.

2. Materials and methods

2.1. Animals

The experiments were performed on male C57BL/6 background (wild type; WT), TNF receptor 1 (TNFR1) deficient ($^{-/-}$) paired with the respective littermate (C57BL/6 background) and IL-10$^{-/-}$ paired with the respective littermate (C57BL/6 background) mice (20-25 g, from University of Sao Paulo, Ribeirao Preto Medical School), which were housed in standard clear plastic cages with free access to food and water. All behavioral testing was performed between 9:00 am and 5:00 pm in a temperature-controlled room. Animals' care and handling procedures were in accordance with the International Association for Study of Pain (IASP) guidelines, with the EC Directive 86/609/EEC for animal experiments and with the approval of the Ethics Committee of the Universidade Estadual de Londrina. All efforts were made to minimize the number of animals used and their suffering.

2.2. Drugs

Drugs were obtained from the following sources: G-CSF (Granulokine®, Filgrastim, recombinant human G-CSF, 100 ng/paw) from Hoffmann La-Roche (Basileia, Swiss), indomethacin (0.5-5 mg/kg) from Prodome (Campinas, SP, Brazil), morphine sulphate (2 and 6 µg/paw) from Cristalia (São Paulo, Brazil), etanercept (10 mg/kg) from Wyeth Indústria Farmacêutica Ltda (São Paulo, Brazil), IL-1ra (30 mg/kg) from NIBSC (National Institute of Biological Standards and Control, UK), thalidomide (α-N-phthalimodoglutarimide, 5-45 mg/kg) from FUNED (Fundação Ezequiel Dias - Belo Horizonte, Brazil), pentoxifylline (methylxanthine derivative, 0.5-13.5 mg/kg) from Sanofi-Aventis Farmacêutica Ltda (Suzano, Brazil). G-CSF, morphine sulphate, etanercept and IL-1 receptor antagonist (IL-1ra) were dissolved in saline, thalidomide and pentoxifylline were dissolved in dimethyl sulfoxide (DMSO) 2% in saline, and indomethacin was dissolved in Tris/HCl (2-amino-2-hydroxymethylpropan-1,3- diol/hydrochloric acid) buffer, pH 8.0.

2.3. Experimental protocols

TNFR1$^{-/-}$, IL-10$^{-/-}$ and the respective WT (C57BL/6 background) mice received intraplantar (i.pl.) injection of G-CSF (100 ng/paw) and mechanical hyperalgesia was evaluated after 1-7 h. Regarding the effect of pharmacological treatments over mechanical hyperalgesia, C57BL/6 mice were treated with etanercept (10 mg/kg, intraperitoneal [i.p.], 48 and 1 h or 1-100 µg/paw, 1 h), IL-1ra (30 mg/kg, i.p., 30 min or 30-300 pg/paw, 30 min), thalidomide (5-45 mg/kg, i.p., 30 min) or pentoxifylline (0.5- 13.5 mg/kg, i.p., 30 min) before i.pl. administration of G-CSF (100 ng/paw) and mechanical hyperalgesia was evaluated after 1-7 h. Cytokine (TNFα, IL-1β and IL-10) levels were determined 2 and 4 h after G-CSF injection (100 ng/paw) or at 2h after G- CSF injection in mice previously treated with thalidomide (45 mg/kg, i.p., 30 min) or pentoxifylline (13.5 mg/kg, i.p., 30 min). In other settings, mice were treated with morphine (2 µg/25 µl, 1 or 4 h after G-CSF stimulus), thalidomide (5 mg/kg, 30 min before), pentoxifylline (0.5 mg/kg, 30 min before), morphine plus thalidomide and morphine plus pentoxifylline, and received G-CSF (100 ng/paw) followed by evaluation of mechanical hyperalgesia at 5 h (peak of hyperalgesia) and cytokine levels at 2 h (peak of cytokine production). The effect of indomethacin (0.5-5 mg/kg, 40 min before G-CSF), and indomethacin (0.5 mg/kg, 40 min before G-CSF) plus thalidomide (5 mg/kg, 30 min before G-CSF) or pentoxifylline (0.5 mg/kg, 30 min before G-CSF) treatments over G-CSF-induced mechanical hyperalgesia was evaluated after 1-7 h. In the last set of experiments, mice were

treated with vehicles (saline i.pl., saline i.p., DMSO 2% in saline i.p. and/or Tris/HCl buffer i.p.), IL-1ra (100 pg/paw or 30 mg/kg i.p.), etanercept (100 µg/paw or 10 mg/kg, i.p.), morphine (6 µg /paw), thalidomide (45 mg/kg, i.p.), pentoxifylline (13.5 mg/kg, i.p.) or indomethacin (5 mg/kg, i.p.) at time points described above before G-CSF (100 ng/paw) stimulus. Twenty four h after G- CSF stimulus blood samples were collected for total and differential leukocyte counts. The doses described above were based on previous studies and standardization in our laboratory (Borghi et al., 2014a; Borghi et al., 2014b; Carvalho et al., 2011; Calil et al., 2013). Saline (25 µl/paw) was used as negative control of G-CSF injection. It is noteworthy to mention that experimenters for behavioral tests were blind to treatment condition.

2.4. Electronic pressure-meter test for mice

Mechanical hyperalgesia was tested in mice as previously reported (Cunha et al., 2004). Briefly, in a quiet room, mice were placed in acrylic cages (12×10×17 cm) with wire grid floors, 15-30 min before the start of testing. The test consisted of evoking a hindpaw flexion reflex with a hand-held force transducer (electronic von Frey anesthesiometer; Insight, Ribeirão Preto, SP, Brazil) adapted with a 0.5 mm^2 contact area polypropylene tip. The investigator was trained to apply the tip perpendicularly to the central area of the hind-paw with a gradual increase in pressure. The end point was characterized by the removal of the paw followed by clear flinching movements. After the paw withdrawal, the intensity of the pressure was recorded automatically. The value for the response was an average of three measurements. The animals were tested before and after treatment. The results are expressed by delta (Δ) withdrawal threshold (in g) calculated by subtracting the zero-time mean measurements from the mean measurements (indicated time points) after stimulus. The basal mechanical withdrawal threshold was 9.5 ± 0.1 g (mean ± S.E.M. of 67 groups, 6 mice per group) before injection of stimulus or vehicle. There was no difference of basal mechanical withdrawal thresholds between groups in the same experiment. Basal values of mechanical thresholds are shown in supplementary material.

2.5. TNF*α*, IL-1β and IL-10 levels determination

Mice received intraplantar injection of G-CSF (100 ng) and 2 and 4 h after samples of paw tissue were collected. In another set of experiments, mice were treated intraperitoneally with vehicle (DMSO 2% in saline), thalidomide (5 – 45 mg/kg i.p.) or pentoxifylline (0.5 – 13.5 mg/kg i.p.) 30 min before G-CSF stimulus. In the last set of experiments dosing cytokine levels, mice were treated with vehicle (saline i.pl., saline i.p., DMSO 2% in saline i.p. and/or Tris/HCl buffer i.p.), morphine (2 µg/paw, 1 h after G-CSF stimulus), thalidomide (5 mg/kg, i.p., 30 min before G-CSF), pentoxifylline (0.5 mg/kg, i.p., 30 min before G-CSF), morphine plus thalidomide and morphine plus pentoxifylline and received intraplantar injection of G-CSF (100 ng/paw) followed by paw tissue sample collection after 2 h (peak of cytokine production). TNFα, IL-1*β* and IL-10 levels were determined as described previously (Verri et al., 2010) by enzyme- linked immunosorbent assay (ELISA) according to manufacturer's instructions (eBioscience). The results were expressed as picograms (pg) of cytokine per 100 mg of tissue.

2.6. Determination of leukocytes in peripheral blood

Mice were treated with vehicles (saline i.pl., saline i.p., DMSO 2% in saline i.p. and/or Tris/HCl buffer i.p.), IL-1ra (100 pg/paw, 30 min before G-CSF or 30 mg/kg, i.p. 30 min

before G-CSF), etanercept (100 µg/paw, 1 h before G-CSF or 10 mg/kg, i.p., 48 and 1 h before G-CSF), morphine (6 µg/paw, 4h after G-CSF), thalidomide (45 mg/kg, i.p., 30 min before G-CSF), pentoxifylline (13.5 mg/kg i.p. 30 min before G-CSF) and indomethacin (5 mg/kg, i.p., 40 min before G-CSF) and received i.pl. injection G-CSF (100 ng/paw). Twenty four h after the administration of G-CSF, samples of blood were collected to evaluate total and differential cell counts. Total cell counts were performed in Neubauer chamber usign Turk solution, and differential cells counts (100 cells per slide) were performed in blood slides stained with panoptic kit (Laborclin Produtos para Laboratórios Ltda., Pinhais, PR, Brazil) under light microscope (Zeiss, Wetzlar, Germany). Results were expressed as total leukocytes, mononuclear cells and neutrophils (cells x 10^5/ml of blood).

2.7. Statistical analysis

Results are presented as means ± S.E.M. of measurements made on 6 mice per group per experiment. The experiments were performed twice. Two-way analysis of variance (ANOVA) was used to compare the groups and doses at all times (curves) when the hyperalgesic responses were measured at different times after the stimulus injection. The analyzed factors were treatments, time and time *versus* treatment interaction. When there was a significant time *versus* treatment interaction, one-way ANOVA followed by Tukey's t-test was performed for each time. On the other hand, when the hyperalgesic responses were measured once after the stimulus injection, the differences between responses were evaluated by one-way ANOVA followed by Tukey's t-test. Statistical differences were considered to be significant at $P < 0.05$.

3. Results

3.1. G-CSF-induced mechanical hyperalgesia depends on hyperalgesic TNFα/TNFR1 and IL-1β signaling pathway and is down-regulated by IL-10 in mice

Firstly, the effect of targeting TNFα, IL-1β and IL-10 action/production in the G-CSF-induced mechanical hyperalgesia was evaluated (Fig. 1). To achieve this aim G- CSF (100 ng/paw) was injected in mice treated with etanercept (10 mg/kg, i.p., 48 and 1 h before) (Fig. 1A), TNFR1$^{-/-}$ mice (Fig. 1B), IL-1ra treated mice (30 mg/kg, i.p., 30 min before) (Fig. 1C) and IL-10$^{-/-}$ mice (Fig. 1D). Intraplantar (i.pl.) injection of saline (25 µl) plus i.p. treatments with saline, etanercept and IL-1ra or TNFR1$^{-/-}$ and IL-10$^{-/-}$ mice were used as negative controls of G-CSF plus treatments/ genetic deficiency. Mechanical hyperalgesia was evaluated after 1-7 h after G-CSF injection (Fig. 1). G- CSF induced significant mechanical hyperalgesia 1-7 h after administration compared to the control groups (G-CSF vehicle, saline + i.p. treatments or G-CSF vehicle injection in deficient mice), reaching its peak at the 5th h (Fig. 1). The treatment with etanercept (Fig. 1A) or TNFR1 deficiency (Fig. 1B) inhibited G-CSF-induced mechanical hyperalgesia. The anti-hyperalgesic effect of etanercept (Fig. 1A) and TNFR1 deficiency (Fig. 1B) was significant between 1-7h after G-CSF administration. IL-1ra (Fig. 1C) treatment also inhibited G-CSF-induced mechanical hyperalgesia between 1-7h. On the other hand, G-CSF-induced mechanical hyperalgesia was significantly higher in IL-10$^{-/-}$ mice compared to WT group between 3-7 h, without differences at 1 h (Fig. 1D). These data demonstrate that TNFα acting on TNFR1 and IL-1β are involved in the

hyperalgesic mechanisms triggered by G-CSF while IL-10 has an anti- hyperalgesic endogenous role. **(Include Fig. 1 here).**

3.2. Local treatment with etanercept and IL-1ra reduced G-CSF-induced mechanical hyperalgesia in mice

Mice received local paw treatment with vehicle (saline), etanercept (1-100 µg, i.pl.) 1 h before, or IL-1ra (30-300 pg, i.pl.) 30 min before ipsilateral stimulus with G- CSF (Fig. 2). Mice that received i.pl. injection of saline, etanercept (100 µg/paw) or IL- 1ra (100 pg/paw) without G-CSF stimulus were used as control groups. G-CSF-induced mechanical hyperalgesia was dose-dependent inhibited by local paw treatment with etanercept (Fig. 2A) and IL-1ra (Fig. 2B). The doses of 1 and 10 µg/paw of etanercept did not affect G-CSF-induced hyperalgesia while 100 µg/paw of etanercept significantly inhibited G-CSF-induced mechanical hyperalgesia between 1-7h (Fig. 2A). The dose of 30 pg/paw of IL-1ra did not affect G-CSF-induced mechanical hyperalgesia and the doses of 100 and 300 pg/paw of IL-1ra inhibited G-CSF-induced mechanical hyperalgesia with similar profile between 1-7h (Fig. 2B). Thus, the doses of 100 µg/paw of etanercept and 100 pg/paw of IL-1ra were chosen for the next set of experiments. Treatment of contralateral paw with etanercept (Fig. 2C) and IL-1ra (Fig. 2D) did not affect G-CSF-induced mechanical hyperalgesia. These data demonstrate the participation of peripheral TNFα and IL-1β in G-CSF-induced mechanical hyperalgesia. **(Include Fig. 2 here).**

3.3. G-CSF injection induces the production of TNFα, IL-1β and IL-10 in the mice paw Mice received i.pl. injection of saline or G-CSF, and TNFα, IL-1β and IL-10

levels were determined 2 and 4 h after stimulus (Fig. 3). G-CSF induced significant TNFα, IL-1β and IL-10 production in the paw skin at 2 h (Fig. 3). Only IL-1β production was still at significantly increased levels at 4h (Fig. 3). Therefore, cytokine levels were determined at 2 h after G-CSF stimulus in the experiments presented at Fig. 5 and 6. These results indicate that G-CSF administration induces local production of TNFα, IL-1β and IL-10. **(Include Fig. 3 here).**

3.4. Thalidomide and pentoxifylline inhibited G-CSF-induced mechanical hyperalgesia in a dose-dependent manner in mice

Mice were treated with vehicle (DMSO 2% in saline, i.p.), thalidomide (5-45 mg/kg, i.p.) or pentoxifylline (0.5-13.5 mg/kg, i.p.) 30 min before i.pl. stimulus with G- CSF and mechanical hyperalgesia was evaluated 1-7 h after (Fig. 4). Negative control groups received i.pl. injection of saline combined with i.p. injection of the DMSO 2% in saline or the higher doses treatments used in the dose-response curves. The dose of 5 mg/kg of thalidomide inhibited G-CSF-induced mechanical hyperalgesia at 3 h only (Fig. 4A). The dose of 15 mg/kg of thalidomide inhibited G-CSF-induced mechanical hyperalgesia 3-7 h after G-CSF injection (Fig. 4A), and the dose of 45 mg/kg of thalidomide inhibited G-CSF-induced mechanical hyperalgesia 1-7 h with significant differences compared to the lower dose of thalidomide tested (5 mg/kg) at 5 and 7 h (Fig. 4A). The dose of 0.5 mg/kg of pentoxifylline did not affect G-CSF-induced mechanical hyperalgesia. On the other hand, pentoxifylline at the dose of 1.5 mg/kg inhibited G-CSF-induced mechanical hyperalgesia at 3 h only (Fig. 4B), and at the doses of 4.5 and 13.5 mg/kg of pentoxifylline inhibited significantly G-CSF-induced mechanical hyperalgesia between 3-7 h with significant differences compared to pentoxifylline at the dose of 0.5 mg/kg group at 7 h (Fig. 4B). Thus, the doses of 45 mg/kg of

thalidomide and 13.5 mg/kg of pentoxifylline were chosen for the next set of experiments on cytokine production. **(Include Fig. 4 here).**

3.5. Thalidomide and pentoxifylline inhibited G-CSF-induced TNFα, IL-1β and IL-10 production in the paw skin of mice

Mice were treated with thalidomide (45 mg/kg, i.p.) and pentoxifylline (13.5 mg/kg, i.p.) 30 min before receiving i.pl. injection of vehicle (saline) or G-CSF and after additional 2h, samples of paw skin were collected for TNFα, IL-1β and IL-10 dosage (Fig. 5). DMSO 2% in saline i.p. was injected in the negative (saline i.pl.) and positive (G-CSF i.pl.) control groups (vehicle was not indicated in the figure). In agreement with the results of Figs. 1-4, G-CSF increased the levels of these three cytokines and pretreatment with thalidomide and pentoxifylline significantly inhibited G-CSF induced TNFα and IL-1β production (Fig. 5). G-CSF-induced IL-10 production was diminished only by pentoxifylline (Fig. 5). **(Include Fig. 5 here).**

3.6. Combined treatment of morphine with thalidomide or pentoxifylline at doses that are ineffective as single treatment reduces G-CSF-induced mechanical hyperalgesia through inhibition of TNFα and IL-1β production

The capability of the combined treatment of the ineffective doses of morphine with thalidomide or pentoxifylline to induce analgesia at the peak (5^{th} h) of G-CSF- induced mechanical hyperalgesia was tested (Fig. 6). Only one time point of evaluation was selected because the analgesic effect of morphine at this protocol is limited to 1 h (Carvalho et al., 2011). Mice received the following single treatments: vehicle (saline, 25 µl/paw and DMSO 2% in saline, 200 µl, i.p.), morphine (2 µg/25 µl, i.pl., 4 h after in panel A and 1 h after in panels B and C), thalidomide (5 mg/kg, i.p., 30 min before), pentoxifylline (0.5 mg/kg, i.p., 30 min before), or co-treatment with morphine and thalidomide or pentoxifylline (same doses described above) at indicated time points before and after G-CSF stimulus. G-CSF induced significant mechanical hyperalgesia at 5 h after stimulus compared to the vehicle group (saline), which was unaffected by single treatment with morphine, thalidomide and pentoxifylline (Fig. 6A). On the other hand, the combined treatments of morphine with thalidomide or pentoxifylline that were ineffective as single treatment significantly inhibited G-CSF-induced mechanical hyperalgesia (Fig. 6A). In order to determine whether the analgesic effects of co- treatments with morphine and thalidomide or pentoxifylline act by inhibiting pro- inflammatory cytokine production, TNFα and IL-1β levels were evaluated at 2 h (peak of cytokine production, Fig. 3) (Figs. 6B and 6C). G-CSF induced significant production of TNFα and IL-1β compared to the vehicle group without alteration under single treatment with morphine, thalidomide and pentoxifylline. However, the combined treatments were effective in inhibiting G-CSF-induced TNFα (Fig. 6B) and IL-1β (Fig. 6C) production, indicating that the mechanism by which the co-treatments induce analgesia depends, at least in part, on targeting peripheral pro-inflammatory cytokine production induced by G-CSF stimulus. **(Include Fig. 6 here).**

3.7. Combined treatment of indomethacin with thalidomide or pentoxifylline at doses that are ineffective as single treatment reduces G-CSF-induced mechanical hyperalgesia

Opioids constitute the analgesic choice to control G-CSF-induced pain. However, non-narcotic analgesics can also be used to control G-CSF-induced pain in humans (Filgrastim package insert). In this sense, mice were treated with indomethacin (cyclooxygenase inhibitor,

0.5-5 mg/kg, i.p.), 40 min before i.pl. injection of vehicle (saline) or G-CSF and mechanical hyperalgesia was evaluated 1-7 h after (Fig. 7A). Negative control groups received i.pl. injection of saline combined with i.p. injection of indomethacin vehicle (Tris/HCl buffer) or the higher dose of indomethacin tested. The dose of 0.5 mg/kg of indomethacin did not affect G-CSF-induced mechanical hyperalgesia. On the other hand, indomethacin at the dose of 5 mg/kg inhibited G-CSF- induced mechanical hyperalgesia between 3-7 h (Fig. 7A). In the following experiment the possibility of inhibiting G-CSF-induced mechanical hyperalgesia was tested using the co-treatment with indomethacin and thalidomide or pentoxifylline at doses that were ineffective alone. Mice received the same treatments (vehicles, thalidomide and pentoxifylline at the same doses, times and routes) applied in the experiment shown at Fig. 6 replacing morphine by indomethacin (0.5 mg/kg, i.p., 40 min before as single dose) and its vehicle (Tris/HCl buffer), or indomethacin plus thalidomide or pentoxifylline (Fig. 7B). G-CSF stimulus induced significant mechanical hyperalgesia when compared to the vehicle group, which again was unaffected by single treatment with indomethacin, thalidomide and pentoxifylline as single treatments. On the other hand, co-treatment with indomethacin and thalidomide or pentoxifylline significantly inhibited G-CSF-induced mechanical hyperalgesia from 3-7 h (Fig. 7B). **(Include Fig. 7 here).**

3.8. Effect of analgesic treatments on G-CSF-induced peripheral blood neutrophil counts.

The major therapeutic use of G-CSF is the increase of circulating neutrophils (Lambertini et al., 2014), and according to the Filgrastim package insert, neutropenia could be reverted in a shorter period such as 24 h after intravenous (i.v.) or subcutaneous (s.c.) administration of G-CSF. Corroborating, we observed increase of neutrophil counts in the peripheral blood of mice 24 h, but not 7 h, after G-CSF administration (data not shown). Therefore, 24 h after G-CSF administration was selected to evaluate the effect of analgesic therapies on G-CSF-induced increase of peripheral blood neutrophil counts. Mice received i.pl. administration of saline or G- CSF (together with the vehicles described at Fig. 8) and total leukocytes, mononuclear cells and neutrophils counts were performed (Fig. 8). G-CSF induced a significant increase in total leukocytes (Fig. 8A), mononuclear cells (Fig. 8B) and neutrophils (Fig. 8C) compared to the saline i.pl. injection. In the neutrophil counts, G-CSF induced the presence of band cells, which were absent in vehicle treated group (data not shown). Mice were treated with IL-1ra (i.pl., 100 pg, 30 min before or i.p., 30 mg/kg, 30 min before), etanercept (i.pl., 100 µg, 1 h before or i.p., 10 mg/kg, 48 and 1 h before), morphine (i.pl., 6 µg/25 µl, 4 h after, Carvalho et al., 2011), thalidomide (i.p., 45 mg/kg, 30 min before), pentoxifylline (i.p., 13,5 mg/kg, 30 min before), indomethacin (i.p., 5 mg/kg, 40 min before) or the respective vehicles (saline i.p., saline i.pl., DMSO 2% in saline i.p. or Tris/HCl buffer i.p., respectively) as indicated and total leukocytes, mononuclear cells and neutrophils counts were determined (Fig. 8). Vehicles did not change G-CSF-induced increase of total leukocytes, mononuclear cells and neutrophil counts in the peripheral blood (Fig. 8). The i.p. treatment with IL-1ra significantly reduced total leukocytes, mononuclear cells and neutrophils counts (Fig 8). IL-1ra, etanercept and morphine at doses with local effect, and etanercept, thalidomide, pentoxifylline and indomethacin at doses with systemic effect did not affect G-CSF- induced increase of total leukocytes, mononuclear cells and neutrophils counts in peripheral blood. **(Include Fig. 8 here).**

4. Discussion

G-CSF is mainly used to increase neutrophil counts in peripheral blood of patients (Lambertini et al., 2014). The most prominent side effect of G-CSF therapy is pain (Battiwalla and McCarthy, 2009; Lambertini et al., 2014). We have previously reported that i.pl. injection of G-CSF is a conceivable model to study G-CSF-induced pain since it occurs at similar dose of G-CSF used in clinical settings and is amenable by morphine treatment as observed in clinical practice (Carvalho et al., 2011). The present study demonstrated that G-CSF-induced mechanical hyperalgesia depends on TNFα and IL-1β hyperalgesic effects while IL-10 presents an endogenous role to control G-CSF-induced mechanical hyperalgesia. In agreement, targeting TNFα and IL- 1β production with thalidomide and pentoxifylline reduced G-CSF-induced mechanical hyperalgesia. TNFα and IL-1β are hyperalgesic cytokines contributing to inflammatory, neuropathic and cancer pain (Cunha et al., 1992; Cunha et al., 2003; Ferreira et al., 1988; Liu et al., 2013; Schäfers et al., 2001; Schäfers et al., 2003; Uçeyler et al., 2009; Zelenka et al., 2005). G-CSF induces TNFα and IL-1β production in other systems not related to pain (Jiang et al., 2013; Schmidt et al., 1999). G-CSF-induced mechanical hyperalgesia was inhibited in TNFR1$^{-/-}$ mice, and by systemic and local treatment with etanercept (a soluble TNF receptor 2) and IL-1ra (IL-1 receptor antagonist), which lined up well with the early G-CSF-induced production of TNFα and IL-1β in the paw skin. These results are not completely expected since G-CSF reduced lipopolysaccharide from gram-negative bacteria (LPS)-induced production of TNFα and IL-1β in human whole blood by translational silencing of LPS-induced TNFα mRNA and inhibiting caspase-1 activation and consequent IL-1β release, respectively (Boneberg & Hartung, 2002). IL-10 is an anti-hyperalgesic cytokine in inflammatory, neuropathic and cancer pain (Kim et al., 2011; Milligan et al., 2005; Poole et al., 1995; Shimizu et al., 2009; Wang et al., 2012). IL-10$^{-/-}$ mice presented enhanced G-CSF-induced mechanical hyperalgesia evidencing the endogenous role of IL-10 as an anti-hyperalgesic cytokine. The anti-hyperalgesic activity of IL-10 has been attributed to inhibition of TNFα and IL-1β production (Akdis et al., 2011; Donnelly et al., 1999; Inoue et al., 2014; Poole et al., 1995) by a mechanism related to the augmented expression of the suppressor of cytokine signaling-1 and -3 genes resulting in reduced cytokine signaling and immune response (Akdis et al., 2011; Donnelly et al., 1999). Cytokine production can be inhibited by drugs such as thalidomide and pentoxifylline, which induce TNFα mRNA degradation (Moreira et al., 1993; Ribeiro et al., 2000) and inhibit TNFα mRNA expression (Verri et al., 2006), respectively. There is also evidence that thalidomide and pentoxifylline inhibit the production of other cytokines such as IL-1β, and that pentoxifylline induce IL-10 production (van Furth et al., 1997; Amirshahrokhi & Ghazi-Khansari, 2012; Amirshahrokhi, 2013; Marcinkiewicz et al., 2000; Ribeiro et al., 2000; Melo et al., 2008; Vale et al., 2004; Wei et al., 2009). The analgesic effects of thalidomide and pentoxifylline have been shown (Cata et al., 2008; Chauhan et al., 2012; Dorazil-Dudzik et al., 2004; Gu et al., 2010; Ribeiro et al., 2000; Vale et al., 2004; Wei et al., 2009), and their lower cost compared to biological therapies associated to known pharmacology, pharmacokinetics and toxicology, suggest their potential therapeutic applicability (Verri et al., 2006). Herein, thalidomide and pentoxifylline inhibited the G-CSF-induced mechanical hyperalgesia and TNFα and IL-1β production, and pentoxifylline also inhibited IL-10 production indicating that their analgesic effect depends on inhibition of hyperalgesic cytokine production rather than inducing anti-hyperalgesic IL-10 production. Morphine combined with thalidomide or pentoxifylline at ineffectively analgesic doses as single treatment reduced G-CSF-induced mechanical hyperalgesia suggesting that these combinations may be useful to reduce the dose of opioid required to control G-CSF-induced pain. Others have observed similar synergy with these drugs. For instance, thalidomide synergizes with morphine to reduce spinal nerve injury-induced neuropathic pain in rats (Lee

et al., 2013). Pentoxifylline potentiated the anti-allodynia and anti-hyperalgesic effects of morphine in chronic constriction injury in rats (Mika et al., 2007) and pentoxifylline also attenuates morphine tolerance in naïve and neuropathic mice (Mika et al., 2009). Importantly, patients that received pentoxifylline presented longer patient-controlled analgesia, faster return of bowel function and consumed less morphine (Lu et al., 2004; Wordliczek et al., 2000). Co-treatment with morphine and thalidomide or pentoxifylline inhibited G-CSF-induced TNFα and IL-1β production indicating a contributing mechanism to this synergy. Therefore, together with our data, the literature suggests that combining morphine with thalidomide or pentoxifylline is a promising therapeutic approach to achieve better analgesic profile and reduce morphine tolerance, side effects and intake (Lee et al., 2013; Lu et al., 2004; Mika et al., 2007; Mika et al., 2009; Wordliczek et al., 2000). Indomethacin (cyclooxygenase inhibitor) inhibited G-CSF-induced mechanical hyperalgesia, and combined treatment with indomethacin and thalidomide or pentoxifylline at ineffective doses as single treatment also reduced G-CSF-induced hyperalgesia. These data corroborate evidence that TNFα and IL-1β induce peripheral mechanical hyperalgesia by triggering prostaglandin production (Verri et al., 2006) and non-narcotic drugs reduce G-CSF-induced pain in humans (Filgrastim package insert). Indomethacin also increases G-CSF-induced differentiation of human promyelocytic leukemia cells (HL60) towards neutrophils (Bunce et al., 1994), suggesting it would eventually contribute to increase neutrophil counts. The mechanism by which G-CSF induces mechanical hyperalgesia also involves spinal activation of PI3K and MAP kinases p38 kinase, c-Jun N-terminal kinase (JNK), and extracellular signal-regulated kinase (ERK) in a synergic/ sequential way (Carvalho et al., 2011). These mechanisms are also endogenously activated by G-CSF in cancer pain (Schweizerhof et al., 2009). The activation of these kinases leads to increases in proinflammatory cytokine production, including TNFα and IL-1β, and may also modulate ion channels, and sensitize nociceptors inducing hyperalgesia (Gao & Ji, 2010; Ji & Strichartz, 2004). On the other hand, this kinase cascade-dependent spinal hyperalgesic mechanism of G-CSF might be a result of peripheral production of cytokines such as TNFα and IL-1β as well as peripheral cytokines induce further cytokine production in the dorsal root ganglia and spinal cord. For instance, peripheral injection of TNFα and IL-1β, or their endogenous production upon injury of peripheral nervous system or inflammatory stimulus induces mechanical hyperalgesia with kinase activation in the spinal cord and dorsal root ganglia (Binshtok et al., 2008; Eijkelkamp et al., 2010; Gaultier et al., 2008; Morell et al., 2013; Willemen et al., 2010). In agreement, G-CSF-induced mechanical hyperalgesia was also inhibited by local paw treatment with etanercept and IL-1ra. Nociceptive neurons express G-CSF receptor indicating possible direct neuronal effect of G-CSF. In fact, there is evidence that G- CSF sensitizes nociceptors (Schweizerhof et al., 2009). Herein, G-CSF-induced mechanical hyperalgesia was dependent on local production/action of TNF-α and IL-1β, which supports the notion that G-CSF also induces peripheral nociceptor sensitization dependent on further production of hyperalgesic molecules. Because increasing neutrophil counts in peripheral blood is the primary therapeutic use of G-CSF (Filgrastim package insert), whether the analgesic approaches proposed in the present study affect the neutrophil counts in peripheral blood should be determined. IL-1ra, but not etanercept, at a dose with systemic effect reduced the G- CSF-induced increase of neutrophil counts in peripheral blood, indicating this G-CSF therapeutic effect depends on systemic IL-1 action. A possible explanation for this pronounced role of IL-1 in G-CSF therapy is that IL-1α and IL-1β do not trigger a robust activation of neutrophils, but rather prolong neutrophil survival (Futosi et al., 2013). On the other hand, TNFα is more related to neutrophil activation, priming and apoptosis, thus, inhibiting TNFα would increase the number of neutrophils (Futosi et al., 2013). Nevertheless, IL-1ra and etanercept at doses with local effect did not change the output of neutrophils from bone marrow indicating that G-

CSF-induced local inflammatory reaction is not of importance to its recruitment of neutrophil from the bone marrow to peripheral blood. IL-1ra, etanercept and morphine at locally acting doses, and etanercept, thalidomide, pentoxifylline and indomethacin at systemic doses are analgesic approaches of potential usefulness in G-CSF-induced hyperalgesia because did not affect G-CSF-induced increase of neutrophil counts in peripheral blood. Interestingly, thalidomide and pentoxifylline reduced G-CSF-induced IL-1β production without affecting the recruitment of bone marrow neutrophils, which is in apparent contradiction to the inhibition of neutrophil counts observed with systemic IL-1ra treatment. However, thalidomine and pentoxifylline partially inhibited G-CSF-induced paw skin IL-1β production while systemic IL-1ra abolished G-CSF-induced recruitment of bone marrow neutrophils. Thus, IL-1β seems to have a more pronounced role in G-CSF- induced recruitment of bone marrow neutrophils compared to its hyperalgesic effect, and the G-CSF-induced hyperalgesia depends on IL-1β and TNFα while TNFα does not have a role in G-CSF-induced bone marrow neutrophil recruitment. Moreover, thalidomide and pentoxifylline have additional mechanisms of action. For instance, thalidomide interacts with protein kinase C (PKC) to modulate chemoattraction (Meierhofer et al., 1999), and inhibits adhesion molecules expression (Settles et al., 2001), and inhibitor of kappa B (IκB) kinase (IKK) activation (Keifer et al., 2001). Pentoxifylline is a competitive nonselective phosphodiesterase inhibitor, which increases intracellular cyclic adenosine monophosphate (cAMP) levels resulting in inhibition of nuclear factor kappa B (NFκB) and nuclear factor of activated T-cells (NFAT) activation (Essayan, 2001; Ribeiro de Jesus et al., 2008), inhibits transforming growth factor-beta (TGFβ)/Smad signaling (Ng et al., 2009) and antioxidant (Vircheva et al., 2010). These mechanisms may contribute to their analgesic effect in addition to reduce TNFα and IL-1β production.

5. Conclusion

The present study demonstrates that TNFα, IL-1β and IL-10 have key roles in G- CSF-induced mechanical hyperalgesia in mice. TNFα and IL-1β mediate the pro- hyperalgesic effect of G-CSF and IL-10 has an endogenous role to limit G-CSF hyperalgesia. Systemic IL-1 seems to have a major role in G-CSF-induced recruitment of neutrophils from the bone marrow to peripheral blood, thus, targeting IL-1 will reduce G-CSF therapeutic effect. Targeting TNFα and IL-1β using biological therapies at locally acting doses, and TNFα at systemic doses can inhibit G-CSF-induced mechanical hyperalgesia without affecting the increased peripheral blood neutrophil counts. In addition to biological therapies, targeting TNFα and IL-1β with thalidomide and pentoxifylline are conceivable therapeutic approaches to control G-CSF-induced mechanical hyperalgesia and to reduce the morphine usage. The inhibition of cyclooxygenase represented by indomethacin is also a conceivable analgesic approach, which can be used in combination with thalidomide and pentoxifylline.

Acknowledgments

This work received financial support from Fundo de Apoio ao Ensino Pesquisa e Extensão/Universidade Estadual de Londrina (FAEPE/UEL 01/2009), Coordenação de Aperfeiçoamento de Pessoal de Nível Superior (CAPES), Fundação de Amparo à Pesquisa do Estado de São Paulo (FAPESP), Conselho Nacional de Desenvolvimento Científico e Tecnológico (CNPq), Ministério da Ciência, Tecnologia e Inovação (MCTI), Secretaria da Ciência, Tecnologia e Ensino Superior (SETI), Fundação Araucária and Governo do Estado do Paraná. The authors declare no conflicts of interest.

References

Akdis, M., Burgler, S., Crameri, R., Eiwegger, T., Fujita, H., Gomez, E., Klunker, S., Meyer, N., O'Mahony, L., Palomares, O., Rhyner, C., Ouaked, N., Schaffartzik, A., Van De Veen, W., Zeller, S., Zimmermann, M., Akdis, C.A., 2011. Interleukins, from 1 to 37, and interferon-γ: receptors, functions, and roles in diseases. J. Allergy Clin. Immunol. 127, 701-721.e1-70.

Amirshahrokhi, K., Ghazi-Khansari, M., 2012. Thalidomide attenuates multiple low- dose streptozotocin-induced diabetes in mice by inhibition of proinflammatory cytokines. Cytokine. 60, 522-527.

Battiwalla, M., McCarthy, P.L., 2009. Filgrastim support in allogeneic HSCT for myeloid malignancies: a review of the role of G-CSF and the implications for current practice. Bone Marrow Transplant. 43, 351-356.

Amirshahrokhi, K., 2013. Anti-inflammatory effect of thalidomide in paraquat-induced pulmonary injury in mice. Int. Immunopharmacol. 17, 210-215.

Bien, E., Krawczyk, M., Izycka-Swieszewska, E., Trzonkowski, P., Kazanowska, B., Adamkiewicz-Drozynska, E., Balcerska, A., 2013. Serum IL-10 and IL-12 levels reflect the response to chemotherapy but are influenced by G-CSF therapy and sepsis in children with soft tissue sarcomas. Postepy Hig. Med. Dosw. 67, 517-528.

Binshtok, A.M., Wang, H., Zimmermann, K., Amaya, F., Vardeh, D., Shi, L., Brenner, G.J., Ji, R.R., Bean, B.P., Woolf, C.J., Samad, T.A., 2008. Nociceptors are interleukin- 1beta sensors. J. Neurosci. 28, 14062-14073.

Borghi, S.M., Zarpelon, A.C., Pinho-Ribeiro, F.A., Cardoso, R.D., Martins-Pinge, M.C., Tatakihara, R.I., Cunha, T.M., Ferreira, S.H., Cunha, F.Q., Casagrande, R., Verri, W.A. Jr, 2014a. Role of TNF-α/TNFR1 in intense acute swimming-induced delayed onset muscle soreness in mice. Physiol. Behav. 128, 277-287.

Borghi, S.M., Zarpelon, A.C., Pinho-Ribeiro, F.A., Cardoso, R.D., Cunha, T.M., Alves- Filho, J.C., Ferreira, S.H., Cunha, F.Q., Casagrande, R., Verri, W.A. Jr, 2014b. Targeting interleukin-1β reduces intense acute swimming-induced muscle mechanical hyperalgesia in mice. J. Pharm. Pharmacol. 66, 1009-1020.

Boneberg, E.M., Hartung, T., 2002. Granulocyte colony-stimulating factor attenuates LPS-stimulated IL-1beta release via suppressed processing of proIL-1beta, whereas TNF-alpha release is inhibited on the level of proTNF-alpha formation. Eur. J. Immunol. 32, 1717-1725.

Breitkreutz, I., Anderson, K.C., 2008. Thalidomide in multiple myeloma--clinical trials and aspects of drug metabolism and toxicity. Expert Opin. Drug Metab. Toxicol. 4, 973- 985.

Bunce, C.M., French, P.J., Durham, J., Stockley, R.A., Michell, R.H., Brown, G., 1994. Indomethacin potentiates the induction of HL60 differentiation to neutrophils, by retinoic acid and granulocyte colony-stimulating factor, and to monocytes, by vitamin D3. Leukemia. 8, 595-604.

Calil, I.L., Zarpelon, A.C., Guerrero, A.T., Alves-Filho, J.C., Ferreira, S.H., Cunha, F.Q., Cunha, T.M., Verri, W.A. Jr, 2014. Lipopolysaccharide induces inflammatory hyperalgesia triggering a TLR4/MyD88-dependent cytokine cascade in the mice paw. PLoS One. 9, e90013.

Carvalho, T.T., Flauzino, T., Otaguiri, E.S., Batistela, A.P., Zarpelon, A.C., Cunha, T.M., Ferreira, S.H., Cunha, F.Q., Verri, W.A. Jr, 2011. Granulocyte-colony stimulating factor (G-CSF) induces mechanical hyperalgesia via spinal activation of MAP kinases and PI3K in mice. Pharmacol. Biochem. Behav. 98, 188-195.

Cata, J.P., Weng, H.R., Dougherty, P.M., 2008. The effects of thalidomide and minocycline on taxol-induced hyperalgesia in rats. Brain Res. 1229, 100-110.

Chauhan, N., Taliyan, R., Sharma, P.L., 2012. Effect of dipyrone and thalidomide alone and in combination on STZ-induced diabetic neuropathic pain. Naunyn Schmiedebergs Arch. Pharmacol. 385, 527-538.

Cunha, F.Q., Poole, S., Lorenzetti, B.B., Ferreira, S.H., 1992. The pivotal role of tumour necrosis factor alpha in the development of inflammatory hyperalgesia. Br. J. Pharmacol. 107, 660-664.

Cunha, J.M., Cunha, F.Q., Poole, S., Ferreira, S.H., 2003. Cytokine-mediated inflammatory hyperalgesia limited by interleukin-1 receptor antagonist. Br. J. Pharmacol. 130, 1418-1424.

Cunha, T.M., Verri, W.A. Jr, Vivancos, G.G., Moreira, I.F., Reis, S., Parada, C.A., Cunha, F.Q., Ferreira, S.H., 2004. An electronic pressure-meter nociception paw test for mice. Braz. J. Med. Biol. Res. 37, 401-407.

Dale, D.C., Bonilla, M.A., Davis, M.W., Nakanishi, A.M., Hammond, W.P., Kurtzberg, J., Wang, W., Jakubowski, A., Winton, E., Lalezari, P., Robinson, W., Glaspy, J.A., Emerson, S., Gabrilove, J., Vincent, M., Boxer, L.A., 1993. A randomized controlled phase III trial of recombinant human granulocyte colony-stimulating factor (filgrastim) for treatment of severe chronic neutropenia. Blood. 81, 2496-2502.

Devulder, J., Jacobs, A., Richarz, U., Wiggett, H., 2009. Impact of opioid rescue medication for breakthrough pain on the efficacy and tolerability of long-acting opioids in patients with chronic non-malignant pain. Br. J. Anaesth. 103, 576-585.

Donnelly, R.P., Dickensheets, H., Finbloom, D.S., 1999. The interleukin-10 signal transduction pathway and regulation of gene expression in mononuclear phagocytes. J. Interferon Cytokine Res. 19, 563-573.

Dorazil-Dudzik, M., Mika, J., Schafer, M.K., Li, Y., Obara, I., Wordliczek, J., Przewłocka, B., 2004. The effects of local pentoxifylline and propentofylline treatment on formalin-induced pain and tumor necrosis factor-alpha messenger RNA levels in the inflamed tissue of the rat paw. Anesth. Analg. 98, 1566-1573.

Eijkelkamp, N., Heijnen, C.J., Willemen, H.L., Deumens, R., Joosten, E.A., Kleibeuker, W., den Hartog, I.J., van Velthoven, C.T., Nijboer, C., Nassar, M.A., Dorn, G.W. 2nd, Wood,

J.N., Kavelaars, A., 2010. GRK2: a novel cell-specific regulator of severity and duration of inflammatory pain. J. Neurosci. 30, 2138-2149.

Essayan, D.M., 2001. Cyclic nucleotide phosphodiesterases. J. Allergy Clin. Immunol. 108, 671-680.

Ferreira, S.H., Lorenzetti, B.B., Bristow, A.F., Poole, S., 1988. Interleukin-1 beta as a potent hyperalgesic agent antagonized by a tripeptide analogue. Nature. 334, 698-700.

Filgrastim Package Insert Kirin-Amgen, Thousand Oaks, CA, 2010. 21, 1-28.

Futosi, K., Fodor, S., Mócsai, A., 2013. Neutrophil cell surface receptors and their intracellular signal transduction pathways. Int. Immunopharmacol. 17, 638-650.

Gao, Y.J., Ji, R.R., 2010. Chemokines, neuronal–glial interactions, and central processing of neuropathic pain. Pharmacol. Ther. 126, 56-68.

Gaultier, A., Arandjelovic, S., Li, X., Janes, J., Dragojlovic, N., Zhou, G.P., Dolkas, J., Myers, R.R., Gonias, S.L., Campana, W.M., 2008. A shed form of LDL receptor- related protein-1 regulates peripheral nerve injury and neuropathic pain in rodents. J. Clin. Invest. 118, 161-172.

Gu, X., Zheng, Y., Ren, B., Zhang, R., Mei, F., Zhang, J., Ma, Z., 2010. Intraperitoneal injection of thalidomide attenuates bone cancer pain and decreases spinal tumor necrosis factor-α expression in a mouse model. Mol. Pain. 6, 64.

Inoue, M., Arikawa, T., Chen, Y.H., Moriwaki, Y., Price, M., Brown, M., Perfect, J.R., Shinohara, M.L., 2014. T cells down-regulate macrophage TNF production by IRAK1-mediated IL-10 expression and control innate hyperinflammation. Proc. Natl. Acad. Sci. U S A. 111, 5295-5300.

Ji, R.R., Strichartz, G., 2004. Cell Signaling and the Genesis of Neuropathic Pain. Sci. STKE. 252, re14.

Jiang, H.M., Wang, H.X., Yang, H., Zeng, X.J., Tang, C.S., Du, J., Li, H.H., 2013. Role for granulocyte colony stimulating factor in angiotensin II-induced neutrophil recruitment and cardiac fibrosis in mice. Am. J. Hypertens. 26, 1224-1233.

Keifer, J.A., Guttridge, D.C., Ashburner, B.P., Baldwin, A.S. Jr, 2001. Inhibition of NF-kappa B activity by thalidomide through suppression of IkappaB kinase activity. J. Biol. Chem. 276, 22382-22387.

Kim, W.M., Jeong, C.W., Lee, S.H., Kim, Y.O., Cui, J.H., Yoon, M.H., 2011. The intrathecally administered kappa-2 opioid agonist GR89696 and interleukin-10 attenuate bone cancer-induced pain through synergistic interaction. Anesth. Analg. 113, 934-940.

Lambertini, M., Del Mastro, L., Bellodi, A., Pronzato, P., 2014. The five "Ws" for bone pain due to the administration of granulocyte-colony stimulating factors (G-CSFs). Crit. Rev. Oncol. Hematol. 89, 112-128.

Lee, H.G., Kim, W.M., Yoon, M.H., Park, A.R., Choi, J.I., 2013. Synergistic anti- allodynic effect between intraperitoneal thalidomide and morphine on rat spinal nerve ligation-induced neuropathic pain. Korean J. Anesthesiol. 65, 331-336.

Liu, S., Liu, Y.P., Song, W.B., Song, X.J., 2013. EphrinB-EphB receptor signaling contributes to bone cancer pain via Toll-like receptor and proinflammatory cytokines in rat spinal cord. Pain. 154, 2823-2835.

Lu, C.H., Chao, P.C., Borel, C.O., Yang, C.P., Yeh, C.C., Wong, C.S., Wu, C.T., 2004. Preincisional intravenous pentoxifylline attenuating perioperative cytokine response, reducing morphine consumption, and improving recovery of bowel function in patients undergoing colorectal cancer surgery. Anesth. Analg. 99, 1465-1471.

Majumder, S., Sreedhara, S.R., Banerjee, S., Chatterjee, S., 2012. TNF-α signaling beholds thalidomide saga: a review of mechanistic role of TNF-α signaling under thalidomide. Curr. Top. Med. Chem. 12, 1456-1467.

Marcinkiewicz, J., Grabowska, A., Lauterbach, R., Bobek, M., 2000. Differential effects of pentoxifylline, a non-specific phosphodiesterase inhibitor, on the production of IL- 10, IL-12 p40 and p35 subunits by murine peritoneal macrophages. Immunopharmacology. 49, 335-343.

Meierhofer, C., Dunzendorfer, S., Wiedermann, C.J., 1999. Protein kinase C-dependent effects on leukocyte migration of thalidomide. J. Infect. Dis. 180, 216-219.

Melo, M.L., Brito, G.A., Soares, R.C., Carvalho, S.B., Silva, J.V., Soares, P.M., Vale, M.L., Souza, M.H., Cunha, F.Q., Ribeiro, R.A., 2008. Role of cytokines (TNF-alpha, IL-1beta and KC) in the pathogenesis of CPT-11-induced intestinal mucositis in mice: effect of pentoxifylline and thalidomide. Cancer Chemother. Pharmacol. 61, 775-784.

Mika, J., Osikowicz, M., Makuch, W., Przewlocka, B., 2007. Minocycline and pentoxifylline attenuate allodynia and hyperalgesia and potentiate the effects of morphine in rat and mouse models of neuropathic pain. Eur. J. Pharmacol. 560, 142- 149.

Mika, J., Wawrzczak-Bargiela, A., Osikowicz, M., Makuch, W., Przewlocka, B., 2009. Attenuation of morphine tolerance by minocycline and pentoxifylline in naive and neuropathic mice. Brain Behav. Immun. 23, 75-84.

Milligan, E.D., Sloane, E.M., Langer, S.J., Cruz, P.E., Chacur, M., Spataro, L., Wieseler-Frank, J., Hammack, S.E., Maier, S.F., Flotte, T.R., Forsayeth, J.R., Leinwand, L.A., Chavez, R., Watkins, L.R., 2005. Controlling neuropathic pain by adeno-associated virus driven production of the anti-inflammatory cytokine, interleukin- 10. Mol. Pain. 1, 9.

Moreira, A.L., Sampaio, E.P., Zmuidzinas, A., Frindt, P., Smith, K.A., Kaplan, G., 1993. Thalidomide exerts its inhibitory action on tumor necrosis factor alpha by enhancing mRNA degradation. J. Exp. Med. 177, 1675-1680.

Morell, M., Souza-Moreira, L., Caro, M., O'Valle, F., Forte-Lago, I., de Lecea, L., Gonzalez-Rey, E., Delgado, M., 2013. Analgesic effect of the neuropeptide cortistatin in murine models of arthritic inflammatory pain. Arthritis Rheum. 65, 1390- 1401.

Murdaca, G., Spanò, F., Contatore, M., Guastalla, A., Magnani, O., Puppo, F., 2014. Efficacy and safety of etanercept in chronic immune-mediated disease. Expert Opin. Drug Saf. 13, 649-661.

Ng, Y.Y., Chen, Y.M., Tsai, T.J., Lan, X.R., Yang, W.C., Lan, H.Y., 2009. Pentoxifylline inhibits transforming growth factor-beta signaling and renal fibrosis in experimental crescentic glomerulonephritis in rats. Am. J. Nephrol. 29, 43-53.

Niu, X., He, D., Deng, S., Li, W., Xi, Y., Xie, C., Jiang, T., Zhang, J.Z., Dong, C., Chen, G., 2011. Regulatory immune responses induced by IL-1 receptor antagonist in rheumatoid arthritis. Mol. Immunol. 49, 290-296.

Obata, K., Yamanaka, H., Dai, Y., Mizushima, T., Fukuoka, T., Tokunaga, A., Noguchi, K., 2004. Differential activation of MAPK in injured and uninjured DRG neurons following chronic constriction injury of the sciatic nerve in rats. Eur. J. Neurosci. 20, 2881-2895.

Pezet, S., Marchand, F., D'Mello, R., Grist, J., Clark, A.K., Malcangio, M., Dickenson, A.H., Williams, R.J., McMahon, S.B., 2008. Phosphatidylinositol 3-kinase is a key mediator of central sensitization in painful inflammatory conditions. J. Neurosci. 28, 4261-4270.

Poh, K.W., Yeo, J.F., Ong, W.Y., 2011. MicroRNA changes in the mouse prefrontal cortex after inflammatory pain. Eur. J. Pain. 15, 801-812.

Poole, S., Cunha, F.Q., Selkirk, S., Lorenzetti, B.B., Ferreira, S.H., 1995. Cytokine- mediated inflammatory hyperalgesia limited by interleukin-10. Br. J. Pharmacol. 115, 684-688.

Putinatti, M.S., Lastória, J.C., Padovani, C.R., 2014. Prevention of repeated episodes of type 2 reaction of leprosy with the use of thalidomide 100 mg/day. An. Bras. Dermatol. 89, 266-272.

Ribeiro, R.A., Vale, M.L., Ferreira, S.H., Cunha, F.Q., 2000. Analgesic effect of thalidomide on inflammatory pain. Eur. J. Pharmacol. 391, 97-103.

Ribeiro de Jesus, A., Luna, T., Pacheco de Almeida, R., Machado, P.R., Carvalho, E.M., 2008. Pentoxifylline down modulate in vitro T cell responses and attenuate pathology in Leishmania and HTLV-I infections. Int. Immunopharmacol. 8, 1344-1353.

Santjohanser, C., Knieper, C., Franz, C., Hirv, K., Meri, O., Schleyer, M., Würfel, W., Toth, B., 2013. Granulocyte-colony stimulating factor as treatment option in patients with recurrent miscarriage. Arch. Immunol. Ther. Exp. (Warsz). 61, 159-164.

Schäfers, M., Brinkhoff, J., Neukirchen, S., Marziniak, M., Sommer, C., 2001. Combined epineurial therapy with neutralizing antibodies to tumor necrosis factor-alpha and interleukin-1 receptor has an additive effect in reducing neuropathic pain in mice. Neurosci. Lett. 310, 113-116.

Schäfers, M., Sorkin, L.S., Sommer, C., 2003. Intramuscular injection of tumor necrosis factor-alpha induces muscle hyperalgesia in rats. Pain. 104, 579-588.

Schmidt, H., Stuertz, K., Brück, W., Chen, V., Stringaris, A.K., Fischer, F.R., Nau, R.,1999. Intravenous granulocyte colony-stimulating factor increases the release of tumour necrosis

factor and interleukin-1beta into the cerebrospinal fluid, but does not inhibit the growth of Streptococcus pneumoniae in experimental meningitis. Scand. J. Immunol. 49, 481-486.

Schweizerhof, M., Stosser, S., Kurejova, M., Njoo, C., Gangadharan, V., Agarwal, N., Schmelz, M., Bali, K.K., Michalski, C.W., Brugger, S., Dickenson, A., Simone, D.A., Kuner, R., 2009. Hematopoietic colony–stimulating factors mediate tumor-nerve interactions and bone cancer pain. Nat. Med. 15, 802-807.

Settles, B., Stevenson, A., Wilson, K., Mack, C., Ezell, T., Davis, M.F., Taylor, L.D., 2001. Down-regulation of cell adhesion molecules LFA-1 and ICAM-1 after in vitro treatment with the anti-TNF-alpha agent thalidomide. Cell Mol. Biol. (Noisy-le-grand). 47, 1105-1114.

Shimizu, K., Guo, W., Wang, H., Zou, S., LaGraize, S.C., Iwata, K., Wei, F., Dubner, R., Ren, K., 2009. Differential involvement of trigeminal transition zone and laminated subnucleus caudalis in orofacial deep and cutaneous hyperalgesia: the effects of interleukin-10 and glial inhibitors. Mol. Pain. 5, 75.

Svensson, C.I., Marsala, M., Westerlund, A., Calcutt, N.A., Campana, W.M., Freshwater, J.D., Catalano, R., Feng, Y., Protter, A.A., Scott, B., Yaksh, T.L., 2003. Activation of p38 mitogen-activated protein kinase in spinal microglia is a critical link in inflammation-induced spinal pain processing. J. Neurochem. 86, 1534-1544.

Uçeyler, N., Schäfers, M., Sommer, C., 2009. Mode of action of cytokines on nociceptive neurons. Exp. Brain Res. 196, 67-78.

Vale, M.L., Benevides, V.M., Sachs, D., Brito, G.A., da Rocha, F.A., Poole, S., Ferreira, S.H., Cunha, F.Q., Ribeiro, R.A., 2004. Antihyperalgesic effect of pentoxifylline on experimental inflammatory pain. Br. J. Pharmacol. 143, 833-844.

van Furth, A.M., Verhard-Seijmonsbergen, E.M., van Furth, R., Langermans, J.A., 1997. Effects of lisofylline and pentoxifylline on the bacterial-stimulated production of TNF-alpha, IL-1beta and IL-10 by human leukocytes. Immunology. 91, 193-196.

Verri, W.A. Jr, Cunha, T.M., Parada, C.A., Poole, S., Cunha, F.Q., Ferreira, S.H., 2006. Hypernociceptive role of cytokines and chemokines: targets for analgesic drug development? Pharmacol. Ther. 112, 116-138.

Verri, W.A. Jr, Souto, F.O., Vieira, S.M., Almeida, S.C., Fukada, S.Y., Xu, D., Alves- Filho, J.C., Cunha, T.M., Guerrero, A.T., Mattos-Guimaraes, R.B., Oliveira, F.R., Teixeira, M.M., Silva, J.S., McInnes, I.B., Ferreira, S.H., Louzada-Junior, P., Liew, F.Y., Cunha, F.Q., 2010. IL-33 induces neutrophil migration in rheumatoid arthritis and is a target of anti-TNF therapy. Ann. Rheum. Dis. 69, 1697-1703.

Vircheva, S., Alexandrova, A., Georgieva, A., Mateeva, P., Zamfirova, R., Kubera, M., Kirkova, M., 2010. In vivo effects of pentoxifylline on enzyme and non-enzyme antioxidant levels in rat liver after carrageenan-induced paw inflammation. Cell Biochem. Funct. 28, 668-672.

Wang, Z.H., Zeng, X.Y., Han, S.P., Fan, G.X., Wang, J.Y., 2012. Interleukin-10 of red nucleus plays anti-allodynia effect in neuropathic pain rats with spared nerve injury. Neurochem. Res. 37, 1811-1819.

Wei, T., Sabsovich, I., Guo, T.Z., Shi, X., Zhao, R., Li, W., Geis, C., Sommer, C., Kingery, W.S., Clark, D.J., 2009. Pentoxifylline attenuates nociceptive sensitization and cytokine expression in a tibia fracture rat model of complex regional pain syndrome. Eur. J. Pain. 13, 253-262.

Willemen, H.L., Eijkelkamp, N., Wang, H., Dantzer, R., Dorn, G.W. 2nd, Kelley, K.W., Heijnen, C.J., Kavelaars, A., 2010. Microglial/macrophage GRK2 determines duration of peripheral IL-1beta-induced hyperalgesia: contribution of spinal cord CX3CR1, p38 and IL-1 signaling. Pain. 150, 550-560.

Wordliczek, J., Szczepanik, A.M., Banach, M., Turchan, J., Zembala, M., Siedlar, M., Przewlocki, R., Serednicki, W., Przewlocka, B., 2000. The effect of pentoxifiline on post-injury hyperalgesia in rats and postoperative pain in patients. Life Sci. 66, 1155- 1164.

Xu, J.T., Tu, H.Y., Xin, W.J., Liu, X.G., Zhang, G.H., Zhai, C.H., 2007. Activation of phosphatidylinositol 3-kinase and protein kinase B/Akt in dorsal root ganglia and spinal cord contributes to the neuropathic pain induced by spinal nerve ligation in rats. Exp. Neurol. 206, 269-279.

Zelenka, M., Schäfers, M., Sommer, C., 2005. Intraneural injection of interleukin-1beta and tumor necrosis factor-alpha into rat sciatic nerve at physiological doses induces signs of neuropathic pain. Pain. 116, 257-263.

Figures

Fig. 1.

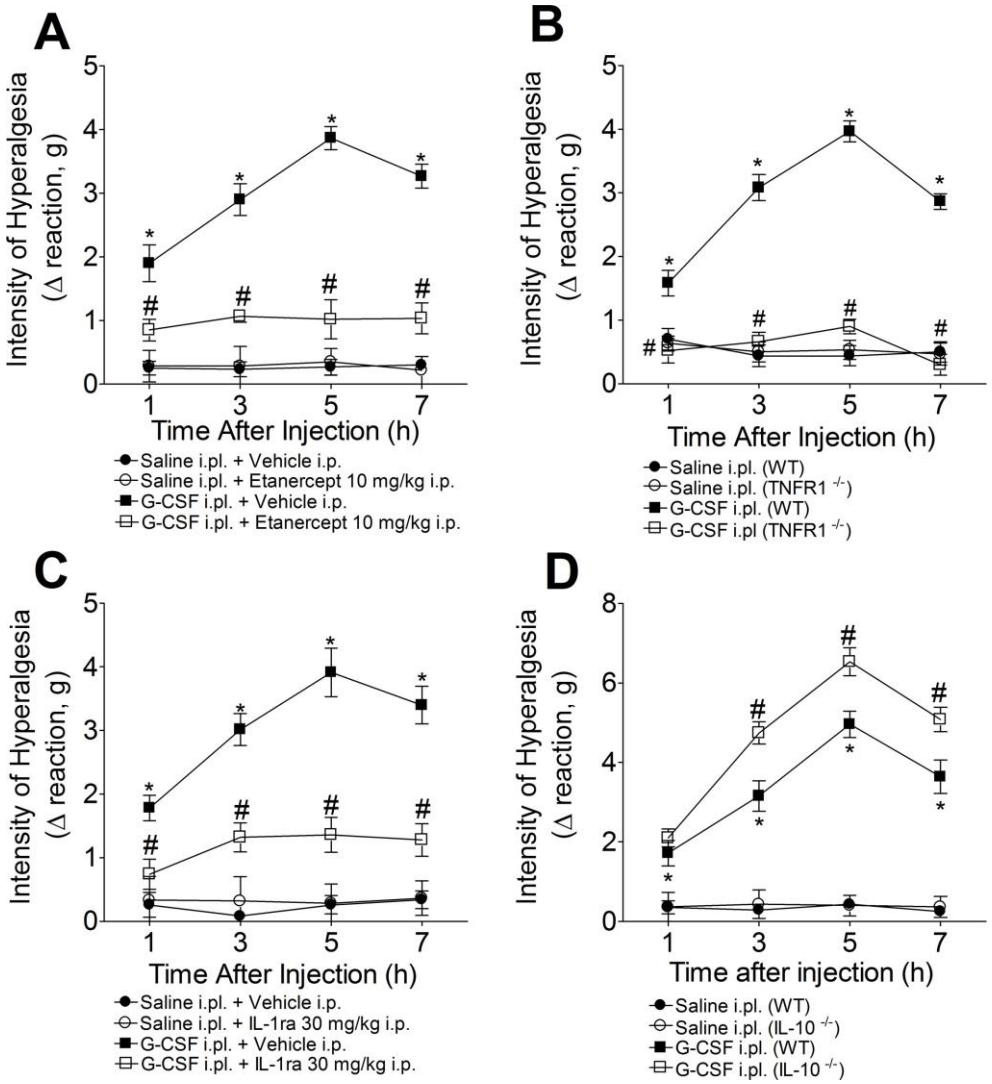
A
Intensity of Hyperalgesia
(Δ reaction, g)
Time After Injection (h)
Saline i.pl. + Vehicle i.p.
Saline i.pl. + Etanercept 10 mg/kg i.p.
G-CSF i.pl. + Vehicle i.p.
G-CSF i.pl. + Etanercept 10 mg/kg i.p.
B
Intensity of Hyperalgesia
(Δ reaction, g)
Time After Injection (h)
Saline i.pl. (WT)
Saline i.pl. (TNFR1 -/-)
G-CSF i.pl. (WT)
G-CSF i.pl (TNFR1 -/-)
C
Intensity of Hyperalgesia
(Δ reaction, g)
Time After Injection (h)
Saline i.pl. + Vehicle i.p.
Saline i.pl. + IL-1ra 30 mg/kg i.p.
G-CSF i.pl. + Vehicle i.p.
G-CSF i.pl. + IL-1ra 30 mg/kg i.p.
D
Intensity of Hyperalgesia
(Δ reaction, g)
Time after injection (h)
Saline i.pl. (WT)
Saline i.pl. (IL-10 -/-)
G-CSF i.pl. (WT)
G-CSF i.pl. (IL-10 -/-)

Fig. 2.

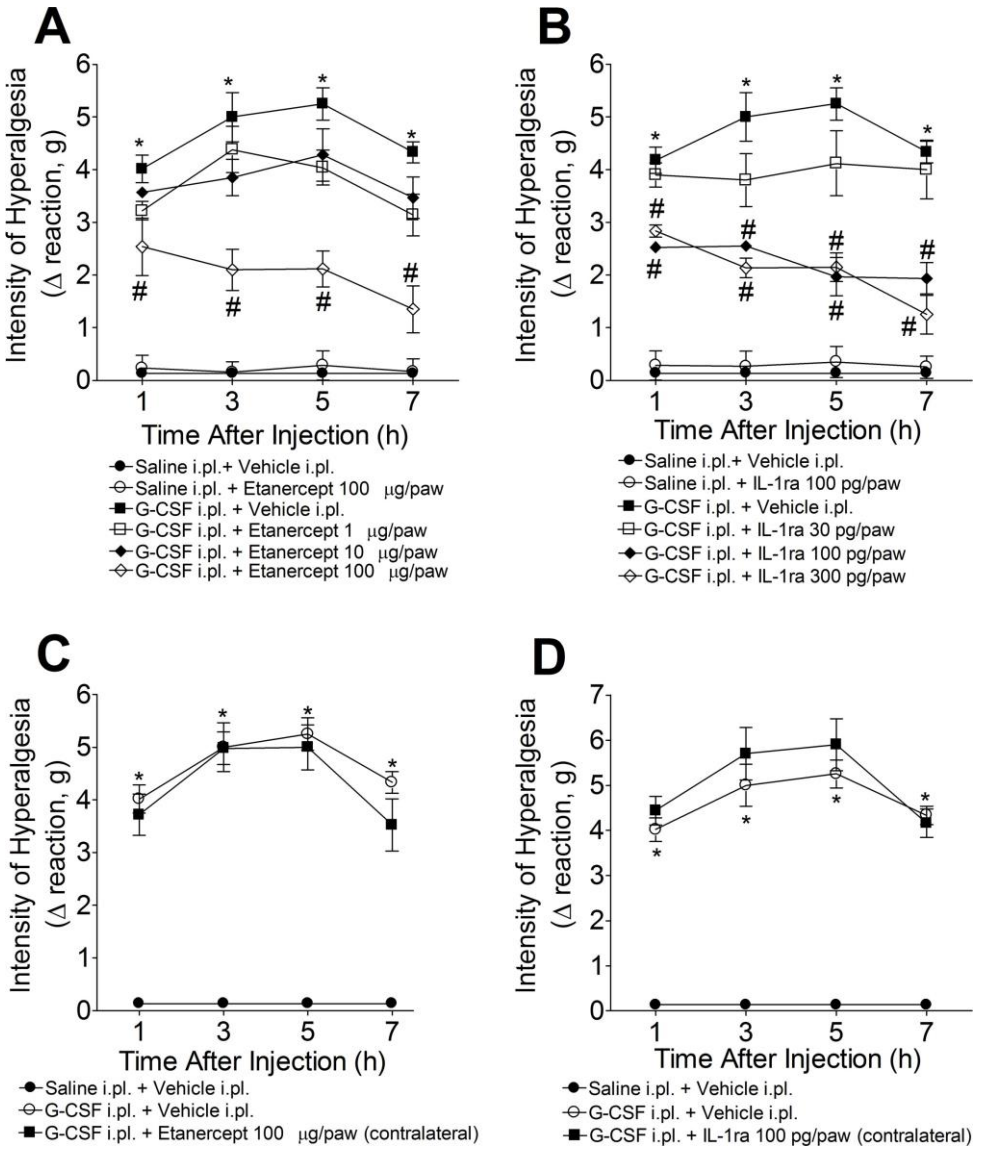
A
Intensity of Hyperalgesia (Δ reaction, g)
Time After Injection (h)
Saline i.pl.+ Vehicle i.pl.
Saline i.pl. + Etanercept 100 μg/paw
G-CSF i.pl. + Vehicle i.pl.
G-CSF i.pl. + Etanercept 1 μg/paw
G-CSF i.pl. + Etanercept 10 μg/paw
G-CSF i.pl. + Etanercept 100 μg/paw
B
Intensity of Hyperalgesia (Δ reaction, g)
Time After Injection (h)
Saline i.pl.+ Vehicle i.pl.
Saline i.pl. + IL-1ra 100 pg/paw
G-CSF i.pl. + Vehicle i.pl.
G-CSF i.pl. + IL-1ra 30 pg/paw
G-CSF i.pl. + IL-1ra 100 pg/paw
G-CSF i.pl. + IL-1ra 300 pg/paw
C
Intensity of Hyperalgesia (Δ reaction, g)
Time After Injection (h)
Saline i.pl. + Vehicle i.pl.
G-CSF i.pl. + Vehicle i.pl.
G-CSF i.pl. + Etanercept 100 μg/paw (contralateral)
D
Intensity of Hyperalgesia (Δ reaction, g)
Time After Injection (h)
Saline i.pl. + Vehicle i.pl.
G-CSF i.pl. + Vehicle i.pl.
G-CSF i.pl. + IL-1ra 100 pg/paw (contralateral)

Fig. 3.

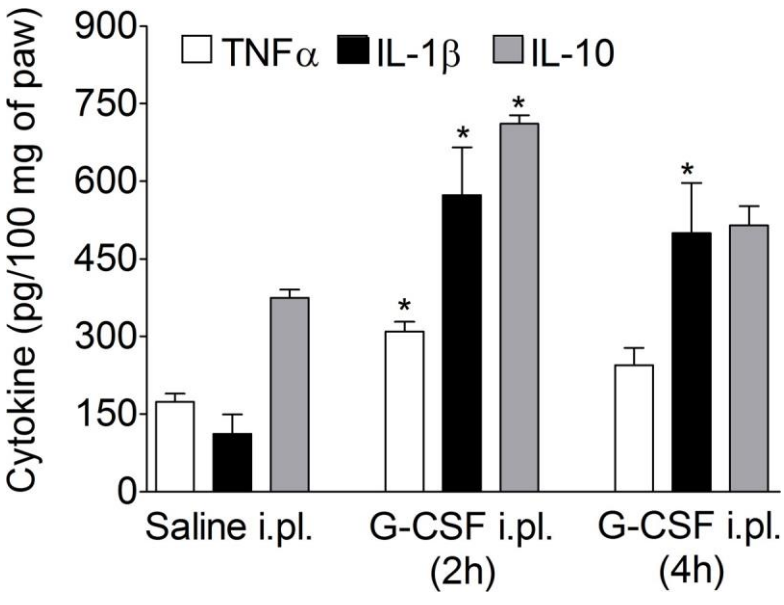
Cytokine (pg/100 mg of paw)
TNFα
IL-1β
IL-10
Saline i.pl.
G-CSF i.pl. (2h)
G-CSF i.pl. (4h)

Fig. 4.

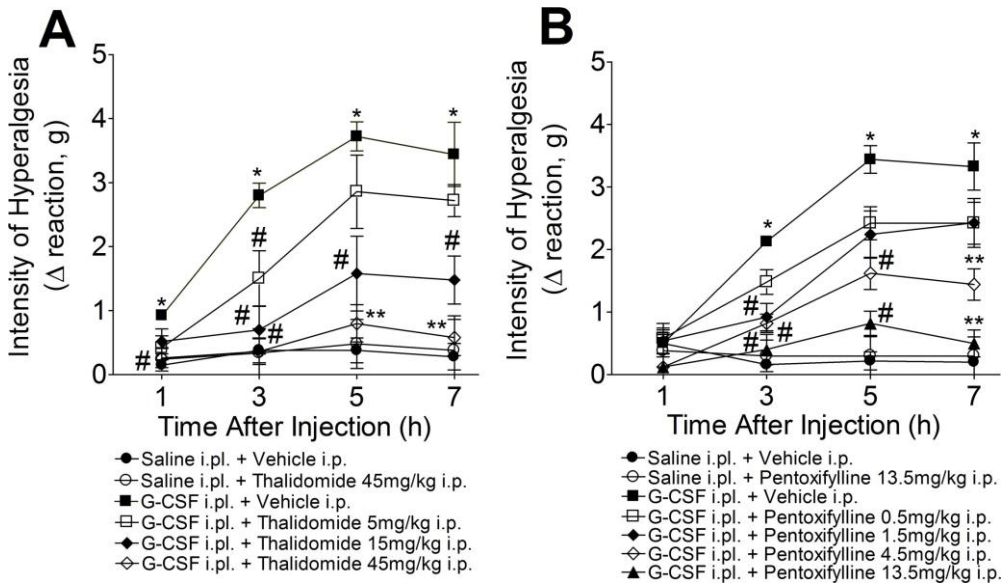
A
B
Intensity of Hyperalgesia
(Δ reaction, g)
Time After Injection (h)
Saline i.pl. + Vehicle i.p.
Saline i.pl. + Thalidomide 45mg/kg i.p.
G-CSF i.pl. + Vehicle i.p.
G-CSF i.pl. + Thalidomide 5mg/kg i.p.
G-CSF i.pl. + Thalidomide 15mg/kg i.p.
G-CSF i.pl. + Thalidomide 45mg/kg i.p.
Saline i.pl. + Pentoxifylline 13.5mg/kg i.p.
G-CSF i.pl. + Pentoxifylline 0.5mg/kg i.p.
G-CSF i.pl. + Pentoxifylline 1.5mg/kg i.p.
G-CSF i.pl. + Pentoxifylline 4.5mg/kg i.p.
G-CSF i.pl. + Pentoxifylline 13.5mg/kg i.p.

Fig. 5.

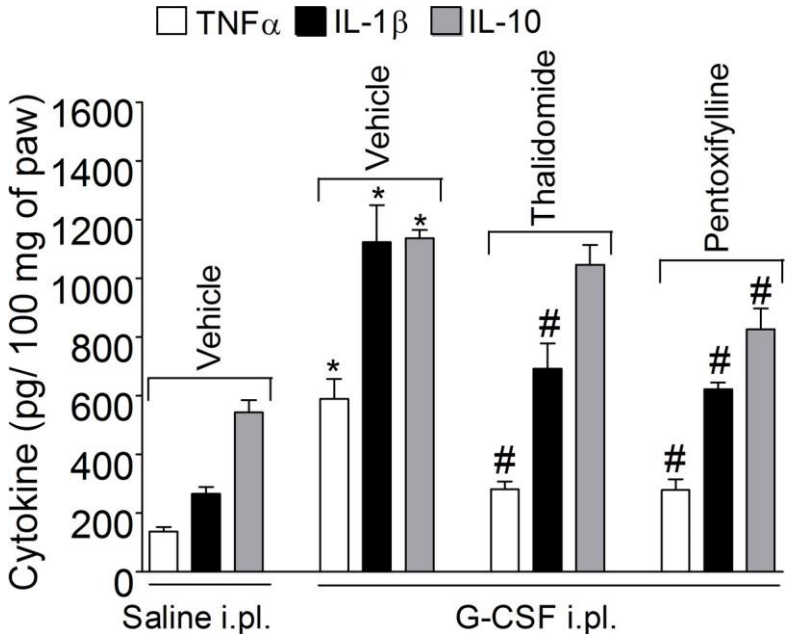
TNFα
IL-1β
IL-10
Cytokine (pg/ 100 mg of paw)
Vehicle
Thalidomide
Pentoxifylline
Saline i.pl.
G-CSF i.pl.

Fig. 6.

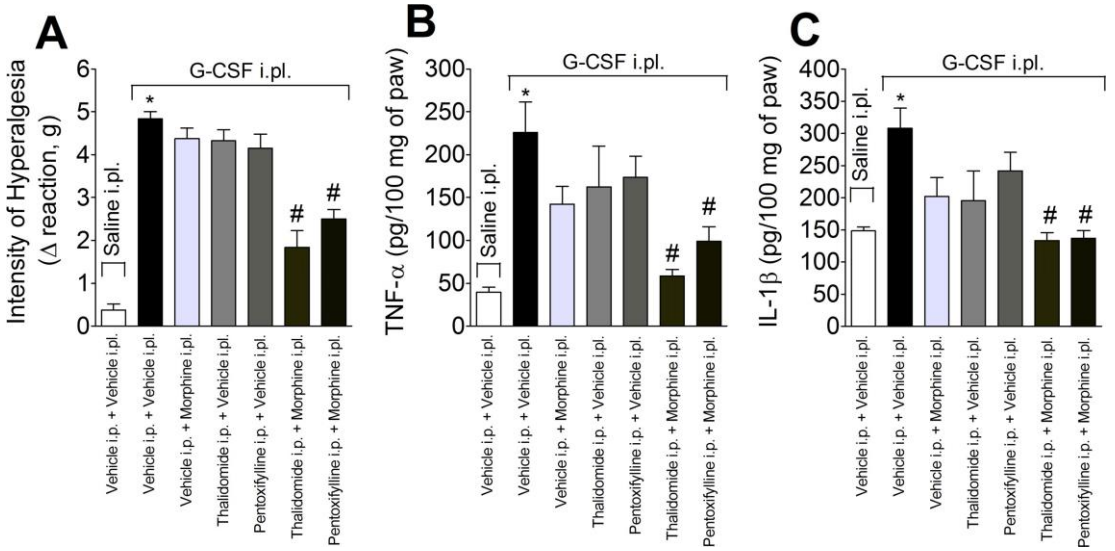
A
B
C
G-CSF i.pl.
Saline i.pl.
Intensity of Hyperalgesia (Δ reaction, g)
TNF-α (pg/100 mg of paw)
IL-1β (pg/100 mg of paw)
Vehicle i.p. + Vehicle i.pl.
Vehicle i.p. + Vehicle i.pl.
Vehicle i.p. + Morphine i.pl.
Thalidomide i.p. + Vehicle i.pl.
Pentoxifylline i.p. + Vehicle i.pl.
Thalidomide i.p. + Morphine i.pl.
Pentoxifylline i.p. + Morphine i.pl.

Fig. 7.

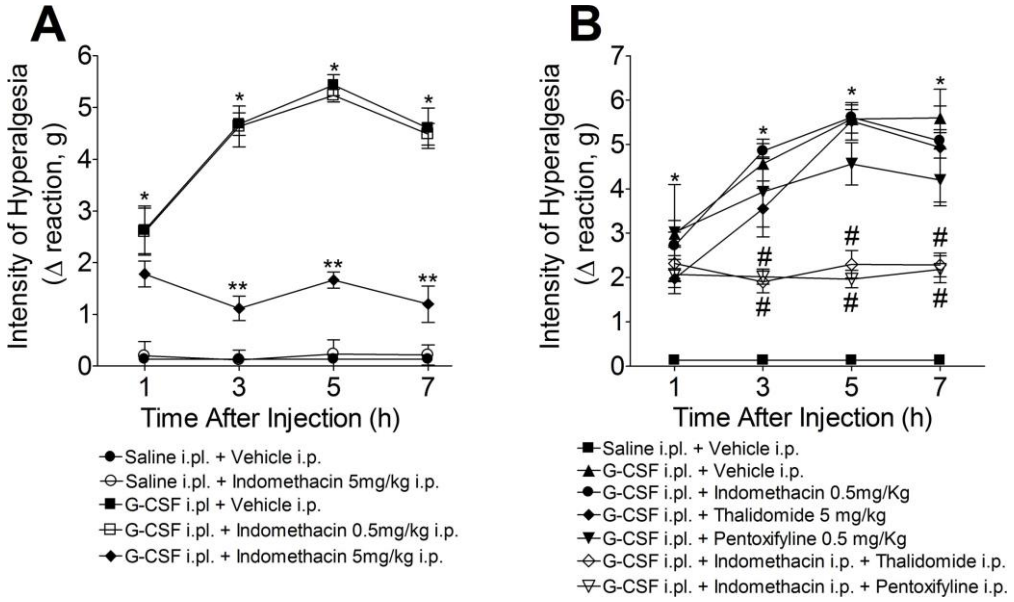
A
B
Intensity of Hyperalgesia (Δ reaction, g)
Time After Injection (h)
Saline i.pl. + Vehicle i.p.
Saline i.pl. + Indomethacin 5mg/kg i.p.
G-CSF i.pl + Vehicle i.p.
G-CSF i.pl. + Indomethacin 0.5mg/kg i.p.
G-CSF i.pl. + Indomethacin 5mg/kg i.p.
Saline i.pl. + Vehicle i.p.
G-CSF i.pl. + Vehicle i.p.
G-CSF i.pl. + Indomethacin 0.5mg/Kg
G-CSF i.pl. + Thalidomide 5 mg/kg
G-CSF i.pl. + Pentoxifyline 0.5 mg/Kg
G-CSF i.pl. + Indomethacin i.p. + Thalidomide i.p.
G-CSF i.pl. + Indomethacin i.p. + Pentoxifyline i.p.

Fig. 8.

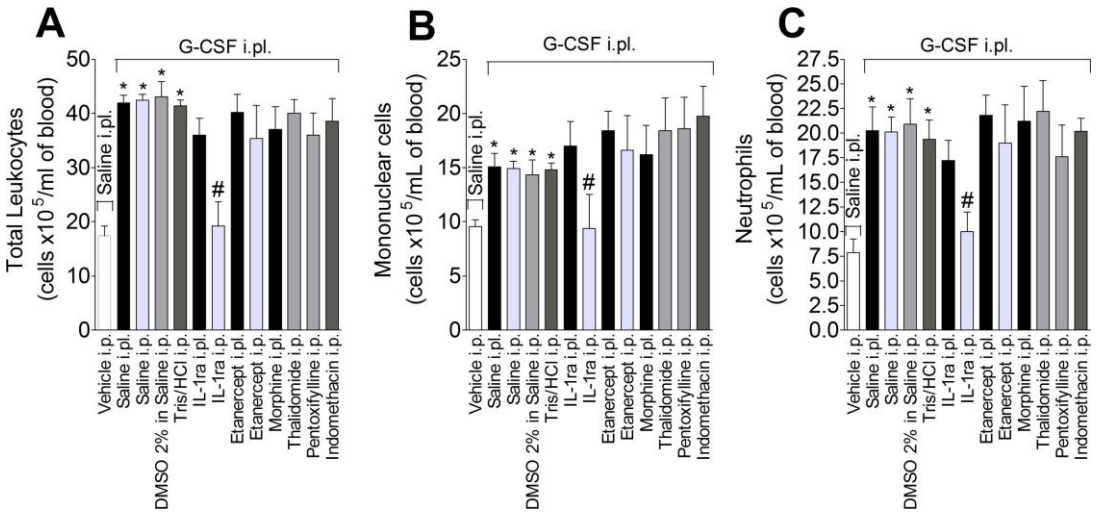

Figure Captions

Fig. 1. TNFα/TNFR1, IL-1β and IL-10 modulate G-CSF-induced mechanical hyperalgesia in mice. G-CSF (100 ng/paw) was injected in mice treated with etanercept (10 mg/kg, i.p., 48 and 1 h before) (Panel A), TNFR1$^{-/-}$ mice (Panel B), IL-1ra treated mice (30 mg/kg, i.p., 30 min before) (Panel C) and IL-10$^{-/-}$ mice (Panel D). Intraplantar (i.pl.) injection of saline (25 µl) + i.p. treatments with saline, etanercept and IL-1ra or TNFR1$^{-/-}$ and IL-10$^{-/-}$ mice were used as negative controls of G-CSF + treatments/ genetic deficiency. Mechanical hyperalgesia was evaluated after 1-7 h. Results are presented as means ± S.E.M. of 6 mice per group per experiment, and are representative of 2 separated experiments. **P*<0.05 compared to saline i.pl. + vehicle i.p. and vehicle i.pl. + treatment i.p./deficient mice control groups; #*P*<0.05 compared to the G-CSF + vehicle i.p./littermate WT groups (One-way ANOVA followed by Tukey's t-test).

Fig. 2. Local paw treatment with etanercept and IL-1ra reduced G-CSF-induced mechanical hyperalgesia in mice. Mice were treated with etanercept (1-100 µg, i.pl., 1 h before) (Panel A) or IL-1ra (30-300 pg, i.pl., 30 min before) (Panel B) and received ipsilateral i.pl. injection of G-CSF (100 ng). Etanercept (100 µg, i.pl., 1 h before) (Panel C) or IL-1ra (100 pg, i.pl., 30 min before) (Panel D) were also injected in the contralateral paw to G-CSF (100 ng) injected paw. Saline (25 µl/paw) plus i.pl. vehicle, etanercept (100 µg/paw) or IL-1ra (100 pg/paw) were used as negative control groups of G-CSF + treatments. Mechanical hyperalgesia was evaluated in paw receiving G-CSF 1-7 h its injection. Results are presented as means ± S.E.M. of 6 mice per group per experiment, and are representative of 2 separated experiments. **P*<0.05 compared to saline i.pl. plus vehicle i.pl./treatments groups; #*P*<0.05 compared to the G-CSF + vehicle group (One-way ANOVA followed by Tukey's t-test).

Fig. 3. G-CSF induces TNFα, IL-1β and IL-10 production in the mice paw skin. Mice received i.pl. injection of saline (25 µl/paw) or G-CSF (100 ng/paw), and after 2 and 4 h, paw skin samples were collected for measurement of TNFα, IL-1β and IL-10 levels by ELISA. Results are presented as means ± S.E.M. of 6 mice per group per experiment, and are representative of 2 separated experiments. **P*<0.05 compared to the vehicle group (One-way ANOVA followed by Tukey's t-test).

Fig. 4. Thalidomide and pentoxifylline inhibited G-CSF-induced mechanical hyperalgesia in a dose-dependent manner. Mice were treated intraperitoneally (i.p.) with vehicle (DMSO 2% in saline), thalidomide (5-45 mg/kg) (Panel A) or pentoxifylline (0.5-13.5 mg/kg) (Panel B) 30 min before the i.pl. injection of saline (25 µl/paw) or G- CSF (100 ng/paw). Mechanical hyperalgesia was evaluated after 1-7 h. Results are presented as means ± S.E.M. of 6 mice per group per experiment, and are representative of 2 separated experiments. **P*<0.05 compared to saline i.pl. + vehicle i.p./control treatment i.p. groups; #*P*<0.05 compared to the G-CSF + vehicle i.p. group; ***P*<0.05 compared to the G-CSF + vehicle i.p. group and 5 mg/kg dose of thalidomide (Panel A) and 0.5 mg/kg dose of pentoxifylline (Panel B) groups (One-way ANOVA followed by Tukey's t-test).

Fig. 5. Effect of thalidomide and pentoxifylline on G-CSF-induced TNFα, IL-1β and IL-10 production in the mice paw skin. Mice were treated intraperitoneally (i.p.) with vehicle (DMSO 2% in saline, not indicated in the figure), thalidomide (45 mg/kg) or pentoxifylline (13.5 mg/kg) 30 min before the i.pl. injection of saline (25 µl/paw) or G- CSF (100 ng/paw), and after 2 h, paw skin samples were collected for TNFα, IL-1β and IL-10 levels determination by ELISA. Results are presented as means ± S.E.M. of 6 mice per group per experiment, and are representative of 2 separated experiments. **P*<0.05 compared to saline group; #*P*<0.05 compared to the G-CSF group (One-way ANOVA followed by Tukey's t-test).

Fig. 6. Combined treatment with morphine and thalidomide or pentoxifylline at doses that are ineffective as single treatment inhibited G-CSF-induced mechanical hyperalgesia and pro-hyperalgesic cytokine production in mice. Mice were treated with vehicle (saline i.pl. 4 h [panel A] or 1 h [panels B and C] after or DMSO 2% in saline i.p. 30 min before), morphine (2 µg/paw 4 h after [panel A], and 1 h after [panels B and C]), thalidomide (5 mg/kg, i.p., diluted in DMSO 2% in saline, 30 min before), pentoxifylline (0.5 mg/kg, i.p., diluted in DMSO 2% in saline, 30 min before), or co- treatment with morphine plus thalidomide or morphine plus pentoxifylline, and received i.pl. injection of G-CSF (100 ng). Mice that received i.pl. injection of saline plus vehicles of morphine (i.pl.) and thalidomide and pentoxifylline (i.p.) were used as negative control group. Mechanical hyperalgesia (Panel A) was evaluated after 5 h (peak of G-CSF-induced mechanical hyperalgesia), and the production of TNFα (Panel B) and IL-1β (Panel C) were evaluated after 2 h (peak of cytokine production). Results are presented as means ± S.E.M. of 6 mice per group per experiment, and are representative of 2 separated experiments. **P*<0.05 compared to saline i.pl. group; #*P*<0.05 compared to the G-CSF + vehicle i.pl. + vehicle i.p. groups (One-way ANOVA followed by Tukey's t-test).

Fig. 7. Indomethacin and combined treatment with indomethacin and thalidomide or pentoxifylline at doses that are ineffective as single treatment inhibited G-CSF-induced mechanical hyperalgesia. In panel A, mice were treated intraperitoneally (i.p.) with vehicle (Tris/HCl buffer) or indomethacin (0.5-5 mg/kg) (Panel A) 40 min before the i.pl. injection of G-CSF (100 ng/paw) (25 µl/paw). In panel B, mice were treated with vehicle (DMSO 2% in saline and Tris/HCl buffer i.p. 30 and 40 min before, respectively), indomethacin (5 mg/kg, i.p., 40 min before), thalidomide (5 mg/kg, i.p., 30 min before), pentoxifylline (0.5 mg/kg, i.p., 30 min before), or co-treatment with indomethacin plus thalidomide or pentoxifylline, and received i.pl. injection of G-CSF or saline (25 µl/paw). Mechanical hyperalgesia was evaluated 1-7 h after G-CSF injection. Results are presented as means ± S.E.M. of 6 mice per group per experiment, and are representative of 2 separated experiments. **P*<0.05 compared to saline i.pl. + vehicles/control treatment groups; #*P*<0.05 compared to the G-CSF + vehicle group; ***P*<0.05 compared to the G-CSF + vehicle group and G-CSF + 0.5 mg/kg dose of indomethacin (One-way ANOVA followed by Tukey's t-test).

Fig. 8. Effect of analgesic treatments on G-CSF-induced peripheral blood neutrophil counts. Mice were treated with the indicated vehicle, IL-1ra (diluted in saline, 100 pg/paw 30 min before and 30 mg/kg i.p. 30 min before), etanercept (diluted in saline, 100 µg/paw 1 h before and 10 mg/kg i.p. 48 and 1 h before), morphine (diluted in saline, 6 µg/25 µl i.pl. 4 h after), thalidomide (diluted in DMSO 2% in saline, 45 mg/kg i.p. 30 min before), pentoxifylline (diluted in DMSO 2% in saline, 13.5 mg/kg i.p. 30 min before) or indomethacin (diluted in Tris/HCl buffer, 5 mg/kg i.p. 40 min before) and received saline i.pl. or G-CSF (100 ng/paw). Total leukocytes (panel A), mononuclear cell (panel B) and neutrophil (panel C) counts were performed 24 h after the i.pl. injection of G-CSF. Results are presented as means ± S.E.M. of 6 mice per group per experiment, and are representative of 2 separated experiments. **P*<0.05 compared to the saline i.pl. + vehicle i.p. group; #*P*<0.05 compared to the G-CSF + saline i.p. groups (One-way ANOVA followed by Tukey's t-test).

3.2 ARTIGO SUBMETIDO AO PERIÓDICO INFLAMMOPHARMACOLOGY

The granulopoietic cytokine granulocyte-colony stimulating factor (G-CSF) induces pain: analgesia by rutin

Thacyana T. Carvalho[a]; Sandra S. Mizokami[a]; Camila R. Ferraz[a]; Marília F. Manchope[a]; Sergio M. Borghi[a,b]; Victor Fattori[a]; Cassia Calixto-Campos[a]; Doumit Camilios-Neto[c]; Rubia Casagrande[d]; Waldiceu A. Verri, Jr[a,*]

[a] Department of Pathology, Center of Biological Sciences, State University of Londrina, Rod. Celso Garcia Cid KM480 PR445, CEP 86057-970, Cx Postal 10.011, Londrina, Brazil

[b] Center for Research in Health Science, University of Northern Paraná - UNOPAR, Rua Marselha, 591, Jardim Piza, CEP 86041-140, Londrina, Paraná, Brazil.

[c] Department of Biochemistry and Biotechnology, Exact Sciences Center, State University of Londrina, Rod. Celso Garcia Cid KM480 PR445, CEP 86057-970, Cx Postal 10.011, Londrina, Brazil.

[d] Department of Pharmaceutical Sciences, Center of Health Sciences, State University of Londrina, Avenida Robert Koch, 60, Hospital Universitário, CEP 86038-350, Londrina, Paraná, Brazil

*Corresponding author. Present address: Department of Pathology, Center of Biological Sciences, State University of Londrina, Rod. Celso Garcia Cid KM480 PR445, CEP 86057-970, Cx Postal 10.011, Londrina, Brazil (ORCID: 0000-0003-2756-9283)

E-mail addresses: waverri@uel.br, waldiceujr@yahoo.com.br (W.A. Verri Jr.)

Acknowledgements

Authors contributions

RC and WAV Jr contributed with funding acquisition, supervision and study design. TTC, SSM, CRF, MFM, SMB, VF, and CC-C conducted the experiments. TTC, SSM, CRF, MFM, SMB, VF, and CC-C analyzed data. DC-N contributed with funding acquisition, supervision, review and editing. TTC, RC, and WAV Jr wrote the paper. All authors read and approved the final version of the manuscript.

Funding

This work was supported by Fundo de Apoio ao Ensino Pesquisa e Extensão/Universidade Estadual de Londrina [FAEPE/UEL 01/2009], Coordenação de Aperfeiçoamento de Pessoal de Nível Superior (CAPES-Brazil), Conselho Nacional de Desenvolvimento Científico e Tecnológico (CNPq-Brazil), Ministério da Ciência, Tecnologia e Inovação (MCTI), Secretaria da Ciência, Tecnologia e Ensino Superior (SETI), Fundação Araucária and Governo do Estado do Paraná. SMB received a post-doctoral fellowship [CNPq process: 435357/2016-6].

Abstract

Rutin is a glycone form of the flavonol quercetin and it reduces inflammatory pain in animal models. On the other hand, therapy with granulocyte-colony stimulating factor (G-CSF) is known by the pain caused as its main side effect. The effect of rutin and its mechanisms of action were evaluated in a model of hyperalgesia induced by G-CSF in mice. The mechanical hyperalgesia induced by G-CSF was reduced by treatment with rutin in a manner dose-dependent. Treatment with both rutin + morphine or rutin + indomethacin, at doses that are ineffectual *per se*, significantly reduced the pain caused by G-CSF. The nitric oxide (NO)−cyclic guanosine monophosphate (cGMP)−protein kinase G (PKG)−ATP-sensitive potassium channel (K_{ATP}) signaling pathway activation is one of the analgesic mechanisms of rutin. Rutin also reduced the pro-hyperalgesic and increased anti-hyperalgesic cytokine production induced by G-CSF. Furthermore, rutin inhibited the activation of the nuclear factor kappa-light-chain enhancer of activated B cells (NFκB), which might explain the inhibition of the cytokine production. Treatment with rutin upregulated the decreased mRNA expression of the nuclear factor (erythroid-derived 2)-like 2 (Nrf2) combined with enhancement of the mRNA expression of the Nrf2 downstream target heme oxygenase (HO-1). Intraperitoneal (i.p.) treatment with rutin did not alter the mobilization of neutrophils induced by G-CSF. The analgesia by rutin can be explained by: NO−cGMP−PKG−K_{ATP} channel signaling activation, inhibition of NFκB and triggering the Nrf2/HO-1 pathway. The present manuscript demonstrates rutin as a promising pharmacological approach to treat the pain induced by G-CSF without impairing its primary therapeutic benefit of mobilizing hematopoietic progenitor cells into the blood.

Keywords: G-CSF; Flavonoids; Hyperalgesia; Rutin; NFκB; Nrf2/HO-1

Introduction

Flavonoids are phenolic compounds widely known for antioxidant effects (Verri et al. 2012). Rutin (3-[[6-*O*-(6-deoxy-α-$_L$-mannopyranosyl)-β-$_D$-glucopyranosyl]oxy]-2-(3',4'-dihydroxyphenyl)-5,7-dihydroxy-4H-1-benzopyran-4-one), a glycoside of the flavonoid quercetin, can be found in many plants such as buckwheat, white mulberry, American elderberry, *Lycopersicon esculentum* Miller leaves, passion flower, apple, *Citrus sinensis* L. Osbeck leaves, green tea, *Betula pendula* leaves, among others (Duke et al. 1992; Hosseinzadeh and Nassiri-Asl 2014; Ugusman 2014; Verri et al. 2012). Rutin is different from quercetin by the sugar rutinose present in position 3 (Guardia et al. 2001). Also known as vitamin P (Haiyun et al. 2003), the advantageous effects of rutin have been reported on inflammation (Feng et al. 2014), cancer (Deschner et al. 1991), diabetic neuropathy (Tian et al. 2016), and cardiovascular diseases (Chung et al. 1993; Sheu et al. 2004).

Concerning anti-inflammatory activity, it has been demonstrated that rutin prevents oxidative stress and neuroinflammation (Tian et al. 2016). For instance, rutin treatment attenuates adjuvant-carrageenan-induced inflammation (ACII) (Guardia et al. 2001), glutamate-induced time spent licking the injected paw (Lapa et al. 2009), oxaliplatin-induced chronic painful peripheral neuropathy (Azevedo et al. 2013), formalin-induced number of paw shakings (Hernandez-Leon et al. 2015) and streptozotocin-induced diabetic neuropathy (Tian et al. 2016). It was shown that rutin acts as an analgesic by inhibiting neuronal activation and neuroplasticity in dorsal horn neurons as observed by reduced Fos expression (Azevedo et al. 2013), decreasing nuclear factor kappa-light-chain enhancer of activated B cells (NFκB) activation, production of interleukin (IL)-6 and tumor nuclear factor alpha (TNFα) in the dorsal root ganglion (DRG) (Tian et al. 2016). Further, in a model of diabetic neuropathy, rutin effects were demonstrated to be due to nuclear factor (erythroid-derived 2)-like-2 factor (Nrf2)/ heme oxygenase-1 (HO-1) pathway activation (Tian et al. 2016). Colony-stimulating factors are often used in the clinical setting to act on hematopoietic cells in order to stimulate proliferation, differentiation, and to activate the end-cell function (Neupogen® [Filgrastim] Package Insert 2013). On this matter, granulocyte colony-stimulating factor (G-CSF) is used to treat neutropenic conditions such as chemotherapy with the view to increase the neutrophil counts (Carvalho et al. 2011; Neupogen® [Filgrastim] Package Insert 2013). Although G-CSF is considered very safe and effective, its usage leads to skeletal pain as the main side effect (Battiwalla and McCarthy 2009; Neupogen® [Filgrastim] Package Insert 2013). Patients suffering from bone pain after G-CSF therapy are treated with non-narcotic or even narcotic drugs (Neupogen® [Filgrastim] Package Insert 2013). Non-narcotic analgesics such as acetaminophen are worldwide used for pain treatment, however, acute overdose may result in serious liver injury and even death (Kociancic and Reed 2003). Also, serious stomach lesions can be caused by the medication with indomethacin (a cyclooxygenase inhibitor) (Valerio et al. 2007). Furthermore, longstanding treatment with opioid analgesics might induce dependence and dose escalation (Devulder et al. 2009).

We previously described that G-CSF injected intraplantarly (i.pl.) evokes pain via spinal cord phosphatidilinositil 3-kinase (PI_3K) and mitogen activated protein (MAP) kinases activation (Carvalho et al. 2011), and that the cytokines TNFα and IL-1β play a relevant role in the pro-hyperalgesic effects of G-CSF therapy in mice (Carvalho et al. 2015).

Considering that new approaches with minimum or no side effects to treat the pain induced by G-CSF are needed and that rutin has been demonstrated to attenuate hyperalgesia in several animal models, here we

analyzed the effect of rutin on reducing the hyperalgesia evoked by G-CSF and the analgesic mechanisms by which rutin acts in this model.

Materials and methods

Experimental mice

In this study, Swiss mice (male, 25-30 g) provided by the State University of Londrina (Londrina, Parana, Brazil) were used to perform all experiments. Animals were kept in standard plastic cages, in a room with temperature-controlled, light–dark cycle of 12/12 h, and had water and food *ad libitum*. All experiments with mice occurred between 9:00 AM and 5:00 PM. All experiments with mice were performed following the guidelines of the International Association for Study of Pain (IASP), Brazilian Council on Animal Experimentation (CONCEA), and EU Directive 2010/63/EU. All animals were used according to the study protocols approved and registered by the Ethics Committee on Animal Use of the State University of Londrina (CEUA-UEL, registration number: 11654.2015.81) accepted on October 8th, 2015. All efforts were made to use the minimum possible number of mice.

Drugs and vehicles

G-CSF (Granulokine®, Filgrastim) was obtained from Hoffmann La-Roche (Basileia, Swiss), rutin (97+% purity) was purchase from Acros Organics (Fair Lawn, NJ, USA), indomethacin from Prodome (Campinas, SP, Brazil), and morphine sulphate from Cristalia (São Paulo, Brazil). L-NAME (N(ω)-nitro-L-arginine methyl ester) from Research Biochemicals (Natick, MA, USA), KT5823 (2,3,9,10,11,12-hexahydro-10R-methoxy-2,9-dimethyl-1-oxo-9S,12R-epoxy-1diindolo [1,2,3-fg:3′,2′,1′-kl] pyrrolo [3,4-i][1,6]benzodiazocine-10-carboxylic acid, methyl ester) from Calbiochem (San Diego, CA, USA), ODQ (1H-[1,2,4]oxadiazolo[4,3-a]quinoxalin-1-one) was purchase from Santa Cruz Biotechnology (Santa Cruz, CA, USA), and glybenclamide from Sigma Chemical Company (St. Louis, MO, USA). G-CSF, morphine sulphate, and L-NAME used saline as vehicle; rutin, KT5823 and ODQ used 2% DMSO in saline as vehicle, Tris (2-amino-2-hydroxymethylpropan-1,3-diol)/HCl (Hydrochloric acid) buffer (pH 8.0) was used as vehicle for indomethacin, and 5% Tween 80 in saline was used as vehicle for glybenclamide.

Experimental protocols

First, mice received rutin (10-100 mg per kg, intraperitoneal [i.p.]) and 30 min after were stimulated with G-CSF (100 ng/paw, intraplantar [i.pl.]) administration and the mechanical hypersensitivity was measured 1-7 h after stimulation. Next, mice received morphine sulphate (2 μg per paw, 1 or 4 h after stimulation), indomethacin (0.5 mg per kg, 45 min of pretreatment [i.p.]), rutin (10 mg per kg, 30 min of pretreatment [i.p.]), morphine + rutin or rutin + indomethacin, and were injected with G-CSF (100 ng per paw) and the hypersensitivity was measured at 5 h. In another set of tests, mice received vehicles (saline [vehicle of L-NAME; i.p.], 2% DMSO in saline [vehicle of rutin, KT5823 and ODQ; i.p.] or 5% Tween 80 in saline [vehicle of glybenclamide; per oral {p.o.}]), L-NAME (90 mg per kg [i.p.], 1h pretreatment), KT5823 (0.5 μg [i.p.], 5 min pretreatment), ODQ (0.3 mg per kg [i.p.], 30 min pretreatment) or glybenclamide (0.3 mg per kg [p.o.], 45 min pretreatment) and were treated with rutin (100 mg per kg [i.p.]) and after additional 30 min G-CSF was injected for mechanical hyperalgesia evaluation (1-7h after stimulation). Cytokine levels (pro-hyperalgesic: TNFα and IL-1β; anti-hyperalgesic: IL-

10) and NFκB were measured by ELISA, and Nrf2 and HO-1 were evaluated by RT-qPCR (2 h after stimulation with G-CSF) in samples of the hindpaw of mice intraperitoneally (i.p.) pretreated or not with rutin (100 mg per kg, 30 min). For the final experiments, mice received: vehicles (saline [vehicle of morphine and negative control for G-CSF; i.pl.], 2% DMSO in saline [vehicle of rutin; i.p.] or Tris/HCl buffer [vehicle of indomethacin; i.p.]), rutin (100 mg per kg [i.p.]), morphine sulphate (6 µg per paw [i.pl.]) or indomethacin (5 mg per kg [i.p.]) pre- or post-G-CSF (100 ng per paw) stimulus, as described above, and after additional twenty-four hours blood samples were collected from the retro-orbital plexus and prepared for leukocyte counts (total and differential). Doses and treatment times were prepared as previous described (Carvalho et al. 2011, 2015; Manchope et al. 2016; Mizokami et al. 2012). Saline (vehicle used for G-CSF [25 µL per paw]) group was used the negative control for G-CSF group (positive control).

Measurement of the mechanical hyperalgesia of the hindpaw of the mice

Mechanical hypersensitivity was verified by using the electronic version of von Frey's test described by Cunha et al. 2004. Measurements on mice were performed before (T0h, baseline) and after stimulation. The basal withdrawal threshold (mechanical) prior to vehicle or stimulation injection was 9.6 ± 0.2 g (mean ± S.E.M. of 62 groups [5 mice/group]). The data are expressed by the intensity of hyperalgesia calculated by the delta (Δ) reaction (in g). To calculate the Δ: subtract the measurements of the T0h from the measurements obtained after stimulation (T1h, T3h, T5h and/or T7h). No difference was found between groups of the baseline in the same test.

Cytokine levels measurement

Animals were pretreated with vehicle or rutin (100 mg/kg [i.p.]) and after 30 min, vehicle or G-CSF (100 ng per paw [i.pl.]) was injected and the hindpaw skin tissues were collected 2h after stimulation. TNFα, IL-1β, and IL-10 concentrations were evaluated by ELISA (enzyme-linked immunosorbent assay) (Ferraz et al. 2015; Verri et al. 2010) following manufacturer's guides and protocols (eBioscience). Data are demonstrated as picograms (pg) of the pro- or anti-hyperalgesic cytokine/100 mg of hindpaw tissue.

NFκB activation

Pretreatment with rutin (100 mg per kg [i.p.]) or vehicle was given to mice 30 min before vehicle or G-CSF injection (100 ng per paw [i.pl.]) and the hindpaw skin tissues were collected 2 h after stimulation. Tissues were disrupted and homogenized with a Tissue-tearor homogenizer in ice-cold cell lysis buffer (#9803; Cell Signaling, Danvers, MA, USA), centrifuged (3000 rpm × 10 min × 4 °C), and the supernatants were frozen at -80 °C until usage. Phosphorylated NFκB p65 and total NFκB p65 quantitation (Calixto-Campos et al. 2015) were performed by using PathScan® Sandwich ELISA Kits (#7834 and #7836; Cell Signaling, Danvers, MA, USA) following the manufacturer's instructions. The data were demonstrated as IOD ratio of phospho-p65/total-p65, thus, an increase in the ratio indicates activation.

Reverse Transcriptase and Quantitative Polymerase Chain Reaction (RT-qPCR)

Hindpaw skin tissues were collected 2 h after vehicle or G-CSF injection (100 ng per paw [i.pl.]) and homogenized in TRIzol™ reagent (Invitrogen™, Life Technologies Corporation, Carlsbad, CA, USA). Isolation

of total RNA was processed following the manufacturer's instructions. Total RNA purity was measured with a spectrophotometer and the wavelength absorption ratio (260/280 nm) was between 1.8 and 2.0 for all preparations. GoTaq® 2-Step RT-qPCR System (Promega, Madison, WI, USA) on a StepOnePlus™ Real-Time PCR System (Applied Biosystems®, Thermo Fisher Scientific, Waltham, MA, USA) were used to the reverse transcription of total RNA to cDNA and qPCR. The relative gene expression was determined using the comparative $2^{-(\Delta\Delta Ct)}$ method. The following primer sequences were used: Nrf2 sense: 5′-TCACACGAGATGAGCTTAGGGCAA-3′, antisense: 5′-TACAGTTCTGGGCGGCGACTTTAT-3′; HO-1 sense: 5´-CCCAAAACTGGC CTGTAAAA-3´, antisense: 5´-CGTGGTCAGTCAACATGGAT-3´; β-actin sense: 5'-AGCTGCGTTTTACACCCTTT-3', antisense: 5'-AAGCCATGCCAATGTTGTCT-3'. β-actin mRNA expression was used to normalize data.

Peripheral blood leukocytes determination

Mice received vehicles (as indicated in the Experimental protocols section), rutin (100 mg per kg [i.p.], 30 min pretreatment prior to stimulation), morphine sulphate (6 µg/paw [i.pl.], 4h after G-CSF) or indomethacin (5 mg per kg, [i.p.], 45 min pretreatment prior to stimulation), and were stimulated or not with G-CSF (100 ng/paw, i.pl.). Twenty-four hours after G-CSF stimulation, the animals were anesthetized with isoflurane 5% by inhalation (Abbott Park, IL, USA) and blood samples were collected from the retro-orbital plexus to perform total and differential cell counts. To count the total number of white blood cells, samples were diluted by using Turk's solution (to lyse the red cells) and the cells were counted manually in a Neubauer chamber. White blood cells differential counts (100 cells/slide) were determined by using panoptic kit (Laborclin Produtos para Laboratórios Ltda., Pinhais, PR, Brazil). A binocular microscope (Olympus CX31, Tokyo, Japan) was used to perform all analysis. Data are presented as cells x 10^5/mL of blood.

Data statistical analysis

Data are expressed as means ± S.E.M. of tests made on 5 or 6 animals in each group (as shown in the legends of the figures). Two-way analysis of variance (ANOVA) was performed when the parameters were analyzed at different time points after stimulation. Treatments, time points, and interaction between time points *vs.* treatment were the parameters analyzed. One-way analysis of variance (ANOVA) and Tukey's post-test were performed for all time point. Results were considered statistically significant when $P < 0.05$.

Results

Rutin attenuates the mechanical hyperalgesia evoked by G-CSF

Animals were treated and stimulated as described in the experimental protocols section and the mechanical hypersensitivity was measured at the time points indicated (Fig. 1). Rutin at 10 mg/kg only reduced the hyperalgesia at 5h (Fig. 1a). The treatment with 30 mg/kg of rutin reduced the hyperalgesia induced by G-CSF at 3, 5, and 7 h after G-CSF administration (Fig. 1a), and rutin at the dose of 100 mg per kg reduced the mechanical hyperalgesia evoked by G-CSF at all time points. Further, rutin (100 mg per kg) inhibition was significant in comparison to the lower dose evaluated (10 mg/kg) at 3, 5, and 7 h (Fig. 1a). Thereby, 10 mg per kg of rutin was used to test possible potentiation when ineffective doses of morphine (Fig. 1b) or indomethacin (Fig. 1c) were given together with rutin at this dose (Carvalho et al. 2011, 2015). The hyperalgesia induced by G-CSF was unaffected by the treatment with rutin, morphine (Fig. 1b) or indomethacin (Fig. 1c) *per se*. On the other hand, the treatment with both rutin + morphine significantly reduced the hyperalgesia induced by G-CSF (Fig. 1b). Also, the combined treatment with rutin + indomethacin at doses ineffectual as single treatment reduced the hyperalgesia induced by G-CSF (Fig. 1c). Thus, rutin can be used in combined treatments with morphine or indomethacin to reduce the doses of these traditional analgesics in the treatment of the hyperalgesia induced by G-CSF. For the next experiments the effective dose of rutin was chosen (100 mg/kg [i.p.]) to determine its analgesic mechanisms.

Rutin activates the nitric oxide (NO)−cyclic guanosine monophosphate (cGMP)−protein kinase G (PKG)−ATP-sensitive potassium channel (K_{ATP}) signaling pathway in the hypersensitivity induced by G-CSF

Nitric oxide (NO)-induced analgesia depends on the cGMP-PKG-K_{ATP} channel signaling pathway activation (Mizokami et al. 2012). In order to test if the anti-hyperalgesic effect of rutin occurs by the activation of NO signaling pathway, treatment with inhibitors of: *i*) NO synthase (L-NAME [i.p.]), *ii*) soluble guanylyl cyclase (ODQ [i.p.]), *iii*) PKG (KT5823 [i.p.]), or *iv*) the K_{ATP} channel (glybenclamide [p.o.]) were given to the animals before rutin. L-NAME (Fig. 2a), ODQ (Fig. 2b), KT5823 (Fig. 2c) and glybenclamide (Fig. 2d) inhibited the anti-hyperalgesic effect of rutin in the hyperalgesia induced by G-CSF. Therefore, the analgesic mechanisms of rutin can be explained by the NO−cGMP−PKG−K_{ATP} channel signaling pathway activation.

The effect of rutin on pro-hyperalgesic cytokines TNFα and IL-1β and anti-hyperalgesic cytokine IL-10 induced by G-CSF stimulation

Next, we analyzed the effect of rutin over pro-hyperalgesic cytokines TNFα and IL-1β and anti-hyperalgesic cytokine IL-10 in the hindpaw skin tissues collected at the peak of cytokine release in this model, which is 2h after stimulus injection (Carvalho et al. 2015) (Fig. 3). Stimulation with G-CSF evoked an increase of TNFα (Fig. 3a) and IL-1β (Fig. 3b) levels and the pretreatment with rutin significantly inhibited the production of these two pro-hyperalgesic cytokines. G-CSF additionally induced an enhancement in the levels of IL-10 (anti-hyperalgesic) that was additionally increased by rutin treatment (Fig. 3c). Thus, rutin reduces the production of pro-hyperalgesic cytokines as well as increases anti-hyperalgesic cytokine suggesting it acts via two different mechanisms regarding the regulation of cytokine production.

Rutin inhibits NFκB activation induced by G-CSF

The activation of NFκB leads to the transcription of several genes, such as cytokines and enzymes. In this sense, we determined in the hindpaw skin tissues collected 2h after stimulation the activation of NFκB (phosphorylated NFκB p65/total NFκB p65 IOD ratio). G-CSF induced NFκB activation, as demonstrated by the increase on the ratio of phosphorylated NFκB p65 per total NFκB p65, and rutin inhibited this activation (Fig. 4). Thus, targeting NFκB activation can be one of the anti-hyperalgesic mechanisms of rutin.

Rutin acts through Nrf2/HO-1 pathway activation in hyperalgesia induced by G-CSF

To test if the analgesic effect of rutin depends on Nrf2/HO-1 pathway, we performed RT-qPCR in the hindpaw skin tissue samples collected 2h after stimulation (Fig. 5). Rutin inhibited the decrease in Nrf2 mRNA expression induced by G-CSF (Fig. 5a). Although G-CSF did not significantly reduced HO-1 mRNA expression, rutin was capable of increasing its expression (Fig. 5b). We also observed that without inflammatory stimulus with G-CSF, rutin reduced basal Nrf2 (mean ± s.e.m.: vehicle [1.057 ± 0.134] and rutin [0.351 ± 0.172]) and HO-1 (mean ± s.e.m.: vehicle [0.887 ± 0.150] and rutin [0.00009 ± 0.00007]) mRNA expression. It is possible that the chemical antioxidant activity of rutin (Verri et al. 2012) reduced basal oxidative stimulus resulting on reduced Nrf2.

Lack of effect of rutin on peripheral blood neutrophil counts induced by G-CSF

The main therapeutic activity of G-CSF is to enhance the counts of neutrophils in the peripheral blood in neutropenic patients (Neupogen® [Filgrastim] Package Insert 2013). In this regard, we assessed the outcome of the analgesic dose of rutin on neutrophil counts induced by G-CSF by counting the total and differential (mononuclear cells and neutrophils) leukocytes at 24 h after G-CSF stimulation (Fig. 6). The treatment with rutin, morphine sulphate or indomethacin did not affect the counts of total leukocytes (Fig. 6a), mononuclear cells (Fig. 6b) and neutrophils (Fig. 6c) induced by G-CSF in the blood stream. Thereby, rutin is a promisor therapeutic approach for the pain control in this model without interfering with its primary pharmacological applicability of accelerating the recovery of neutrophil counts.

Discussion and Conclusions

The treatment of patients with severe neutropenic conditions with granulocyte colony-stimulating factor (G-CSF) aims to: reduce the incidence of infectious diseases; reduce neutrophil recovery time and the duration of total fever episodes; reduce the duration of neutropenia; and induce hematopoietic stem cells mobilization into the blood stream in order to collect by leukapheresis (Neupogen® [Filgrastim] Package Insert 2013). G-CSF therapy is considered safe and effective, but it presents significant side effects such as skeletal pain (Battiwalla and McCarthy 2009; Carvalho et al. 2011; Neupogen® [Filgrastim] Package Insert 2013). In the present manuscript, it was demonstrated that the treatment with rutin was capable of reducing G-CSF-induced mechanical hyperalgesia via NO−cGMP−PKG−ATP-K_{ATP} channel signaling pathway activation, inhibition of the pro-hyperalgesic cytokines TNFα and IL-1β release, increasing anti-hyperalgesic cytokine IL-10 levels, inhibition of NFκB activation, and increasing the Nrf2 and HO-1 mRNA expression.

The hyperalgesic effect of G-CSF was previous reported by our group using the electronic version of von Frey's filaments test (Carvalho et al. 2011, 2015). The stimulation with G-CSF (intraplantar [i.pl.]) induced hypersensitivity via spinal cord PI_3K and MAP kinases (Carvalho et al. 2011). In addition, we recently demonstrated that the pro-hyperalgesic TNFα and IL-1β and the anti-hyperalgesic IL-10 are key cytokines in the hyperalgesia evoked by G-CSF (Carvalho et al. 2015). Here, we observed that treatment with rutin presented dose-dependent anti-hyperalgesic effect in mice after G-CSF stimulation.

Opioids as well as non-steroidal anti-inflammatory drugs (NSAIDs) are effective treatments for the moderate to severe pain caused by G-CSF therapy (Neupogen® [Filgrastim] Package Insert 2013). Considering that treatment with these drugs can lead to many adverse effects (Devulder et al. 2009; Kociancic and Reed 2003; Valerio et al. 2007), we tested the effect of potentiation by treating the mice with a combination of morphine + rutin or indomethacin + rutin at doses that are ineffective as analgesics *per se* over the hyperalgesia induced by G-CSF. Rutin given together with morphine or indomethacin reduced the mechanical hyperalgesia induced by G-CSF proposing that these arrangements can be beneficial to reach better pain control and decrease dosage, tolerance and side effects induced by the usage of these drugs.

The analgesic mechanisms of opioids and NSAIDs under clinical use, such as morphine (Ferreira, Duarte and Lorenzetti 1991), dipyrone (Duarte et al. 1992), diclofenac (Tonussi and Ferreira 1994) and ketorolac (Granados-Soto et al. 1995) are, at least in part, due to increased nitric oxide (NO) release which, in turn, stimulates the cGMP/PKG pathway leading to up-regulation of K_{ATP} currents, then, promoting the hyperpolarization of primary nociceptive neurons and blocking nociceptor neuron sensitization (Cunha et al. 2010; Duarte, Lorenzetti and Ferreira 1990; Sachs, Cunha and Ferreira 2004). The NO−cGMP−PKG− K_{ATP} channel signaling pathway activation is one of the mechanisms by which flavonoids can inhibit hyperalgesia (Bertozzi et al. 2017; Manchope et al. 2016; Pinho-Ribeiro et al. 2016a). Supporting these results, the analgesic effect of rutin was blocked by the inhibitors of the NO synthase (L-NAME), guanylate cyclase (ODQ), PKG (KT5823), and K_{ATP} channel (glybenclamide) revealing that the analgesic mechanisms of rutin are dependent, at least in part, on the activation of the NO−cGMP−PKG− K_{ATP} channel signaling pathway.

Rutin has been shown to present antinociceptive effects in several rodent models of pain, such as: glutamate (Lapa et al. 2009), oxaliplatin (Azevedo et al. 2013), formalin (Hernandez-Leon et al. 2015) and diabetic neuropathy (Tian et al. 2016). After recognizing an inflammatory stimulus, resident cells release a cascade of cytokines, including IL-1β, IL-6 and TNFα, known to participate in the development of inflammatory pain (Verri

et al. 2006; Zhang and An 2007). G-CSF-induced pain has been demonstrated to depend on the hyperalgesic effects of both TNFα and IL-1β (Carvalho et al. 2015). Rutin inhibited the release of TNFα and IL-1β induced by G-CSF in the paw skin which corroborates to its effect on inhibiting TNFα levels in diabetic neuropathy model (Tian et al. 2016). Also, rutin increased IL-10 levels, an anti-hyperalgesic cytokine described to act by the inhibition of pro-hyperalgesic cytokines production such as IL-1β, IL-6 and TNFα (Borghi et al. 2015; Verri et al. 2006; Zhang and An 2007).

NFκB activation occurs once the IκB proteins are phosphorylated and undergo degradation by the proteasome (Verri et al. 2006). As soon as IκB degrades, NFκB can translocate to nucleus and upregulate the transcription of several genes, including pro-hyperalgesic cytokines, cycloxygenase-2 (COX-2) and inducible NO synthase (iNOS) (Li and Verma, 2002). Accordingly, we further examined NFκB activation in both rutin and vehicle-treated mice, since inhibition of NFκB activation has been shown to be an effective mechanism to control inflammatory pain (Calixto-Campos et al. 2015; Ferraz et al. 2015; Pinho-Ribeiro et al. 2016b; Possebon et al. 2014). It was found that G-CSF significantly induced NFκB activation as shown by an increase of phosphorylated NFκB p65/total NFκB p65 ratio, and rutin treatment completely inhibited this activation, suggesting that NFκB inhibition is one of the anti-hyperalgesic mechanisms of rutin in this model. Rutin treatment also caused an increase of Nrf2 mRNA expression higher than basal levels, which we speculate to be explained by the sharing of intracellular pathways by NFκB and Nrf2 and that both transcription factors are sensitive to redox signaling (Staurengo-Ferrari et al. 2019). Rutin reduced NFκB activation, which would favor Nrf2 activity since NFκB p65 and Nrf2 compete for the transcriptional co-activator CBP–p300 complex (Gerritsen et al. 1997; Wardyn, Ponsford and Sanderson 2015). This complex exposes the DNA for transcription due to its histone acetylation activity. We also observed that rutin reduced NFκB p65 phosphorylation, which would otherwise bind to CBP and limit the availability of CBP to Nrf2 binding and transcriptional activity (Staurengo-Ferrari et al. 2019; Wardyn, Ponsford and Sanderson 2015). NFκB also promotes the binding of MafK (small musculoaponeurotic fibrosarcoma K) to histone deacetylase (HDAC)3, thus, reducing the formation of MafK/Nrf2 dimer with consequent diminishing of transcription. Keap-1 (Kelch-like ECH-associated protein 1) on the other hand, stabilizes IKK resulting in reduced NFκB phosphorylation (Lee et al. 2009; Staurengo-Ferrari et al. 2019; Wardyn, Ponsford and Sanderson 2015). The transcription factor Nrf2 is responsible for upregulating antioxidant genes and phase 2 detoxification enzymes, such as thioredoxin system, γ–glutamyl cysteine synthase (γ-GCS), heme oxygenase-1 (HO-1), and NQO1 (NAD(P)H dehydrogenase, quinone 1) and several members of the glutathione S-transferase (GST) family (Manchope et al. 2016; Pinho-Ribeiro et al. 2016b; Rangasamy et al. 2004; Yu et al. 2011). The present shows that rutin inhibited the decrease in the mRNA expression of Nrf2 induced by G-CSF and increased mRNA expression of HO-1. Corroborating the present data, the Nrf2/HO-1 pathway activation inhibits the pro-hyperalgesic cytokine release (So et al. 2008; Yeligar et al. 2010) and HO-1 limits NFκB activity (Staurengo-Ferrari et al. 2019; Wardyn, Ponsford and Sanderson 2015).

The G-CSF therapeutic usage aims to mobilize hematopoietic stem cells into the blood stream to increase the neutrophil counts in patients after chemotherapy to avoid infections and reduce febrile stages (Neupogen® [Filgrastim] Package Insert 2013). In this regard, we tested whether rutin would affect the mobilization of neutrophils to the blood stream induced by G-CSF. The output of proliferating precursors and mature neutrophils from the bone marrow to the blood stream was not affected by the treatment with rutin, thus indicating that rutin

is safe to be used as analgesic, antioxidant and anti-hyperalgesic compound for the hyperalgesia induced by G-CSF without interfering with its primary pharmacological activity.

The data presented in this work demonstrates that rutin inhibits the mechanical hyperalgesia induced by G-CSF through the NO−cGMP−PKG−K_{ATP} channel signaling pathway activation, inhibition of pro-hyperalgesic cytokine release, increasing the anti-hyperalgesic cytokine IL-10, in addition of inducing the mRNA expression of Nrf2 and HO-1. Moreover, rutin did not affect the leucocyte recruitment to the blood stream. Taken together, our results demonstrated that the analgesic effect and mechanisms of rutin are promising to suggest rutin as a therapeutic approach to treat the pain induced by G-CSF without inhibiting the mobilization of hematopoietic stem cells and neutrophils from the bone marrow induced by this granulopoietic cytokine to the blood stream. Our data also showed that rutin can be used alone or in combination with morphine or indomethacin in order to decrease the dosage of these drugs and, in turn, reduce the use of opioids and NSAIDs, again, without affect the therapeutic use of G-CSF.

Compliance with ethical standards

Conflict of interest

The authors declare that they have no conflict of interest.

Ethical approval

Animal care and manipulation were carried out following the experimental guidelines from the International Association for Study of Pain (IASP), EU Directive 2010/63/EU, and the Brazilian Council on Animal Experimentation (CONCEA). All experiments with animals in the present study were conducted according to the protocols approved by the process registered under the number 11654.2015.81, dated from October 8th, 2015 of the Ethics Committee on Animal Use of the State University of Londrina (CEUA-UEL).

This article does not contain any studies with human participants performed by any of the authors.

References

Azevedo MI, Pereira AF, Nogueira RB, Rolim FE, Brito GA, Wong DV, Lima-Júnior RC, de Albuquerque Ribeiro R, Vale ML (2013) The antioxidant effects of the flavonoids rutin and quercetin inhibit oxaliplatin-induced chronic painful peripheral neuropathy. Mol Pain 9:1-14. https://doi.org/10.1186/1744-8069-9-53.

Battiwalla M, McCarthy PL (2009) Filgrastim support in allogeneic HSCT for myeloid malignancies: a review of the role of G-CSF and the implications for current practice. Bone Marrow Transplant 43:351-356. https://doi.org/10.1038/bmt.2008.443.

Bertozzi MM, Rossaneis AC, Fattori V, Longhi-Balbinot DT, Freitas A, Cunha FQ, Alves-Filho JC, Cunha TM, Casagrande R, Verri WA, Jr (2017) Diosmin reduces chronic constriction injury-induced neuropathic pain in mice. Chem Biol Interact 273:180-189. https://doi.org/10.1016/j.cbi.2017.06.014.

Borghi SM, Pinho-Ribeiro FA, Zarpelon AC, Cunha TM, Alves-Filho JC, Ferreira SH, Cunha FQ, Casagrande R, Verri WA, Jr (2015) Interleukin-10 limits intense acute swimming-induced muscle mechanical hyperalgesia in mice. Exp Physiol 100:531-544. https://doi.org/10.1113/EP085026.

Calixto-Campos C, Carvalho TT, Hohmann MSN, Pinho-Ribeiro FA, Fattori V, Manchope MF, Zarpelon AC, Baracat MM, Georgetti SR, Casagrande R, Verri WA, Jr (2015) Vanillic Acid Inhibits Inflammatory Pain by

Inhibiting Neutrophil Recruitment, Oxidative Stress, Cytokine Production, and NFκB Activation in Mice. J Nat Prod 78:1799-1808. https://doi.org/10.1021/acs.jnatprod.5b00246.

Carvalho TT, Borghi SM, Pinho-Ribeiro FA, Mizokami SS, Cunha TM, Ferreira SH, Cunha FQ, Casagrande R, Verri WA, Jr (2015) Granulocyte-colony stimulating factor (G-CSF)-induced mechanical hyperalgesia in mice: Role for peripheral TNFα, IL-1β and IL-10. Eur J Pharmacol 749:62-72. https://doi.org/10.1016/j.ejphar.2014.12.023.

Carvalho TT, Flauzino T, Otaguiri ES, Batistela AP, Zarpelon AC, Cunha TM, Ferreira SH, Cunha FQ, Verri W.A., Jr (2011) Granulocyte-colony stimulating factor (G-CSF) induces mechanical hyperalgesia via spinal activation of MAP kinases and PI_3K in mice. Pharmacol Biochem Behav 98:188-195. https://doi.org/10.1016/j.pbb.2010.12.027.

Chung MI, Gan KH, Lin CN, Ko FN, Teng CM (1993) Antiplatelet effects and vasorelaxing action of some constitutes of Formosan plants. J Nat Prod 56:929-934. https://doi.org/10.1021/np50096a018.

Cunha TM, Roman-Campos D, Lotufo CM, Duarte HL, Souza GR, Verri WA, Funez MI, Dias QM, Schivo IR, Domingues AC, Sachs D, Chiavegatto S, Teixeira MM, Hothersall JS, Cruz JS, Cunha FQ, Ferreira SH (2010) Morphine peripheral analgesia depends on activation of the PI3Kγ/AKT/nNOS/NO/K_{ATP} signaling pathway. PNAS 107:4442-4447. https://doi.org/10.1073/pnas.0914733107.

Cunha TM, Verri WA, Vivancos GG, Moreira IF, Reis S, Parada CA, Cunha FQ, Ferreira SH (2004) An electronic pressure-meter nociception paw test for mice. Braz J Med Biol Res 37:401-407. http://dx.doi.org/10.1590/S0100-879X2004000300018.

Deschner EE, Ruperto J, Wong G, Newmark HL (1991) Quercetin and rutin as inhibitors of azoxymethanol-induced colonic neoplasia. Carcinogenesis 12:1193-1196. https://doi.org/10.1093/carcin/12.7.1193.

Devulder J, Jacobs A, Richarz U, Wiggett H (2009) Impact of opioid rescue medication for breakthrough pain on the efficacy and tolerability of long-acting opioids in patients with chronic non-malignant pain. Br J Anaesth 103:576-585. https://doi.org/10.1093/bja/aep253.

Duarte IDG, Lorenzetti BB, Ferreira SH (1990) Peripheral analgesia and activation of the nitric oxide-cyclic GMP pathway. Eur J Pharmacol 186:289-293. https://doi.org/10.1016/0014-2999(90)90446-D.

Duarte IDG, Santos IR, Lorenzetti BB, Ferreira SH (1992) Analgesia by direct antagonism of nociceptor sensitization involves the arginine-nitric oxide-cGMP pathway. Eur J Pharmacol 217:225-227. https://doi.org/10.1016/0014-2999(92)90881-4.

Duke JA (1992) Handbook of phytochemical constituents of GRAS herbs and other economic plants, CRC Press, Boca Raton.

Feng L, Wang D, He J, Qi D (2014) Protective effect of rutin against lipopolysaccharide-induced acute lung injury in mice. Nan Fang Yi Ke Da Xue Xue Bao 34:1282-1285.

Ferraz CR, Calixto-Campos C, Manchope MF, Casagrande R, Clissa PB, Baldo C, Verri WA, Jr (2015) Jararhagin-induced mechanical hyperalgesia depends on TNF-α, IL-1β and NFkB in mice. Toxicon 103:119-128. https://doi.org/10.1016/j.toxicon.2015.06.024.

Ferreira SH, Duarte ID, Lorenzetti BB (1991) The molecular mechanism of action of peripheral morphine analgesia: Stimulation of the cGMP system via nitric oxide release. Eur J Pharmacol 201:121–122. https://doi.org/10.1016/0014-2999(91)90333-L.

Gerritsen ME, Williams AJ, Neish AS, Moore S, Shi Y, Collins T (1997) CREB-binding protein/p300 are transcriptional coactivators of p65. Proc Natl Acad Sci USA (94) 2927. https://doi.org/10.1073/pnas.94.7.2927.

Granados-Soto V, Flores-Murrieta FJ, Castañeda-Hernández G, López-Muñoz FJ (1995) Evidence for the involvement of nitric oxide in the antinociceptive effect of ketorolac. Eur J Pharmacol 277:281-284. https://doi.org/10.1016/0014-2999(95)00123-3.

Guardia T, Rotelli AE, Juarez AO, Pelzer LE (2001) Anti-inflammatory properties of plant flavonoids. Effects of rutin, quercetin and hesperidin on adjuvant arthritis in rat. Il Farmaco 56:683-687. https://doi.org/10.1016/S0014-827X(01)01111-9.

Haiyun D, Jianbin C, Guomei Z, Shaomin S, Jinhao P (2003) Preparation and spectral investigation on inclusion complex of β-cyclodextrin with rutin. Spectrochim Acta A Mol Biomol Spectrosc 59:3421-3429. https://doi.org/10.1016/S1386-1425(03)00176-8.

Hernandez-Leon A, Fernández-Guasti A, González-Trujano ME (2016) Rutin antinociception involves opioidergic mechanism and descending modulation of ventrolateral periaqueductal grey matter in rats. Eur J Pain 20:274-283. https://doi.org/10.1002/ejp.720.

Hosseinzadeh H, Nassiri-Asl M (2014) Review of the protective effects of rutin on the metabolic function as an important dietary flavonoid. J Endocrinol Invest 37:783-788. https://doi.org/10.1007/s40618-014-0096-3.

Kociancic T, Reed MD (2003) Acetaminophen Intoxication and Length of Treatment: How Long Is Long Enough? Pharmacother 23:1052-1059. https://doi.org/10.1592/phco.23.8.1052.32884.

Lapa FR, Gadotti VM, Missau FC, Pizzolatti MG, Marques MC, Dafré AL, Farina M, Rodrigues AL, Santos AR (2009) Antinociceptive properties of the hydroalcoholic extract and the flavonoid rutin obtained from *Polygala paniculata* L. in mice. Basic Clin Pharmacol Toxicol 104:306-315. https://doi.org/10.1111/j.1742-7843.2008.00365.

Lee DF, Kuo HP, Liu M, Chou CK, Xia W, Du Y, Shen J, Chen CT, Huo L, Hsu MC, Li CW, Ding Q, Liao TL, Lai CC, Lin AC, Chang YH, Tsai SF, Li LY, Hung MC (2009) KEAP1 E3 ligase-mediated downregulation of NF-kappaB signaling by targeting IKKbeta. Mol Cell 36:131-140. https://doi.org/10.1016/j.molcel.2009.07.025.

Li Q, Verma IM (2002) NF-κB Regulation in the Immune System. Nat Rev Immunol 2:725-734. https://doi.org/10.1038/nri910.

Manchope MF, Calixto-Campos C, Coelho-Silva L, Zarpelon AC, Pinho-Ribeiro FA, Georgetti SR, Baracat MM, Casagrande R, Verri WA, Jr (2016) Naringenin inhibits superoxide anion-induced inflammatory pain: role of oxidative stress, cytokines, Nrf-2 and the NO-cGMP-PKG-K_{ATP} Channel signaling pathway. PLoS One 11:e0153015. https://doi.org/10.1371/journal.pone.0153015.

Mizokami SS, Arakawa NS, Ambrosio SR, Zarpelon AC, Casagrande R, Cunha TM, Ferreira SH, Cunha FQ, Verri WA, Jr (2012) Kaurenoic acid from *Sphagneticola trilobata* Inhibits Inflammatory Pain: effect on cytokine production and activation of the NO-cyclic GMP-protein kinase G-ATP-sensitive potassium channel signaling pathway. J Nat Prod 75:896-904. https://doi.org/10.1021/np200989t.

Neupogen® [Filgrastim] Package Insert Kirin-Amgen (2013) Thousand Oaks, CA. https://www.accessdata.fda.gov/drugsatfda_docs/label/2013/103353s5157lbl.pdf. Accessed 26 July 2018.

Pinho-Ribeiro FA, Zarpelon AC, Fattori V, Manchope MF, Mizokami SS, Casagrande R, Verri WA, Jr (2016a) Naringenin reduces inflammatory pain in mice. Neuropharmacol 105:508-519. https://doi.org/10.1016/j.neuropharm.2016.02.019.

Pinho-Ribeiro FA, Fattori V, Zarpelon AC, Borghi SM, Staurengo-Ferrari L, Carvalho TT, Alves-Filho JC, Cunha FQ, Cunha TM, Casagrande R, Verri WA, Jr (2016b) Pyrrolidine dithiocarbamate inhibits superoxide anion-induced pain and inflammation in the paw skin and spinal cord by targeting NF-κB and oxidative stress. Inflammopharmacol 24:97-107. https://doi.org/10.1007/s10787-016-0266-3.

Possebon MI, Mizokami SS, Carvalho TT, Zarpelon AC, Hohmann MSN, Staurengo-Ferrari L, Ferraz CR, Hayashida TH, de Souza AR, Ambrosio SR, Arakawa NS, Casagrande R, Verri WA, Jr (2014) Pimaradienoic acid inhibits inflammatory pain: inhibition of NF-kappaB activation and cytokine production and activation of the NO-cyclic GMP-protein kinase G-ATP-sensitive potassium channel signaling pathway. J Nat Prod 77:2488-2496. https://doi.org/10.1021/np500563b.

Rangasamy T, Cho CY, Thimmulappa RK, Zhen L, Srisuma SS, Kensler TW, Yamamoto M, Petrache I, Tuder RM, Biswal S (2004) Genetic ablation of Nrf2 enhances susceptibility to cigarette smoke-induced emphysema in mice. J Clin Invest 114:1248-1259. https://doi.org/10.1172/JCI200421146.

Sachs D, Cunha FQ, Ferreira SH (2004) Peripheral analgesic blockade of hypernociception: Activation of arginine/NO/cGMP/protein kinase G/ATP-sensitive K^+channel pathway. Proc Natl Acad Sci USA 101:3680-3685. https://doi.org/10.1073/pnas.0308382101.

Sheu JR, Hsiao G, Chou PH, Shen MY, Chou DS (2004) Mechanisms Involved in the Antiplatelet Activity of Rutin, a Glycoside of the Flavonol Quercetin, in Human Platelets. J Agric Food Chem 52:4414-4418. https://doi.org/10.1021/jf040059f.

So H, Kim H, Kim Y, Kim E, Pae HO, Chung HT, Kim HJ, Kwon KB, Lee KM, Lee HY, Moon SK, Park R (2008) Evidence that cisplatin-induced auditory damage is attenuated by downregulation of pro-inflammatory cytokines via Nrf2/HO-1. J Assoc Res Otolaryngol 9:290-306. https://doi.org/10.1007/s10162-008-0126-y.

Staurengo-Ferrari L, Badaro-Garcia S, Hohmann MSN, Manchope MF, Zaninelli TH, Casagrande R, Verri WA, Jr (2019) Contribution of Nrf2 Modulation to the Mechanism of Action of Analgesic and Anti-inflammatory Drugs in Pre-clinical and Clinical Stages. Front Pharmacol 11;9:1536. https://doi.org/10.3389/fphar.2018.01536.

Tian R, Yang W, Xue Q, Gao L, Huo H, Ren D, Chen X (2016) Rutin ameliorates diabetic neuropathy by lowering plasma glucose and decreasing oxidative stress via Nrf2 signaling pathway in rats. Eur J Pharm 771:84-92. https://doi.org/10.1016/j.ejphar.2015.12.02.

Tonussi CR, Ferreira SH (1994) Mechanism of diclofenac analgesia: direct blockade of inflammatory sensitization. Eur J Pharmacol 251:173-179. https://doi.org/10.1016/0014-2999(94)90398-0.

Ugusman A, Zakaria Z, Chua KH, Nordin NAMM, Mahdy ZA (2014) Role of Rutin on Nitric Oxide Synthesis in Human Umbilical Vein Endothelial Cells. Scientific World J 2014:169370. https://doi.org/10.1155/2014/169370.

Valerio DA, Cunha TM, Arakawa NS, Lemos HP, Da Costa FB, Parada CA, Ferreira SH, Cunha FQ, Verri WA, Jr (2007) Anti-inflammatory and analgesic effects of the sesquiterpene lactone budlein A in mice: inhibition of cytokine production dependent mechanism. Eur J Pharmacol 562:155-163. https://doi.org/10.1016/j.ejphar.2007.01.029.

Verri WA, Jr, Cunha TM, Parada CA, Poole S, Cunha FQ, Ferreira SH (2006) Hypernociceptive role of cytokines and chemokines: targets for analgesic drug development? Pharmacol Ther 112:116-138. https://doi.org/10.1016/j.pharmthera.2006.04.001.

Verri WA, Jr, Souto FO, Vieira SM, Almeida SC, Fukada SY, Xu D, Alves-Filho JC, Cunha TM, Guerrero AT, Mattos-Guimaraes RB, Oliveira FR, Teixeira MM, Silva JS, McInnes IB, Ferreira SH, Louzada-Junior P, Liew FY, Cunha FQ (2010) IL-33 induces neutrophil migration in rheumatoid arthritis and is a target of anti-TNF therapy. Ann Rheum Dis 69:1697-1703. https://doi.org/10.1136/ard.2009.122655.

Verri, WA, Jr, Vicentini FTMC, Baracat MM, Georgetti SR, Cardoso RDR, Cunha TM, Ferreira SH, Cunha FQ, Fonseca MJV, Casagrande R (2012) Flavonoids as Anti-Inflammatory and Analgesic Drugs: Mechanisms of Action and Perspectives in the Development of Pharmaceutical Forms. In: Atta-ur-Rahman (Ed.), Studies in Natural Products Chemistry, Elsevier, Amsterdam, pp. 297-322. https://doi.org/10.1016/B978-0-444-53836-9.00026-8.

Wardyn JD, Ponsford AH, Sanderson CM (2015) Dissecting molecular cross-talk between Nrf2 and NF-κB response pathways. Biochem Soc Trans 43(4):621-626. https://doi.org/10.1042/BST20150014.

Yeligar SM, Machida K, Kalra VK (2010) Ethanol-induced HO-1 and NQO1 are differentially regulated by HIF-1alpha and Nrf2 to attenuate inflammatory cytokine expression. J Biol Chem 285:35359-35373. https://doi.org/10.1074/jbc.M110.138636.

Yu M, Li H, Liu Q, Liu F, Tang L, Li C, Yuan Y, Zhan Y, Xu W, Li W, Chen H, Ge C, Wang J, Yang X (2011) Nuclear factor p65 interacts with Keap1 to repress the Nrf2-ARE pathway. Cell Signal 23:883–892. https://doi.org/10.1016/j.cellsig.2011.01.014.

Zhang JM, An J (2007) Cytokines, inflammation, and pain. Int Anesthesiol Clin Spring 45:27-37. https://doi.org/10.1097/AIA.0b013e318034194e.

Figure Captions

Fig. 1 Effect of rutin alone or combined with morphine or indomethacin in the mechanical hyperalgesia induced by G-CSF. Saline (vehicle used for G-CSF [25 µL per paw]) or G-CSF (100 ng per paw [i.pl.]) was administrated in animals pretreated with rutin (10-100 mg per kg [i.p.], 30 min) and mechanical hypersensitivity was measured after 1-7 h (a). Mice received vehicle (saline [i.pl.] 4 h, 2% DMSO in saline [i.p.] or Tris/HCl buffer [i.p.]), morphine sulphate (2 µg per paw [i.pl.], 4 h after), rutin (10 mg per kg [i.p.]) or morphine + rutin (b) or indomethacin + rutin (c) and were stimulated with G-CSF (100 ng [i.pl.]) and the mechanical hypersensitivity was measured at 5h after stimulation (peak of hypersensitivity and because the effect of this dose of morphine lasts for approximately 1.5 h). Saline (25 µL [i.pl.]) + 2% DMSO in saline (100 µL [i.p.]) or Tris/HCl buffer (100 µL [i.p.]) groups were used as negative controls of G-CSF + treatments and G-CSF + vehicles i.p. or i.pl. were used as positive control groups. Data are presented as means ± S.E.M. of 5 animals/group/experiment. Data represents two separate experiments. [*P<0.05 of data against to negative control groups; #P<0.05 of data against to positive control groups; **P<0.05 of data against to the smallest dose of rutin]

Fig. 2 Rutin reduces the hyperalgesia induced by G-CSF via NO-cGMP-PKG-K_{ATP} channel signaling pathway activation. Animals were treated with L-NAME (NOS inhibitor; i.p., 90 mg/kg, 1 h) (a), ODQ (guanylate cyclase inhibitor; i.p., 0.3 mg/kg, 30 min) (b), KT5823 (PKG inhibitor; i.p., 0.5 µg/mice, 5 min) (c), or glybenclamide (K_{ATP} channel inhibitor; p.o., 0.3 mg/kg, 45 min) (d) before rutin (100 mg/kg [i.p.]) administration. After additional 30 min, animals were stimulated with G-CSF (100 ng [i.pl.]). The mechanical

hypersensitivity was measured at 1, 3, 5, and 7 h after G-CSF stimulation. Saline (25 µL [i.pl.]) + vehicles i.p. or p.o. groups were controls (negative) of G-CSF + treatments and G-CSF + vehicles i.p. or p.o. were used as positive control groups. Data are presented as means ± S.E.M. of 5 animals/group/experiment. Data represents two separate experiments. [*P<0.05 of data against to the negative groups; #P<0.05 of data against to the positive groups]

Fig. 3 Rutin reduces the levels of the pro-hyperalgesic cytokines TNFα and IL-1β and increases the release of IL-10 induced by G-CSF in hindpaw skin of mice. Animals were treated with rutin (100 mg per kg [i.p.]) and after 30 min they received i.pl. injection of G-CSF (100 ng). Two h after stimulation, hindpaw skin tissue samples were collected and processed for TNFα (a), IL-1β (b) and IL-10 (c) measurement by ELISA. Data are presented as means ± S.E.M. of 6 animals/group/experiment. Data represents two separate experiments. [*P<0.05 of data against to the negative control group; #P<0.05 of data against to the positive group]

Fig. 4 Rutin inhibits the activation of NFκB in mice induced by G-CSF. Mice were treated with rutin (100 mg per kg [i.p.]) and 30 min after the injection of G-CSF (100 ng per paw [i.pl.]) was performed. Two h after stimulation, hindpaw skin tissue samples were collected and processed for NFκB activation assay by ELISA. Results are shown by the IOD ratio of phospho-p65/total-p65 and presented as means ± S.E.M. of 6 animals/group/experiment. Data represents two separate experiments. [*P<0.05 of data against to the negative control group; #P<0.05 of data against to the positive control group]

Fig. 5 Rutin acts through Nrf2/HO-1 pathway activation in the hyperalgesia evoked by G-CSF. Mice received rutin (100 mg per kg [i.p.]) pretreatment and 30 min after G-CSF (100 ng/paw [i.pl.]) stimulations was performed. Two h after stimulation, hindpaw skin tissue samples were taken and processed for mRNA expression analysis of Nrf2 (a) and HO-1 (b) by RT-qPCR. β-actin was used to normalize the data. Data are presented as means ± S.E.M. of 6 animals/group/experiment. Data represents two separate experiments. [*P<0.05 of data against to the negative control group; **P<0.05 of data against to the positive control group and to the negative control group]

Fig. 6 The effect of rutin on peripheral blood counts induced by G-CSF. Mice were pre- or post-treated with vehicles (saline [i.pl.], 2% DMSO in saline [i.p.] or Tris/HCl buffer [i.p.]), rutin (100 mg per kg, 30 min pretreatment [i.p.]), morphine (6 µg per paw [i.pl.], 4 h post-treatment) or indomethacin (5 mg per kg, 45 min pretreatment [i.p.]) and were injected with vehicle (saline [i.pl.]) or G-CSF (100 ng per paw [i.pl.]). Twenty-four h after stimulation, counts of total leukocytes (a), mononuclear cells (b) and neutrophils (c) were carried out. Saline (25 µL [i.pl.]) + vehicles i.p. or i.pl. group was used as negative control of G-CSF + treatments. Data are presented as means ± S.E.M. of 6 animals/group/experiment. Data represents two separate experiments. [*P<0.05 compared to the negative control group]

Figures

Fig. 1

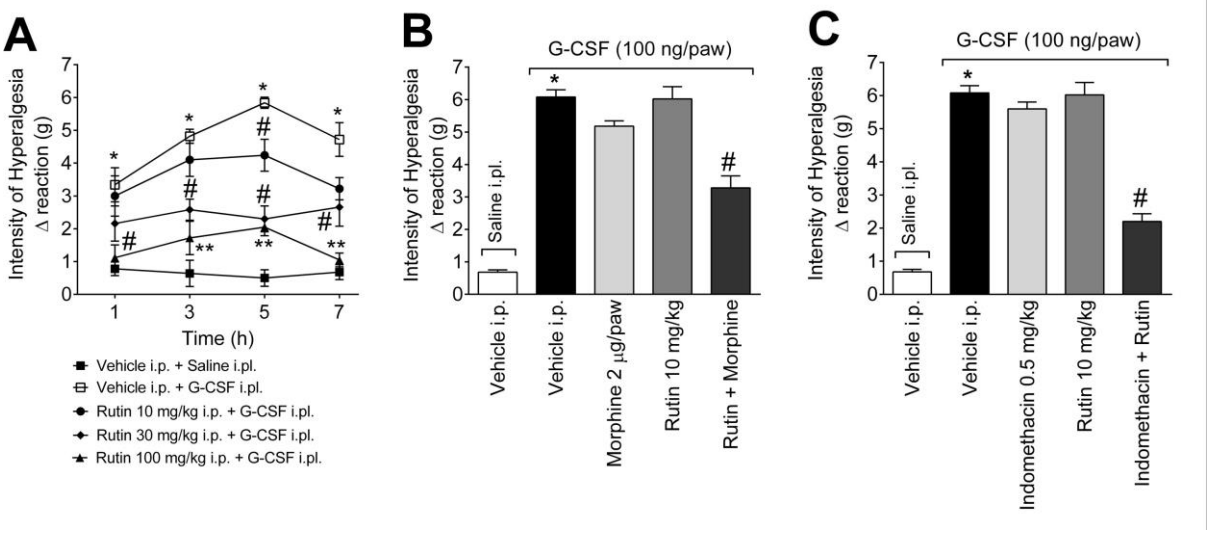
A
Intensity of Hyperalgesia
Δ reaction (g)
Time (h)
Vehicle i.p. + Saline i.pl.
Vehicle i.p. + G-CSF i.pl.
Rutin 10 mg/kg i.p. + G-CSF i.pl.
Rutin 30 mg/kg i.p. + G-CSF i.pl.
Rutin 100 mg/kg i.p. + G-CSF i.pl.
B
G-CSF (100 ng/paw)
Saline i.pl.
Vehicle i.p.
Vehicle i.p.
Morphine 2 μg/paw
Rutin 10 mg/kg
Rutin + Morphine
C
G-CSF (100 ng/paw)
Saline i.pl.
Vehicle i.p.
Vehicle i.p.
Indomethacin 0.5 mg/kg
Rutin 10 mg/kg
Indomethacin + Rutin

Fig. 2

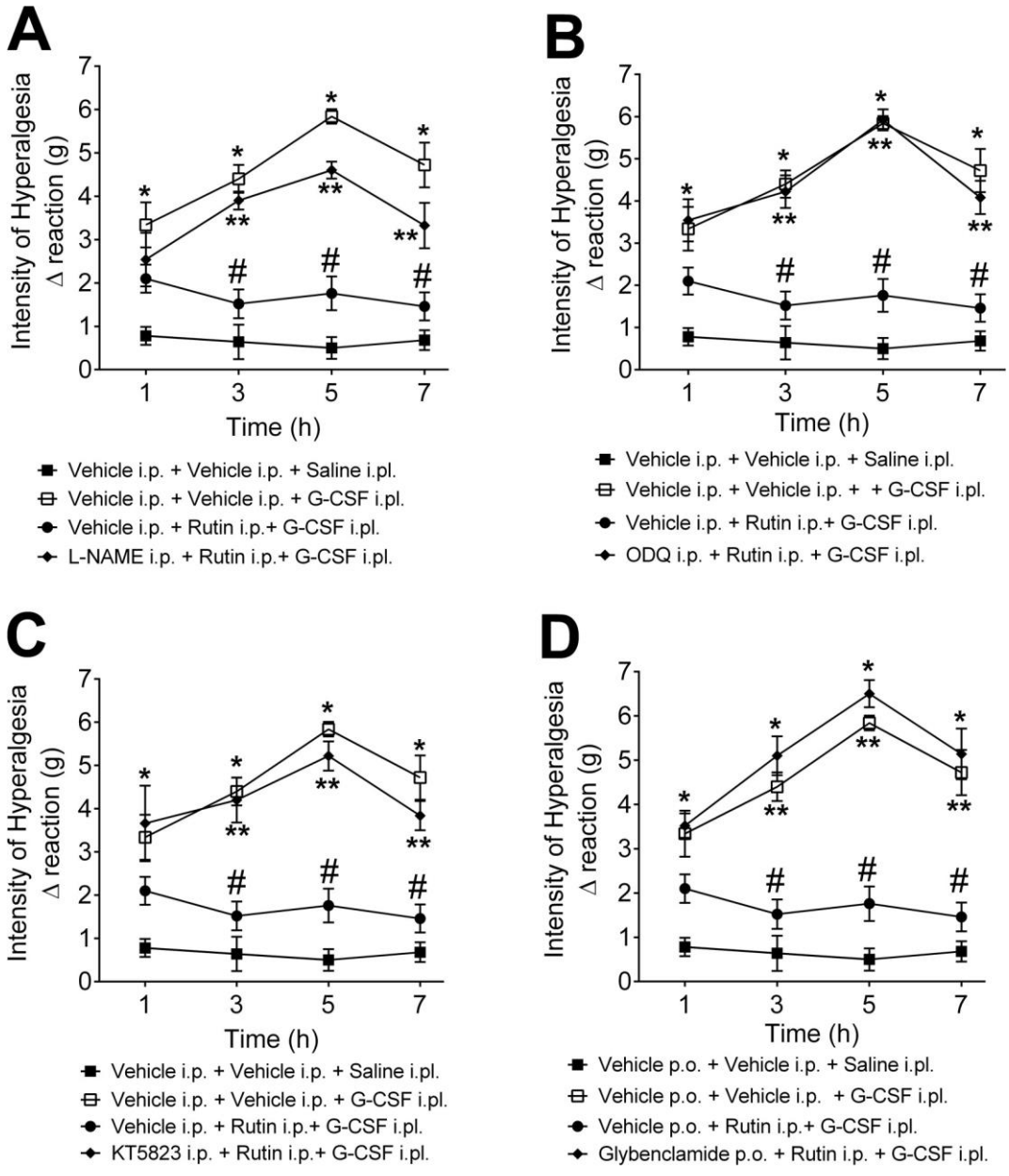
A
Intensity of Hyperalgesia
Δ reaction (g)
Time (h)
Vehicle i.p. + Vehicle i.p. + Saline i.pl.
Vehicle i.p. + Vehicle i.p. + G-CSF i.pl.
Vehicle i.p. + Rutin i.p.+ G-CSF i.pl.
L-NAME i.p. + Rutin i.p.+ G-CSF i.pl.
B
Intensity of Hyperalgesia
Δ reaction (g)
Time (h)
Vehicle i.p. + Vehicle i.p. + Saline i.pl.
Vehicle i.p. + Vehicle i.p. + + G-CSF i.pl.
Vehicle i.p. + Rutin i.p.+ G-CSF i.pl.
ODQ i.p. + Rutin i.p. + G-CSF i.pl.
C
Intensity of Hyperalgesia
Δ reaction (g)
Time (h)
Vehicle i.p. + Vehicle i.p. + Saline i.pl.
Vehicle i.p. + Vehicle i.p. + G-CSF i.pl.
Vehicle i.p. + Rutin i.p.+ G-CSF i.pl.
KT5823 i.p. + Rutin i.p.+ G-CSF i.pl.
D
Intensity of Hyperalgesia
Δ reaction (g)
Time (h)
Vehicle p.o. + Vehicle i.p. + Saline i.pl.
Vehicle p.o. + Vehicle i.p. + G-CSF i.pl.
Vehicle p.o. + Rutin i.p.+ G-CSF i.pl.
Glybenclamide p.o. + Rutin i.p. + G-CSF i.pl.

Fig. 3

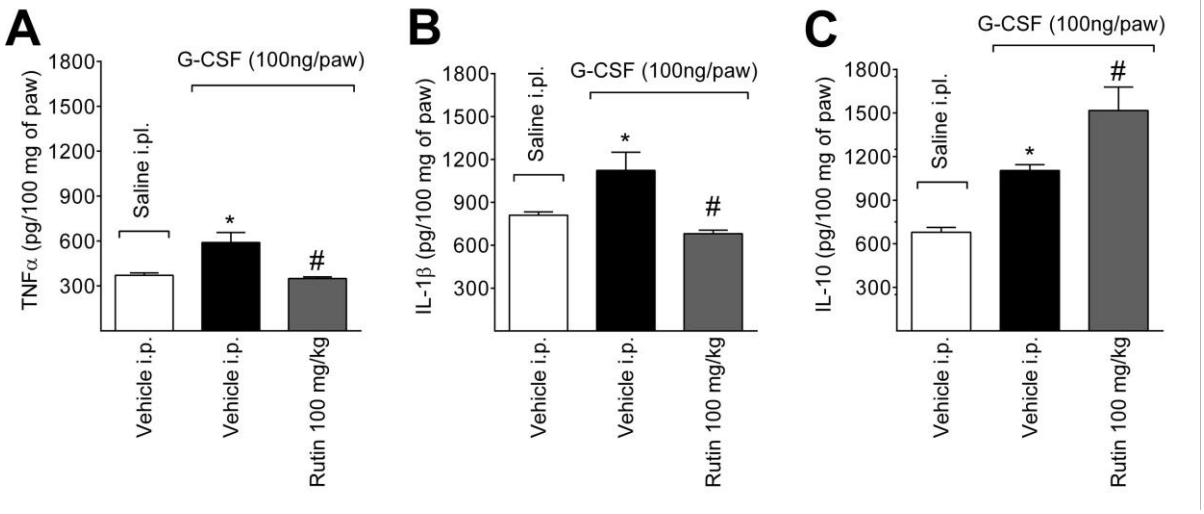
A
B
C
G-CSF (100ng/paw)
Saline i.pl.
TNFα (pg/100 mg of paw)
IL-1β (pg/100 mg of paw)
IL-10 (pg/100 mg of paw)
1800
1500
1200
900
600
300
*
#
Vehicle i.p.
Vehicle i.p.
Rutin 100 mg/kg

Fig. 4

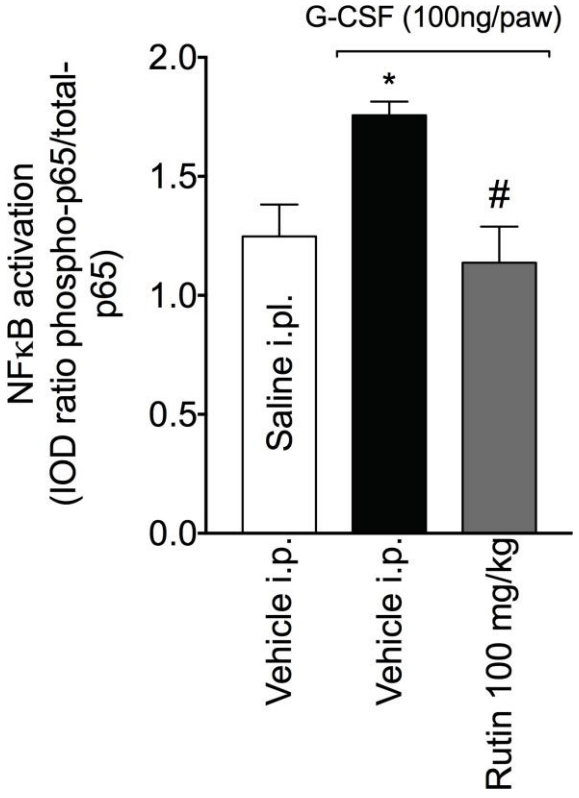
G-CSF (100ng/paw)
NFκB activation
(IOD ratio phospho-p65/total-p65)
2.0
1.5
1.0
0.5
0.0
*
#
Saline i.pl.
Vehicle i.p.
Vehicle i.p.
Rutin 100 mg/kg

Fig. 5

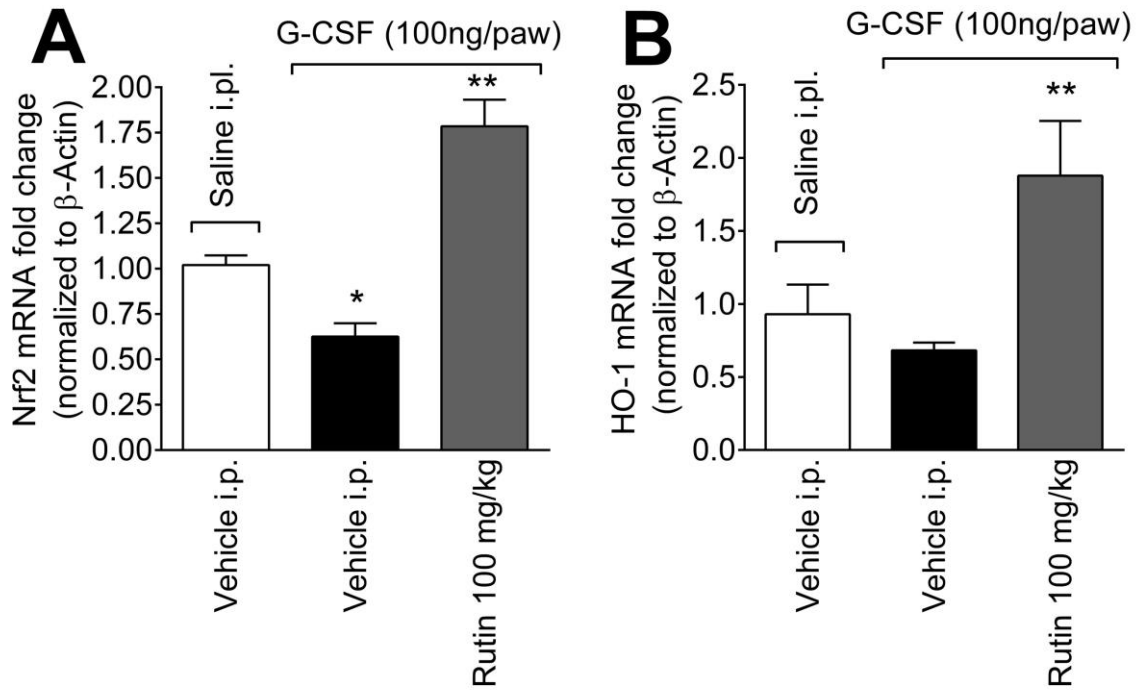
A
G-CSF (100ng/paw)
Nrf2 mRNA fold change (normalized to β-Actin)
Saline i.pl.
Vehicle i.p.
Vehicle i.p.
Rutin 100 mg/kg
B
G-CSF (100ng/paw)
HO-1 mRNA fold change (normalized to β-Actin)
Saline i.pl.
Vehicle i.p.
Vehicle i.p.
Rutin 100 mg/kg

Fig. 6

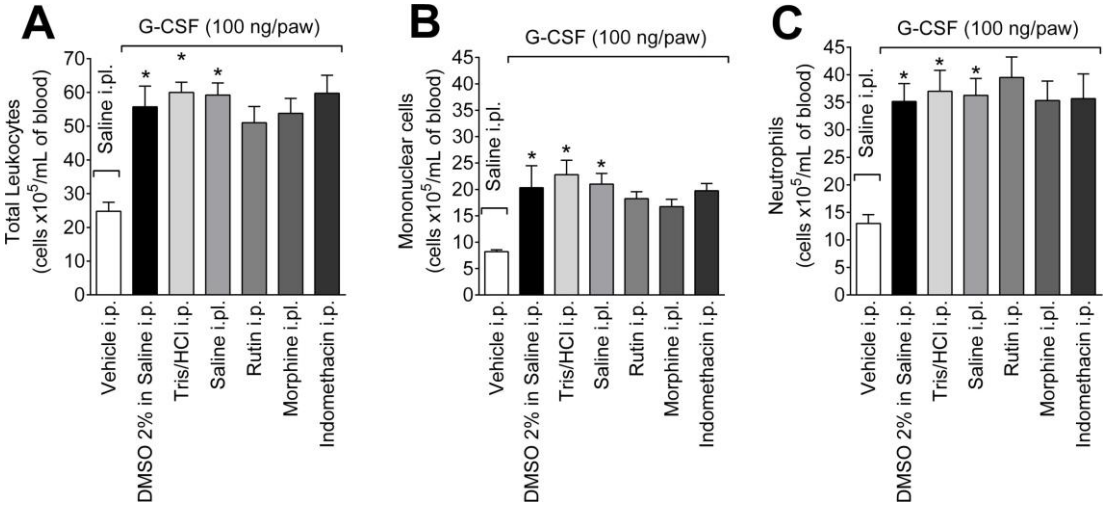
A
G-CSF (100 ng/paw)
Total Leukocytes (cells x10⁵/mL of blood)
Saline i.pl.
B
G-CSF (100 ng/paw)
Mononuclear cells (cells x10⁵/mL of blood)
Saline i.pl.
C
G-CSF (100 ng/paw)
Neutrophils (cells x10⁵/mL of blood)
Saline i.pl.
Vehicle i.p.
DMSO 2% in Saline i.p.
Tris/HCl i.p.
Saline i.pl.
Rutin i.p.
Morphine i.pl.
Indomethacin i.p.

3.3 Artigo derivado do período de doutorado sanduíche no Cedars-Sinai Medical Center a ser submetido ao periódico Arteriosclerosis, Thrombosis, and Vascular Biology

Role of IL-33 in LCWE-induced Kawasaki Disease Vasculitis and Aneurysms

Thacyana T. Carvalho[1,2], Masanori Abe[2], Michael Franklin[2], Waldiceu Ap. Verri[1], Moshe Arditi[2,3] and Magali Noval Rivas[2,*]

[1]Department of Pathological Sciences, Center of Biological Sciences, State University of Londrina, Rod. Celso Garcia Cid KM480 PR445, CEP 86057-970, Cx Postal 10.011, Londrina, Brazil
[2]Division of Pediatric Infectious Diseases and Immunology, Burns and Allen Research Institute, Cedars-Sinai Medical Center, 8700 Beverly Blvd. Davis Building, 90048, Los Angeles, California
[3]David Geffen School of Medicine at University of California Los Angeles (UCLA), Los Angeles, California

Running Title: Role of IL-33 in a mouse model of Kawasaki Disease

*Corresponding author. Magali Noval Rivas, PhD; Division of Pediatric Infectious Diseases and Immunology, Burns and Allen Research Institute, Cedars-Sinai Medical Center, 8700 Beverly Blvd, Room 4225, Los Angeles, CA 90048. Tel.: (310) 423-4471, magali.novalrivas@csmc.edu

Keywords: Kawasaki Disease; Interleucina-33; ST2; LCWE; vasculitis

Subject codes: Animal Models of Human Disease; Cell Signaling/Signal Transduction; Growth Factors/Cytokines; Inflammation; Mechanisms; Cardiovascular Disease; Pediatrics; Inflammatory Heart Disease; Acute Coronary Syndromes; Coronary Artery Disease
Word count: 4.305
Total number of figures: 3
TOC category: Basic, Translational, and Clinical Research
TOC subcategory: Animal Models of Human Disease

Abstract

Objective: Kawasaki disease (KD) is a multisystem inflammatory disease of unknown cause resulting in an acute febrile syndrome that affects predominantly children under 5 years of age. Intraperitoneal administration of a *Lactobacillus casei* cell-wall extract (LCWE) induces local arteritis with histopathological changes similar to coronary artery lesions found in KD patients. It is been demonstrated that the Interleukin (IL)-33 is involved in cardiovascular diseases, such as atherosclerosis. In this sense, we aimed to evaluate the role of IL-33 in the LCWE-induced mouse model of KD vasculitis.

Approach and Results: In this study, we showed by RNA sequencing that IL-33 gene expression is increased in both heart and abdominal aorta (AA) of mice stimulated with LCWE compared to PBS mice. No difference was observed in the IL-33 production in the serum of LCWE-stimulated mice compared to PBS injected mice. Neutralization of IL-33 reduced coronary artery (CA) lesions and abdominal aortic aneurysm (AAA) formation in mice. Also, IL-33 expression is increase in the AA and did not co-localize with infiltrated macrophages. There was no difference in ST2 production in serum or expression in the AA.

Conclusions: In conclusion, IL-33 may play a significant role in modulating the systemic and local immune responses leading to development of KD vasculitis. Together these data demonstrate that targeting IL-33 can be a conceivable therapeutic approach for KD treatment.

Nonstandard Abbreviations and Acronyms

KD - Kawasaki Disease

AAA - abdominal aortic aneurysm

LCWE - *Lactobacillus casei* cell-wall extract

IVIG - intravenous immunogolubulin

CAA - coronary artery

INTRODUCTION

Kawasaki disease (KD) is a multisystem inflammatory disease of unknown etiology that results in an acute febrile syndrome.[1,2] The disease affects predominantly children under 5 years of age and it is characterized by fever, bilateral nonexudative conjunctivitis, erythema of the lips and oral mucosa, changes in the extremities, rash, and cervical lymphadenopathy.[3] Although it is been thought that KD is triggered by an infectious agent, the etiology of KD still remains unknown.[3] The current treatment with a high dose of intravenous immunoglobulin (IVIG) is focused in reducing the acute inflammation and the prolonged fever, however, up to 20% of the patients are IVIG resistant making them a high-risk population for the development of heart problems and highlighting the necessity to develop new therapeutics.[4,5] Occurrence of KD in childhood is also associated with the development of early atherosclerosis and cardiovascular diseases in adult life.[2,6] Interleukin (IL)-1β plays a key role in the induction of KD vasculitis,[7,8] however, the mechanisms involved in KD vasculitis development are still poorly understood. Intraperitoneal administration of *Lactobacillus casei* cell-wall extract (LCWE) in Wild Type (WT) C57 BL/6 mice induces coronary arteritis with histopathological lesions similar to the ones observed in human KD.[9-11]

IL-33 is a recently discovered cytokine member of the IL-1 family, its structure is related to IL-18 and IL-1β.[12] IL-33 binds the receptor suppression of tumorigenicity 2 (ST2), an IL-1 family member receptor.[12] The *ST2* gene encodes two receptors: a transmembrane form (ST2L) responsible for IL-33 signaling, and a soluble form (sST2) that can serve as a decoy receptor.[12,13] An increased concentration of sST2 in the serum of patients with chronic heart failure[14] or acute myocardial infarction[15] is an indicative of a poor prognosis. It was observed that IL-33 and TNF-α levels are elevated in the serum of KD patients even after IVIG treatment.[16] However, the specific roles of IL-33/ST2 signaling during KD have not yet been investigated. Therefore, we hypothesize that IL-33/ST2 signaling contributes to the coronary artery lesions formation and this pathway may play a significant role in modulating the systemic and local immune responses that further contributes to KD vasculitis development.

MATERIALS AND METHODS

Mice

C57BL/6 mice were purchased from the Jackson Laboratory (Bar Harbor, ME). All animals were housed under specific pathogen-free conditions at the animal center of the Cedars-Sinai Medical Center and experiments conducted under approved IACUC protocols.

Preparation of *Lactobacillus casei* cell wall extract (LCWE)

Lactobacillus casei (ATCC 11578) cell wall extract was prepared as previously described.[9,10] In brief, *L. casei* were grown in *Lactobacillus* de Man, Rogosa, and Sharpe broth (Difco) for 48 hours, harvested, and washed with PBS. The harvested bacteria were disrupted by 2 packed volumes of 4% SDS/PBS overnight. Cell wall fragments were washed 8 times with SDS-Out™ SDS Precipitation Kit (Thermo Fisher Scientific, Rockford, IL, USA) to remove any residual SDS. The SDS-treated cell wall fragment was sonicated for 2 hours with a 3⁄4-in horn and a garnet tip at maximum power maintained in a dry ice/ethanol bath. After sonication, the cell wall fragments were spun for 20 minutes at 12 000 rpm and 4°C. The supernatant was centrifuged for 1 hour at 38 000 rpm and 4°C, and the pellet was discarded. The total Rhamnose content of the cell wall extract was determined by a colorimetric phenol-sulfuric assay as described previously.[9]

***Lactobacillus casei* cell wall extract (LCWE) murine model of Kawasaki Disease**

5 weeks old male mice were injected i.p. with either 500 µg of LCWE or PBS. At 14 days after LCWE injection, blood was collected for serum separation and the mice were euthanized. Heart perfusion with PBS containing heparin was performed and hearts were removed and embedded in Optimal Cutting Temperature (OCT) compound for histological examination. Aortas were dissected, photographed, removed and embedded in OCT compound for histological examination. Serial cryosections (7 µm) of heart and abdominal aorta tissues were stained with hematoxilyn and eosin (H&E) and histopathological scoring of coronary arteritis, aortic root vasculitis, and myocarditis were performed in the heart sections by an experimenter blinded to the experimental set up.

RNA-sequencing

Heart tissues and abdominal aorta were collected from PBS (n=5) and LCWE-injected (n=5) C57 BL/6 WT mice 7 day after injection. RNA was extracted by using a

RNeasy Mini Kit (Qiagen). RNA quality was further determined by using a Bioanalyzer (Agilent); only samples with a RIN score higher that 7 were used. RNA-Sequencing and analysis were performed as previously described (Wakita et al., 2016). Molecule Activity Predictor (MAP), Upstream Regulator Analysis, Mechanistic Networks and Interaction Network Analysis were performed by using Ingenuity® Pathway Analysis (IPA®) (Qiagen Bioinformatics).

Cytokine Measurement

Peripheral blood was collected from the retro-orbital vein by using Heparinized capillary on day 14 after LCWE or PBS i.p. injection. Samples were centrifuged for 10 min at 8000 rpm and serum was separated and stored at -80°C until usage. IL-33 (Mouse IL-33 DuoSet ELISA, R&D Systems, Inc., Minneapolis, USA) and sST2 (ST2 Mouse Uncoated ELISA Kit, Thermo Fisher Scientific, USA) quantitation in the serum were determined by enzyme-linked immunosorbent assay (ELISA) according to manufacturer's instructions. Results were presented by pictograms (pg) of cytokine per mL of serum.

Neutralization experiments

5 weeks old male mice were injected i.p. with anti-IL-33 Ab (Goat Anti-Mouse IL-33 Antigen Affinity-purified Polyclonal Antibody - AF3626, R&D Systems, Minneapolis, MN, USA) or Goat IgG isotype (IgG from Goat serum - I5256, Sigma-Aldrich Co., St. Louis, MO, USA) 6h before, 2 and 7 days after either 500 µg of LCWE or PBS. At 14 days after LCWE injection, blood was collected for serum separation and the mice were euthanized. Heart perfusion was performed and hearts were removed and embedded in OCT compound for histological examination. Aortas were dissected, photographed, removed and embedded in OCT compound for histological examination as described above.

Heart histopathological scoring

Severity of heart vessels inflammation was scored as follow: 0, no inflammation; 1, rare inflammatory cells; 2, scattered inflammatory cells; 3, diffuse infiltrate of inflammatory cells; and 4, dense cluster of inflammatory cells. Myocardial inflammation was scored as followed: 0, no myocardial fibrosis; 1, very minimal focal subepicardial interstitial fibrosis just infiltrating beneath epicardial fat; 2, mild

subepicardial interstitial fibrosis infiltrating deeper into subepicardial myocardium; 3, multifocal subepicardial interstitial fibrosis; and 4, replacement fibrosis.[17] Imaging of the sections was performed on a Biorevo BZ-9000 (Keyence).

Aorta diameter measurement

After heart was perfused, aorta dissection was performed and with the help of a ruler the aortas were photographed by using a Panasonic Lumix camera (DMC-LX7, Panasonic Corporation, Japan) for aorta diameters measurement. The diameters of abdominal aorta were measured at 5 different parts (below the left renal artery) and average and maximal abdominal aorta diameters were calculated by using the ImageJ 1.47t software (National Institutes of Health).

Immunofluorescence

Frozen abdominal aorta sections of PBS and LCWE-injected mice were stained with the following antibodies: Goat anti-mouse IL-33 (Polyclonal – AF33626, R&D Systems), Rabbit anti-mouse ST2 (Polyclonal – ab25877, Abcam) and Rat anti-mouse F4/80 (Clone BM8.1 – 70-4801; Tonbo Biosciences). Isotype controls were used as negative controls. Before imaging, the nuclei were counterstained with ProLong Gold Antifade Reagent containing DAPI (Invitrogen). Images were obtained using a Biorevo BZ-9000 (Keyence) fluorescent microscope.

Statistical analysis

All data were analyzed using Prism 5.0 statistical program (GraphPad sofware, Inc.). We used one-way ANOVA with Tukey's post hoc test for analysis with three or greater groups. A P value less than 0.05 was considered statistically significant.

RESULTS

IL-33 gene expression is highly increased in the heart and abdominal aorta and IL-33 production had no difference in the serum of LCWE-induced KD vasculitis mouse

We first investigated the gene expression by RNA sequencing in the heart and abdominal aortas in the LCWE-induce KD vasculitis at Day 14 after the intraperitoneal (i.p.) injection of LCWE (500 µL) or PBS (500 µL) into male C57 BL/6 mice. LCWE injected mice presented significantly increase in *il33* gene expression

compared to PBS injected mice in both heart and abdominal aorta tissues (Fig. 1A). With the results obtained by RNA sequencing a pathway interaction MAP of IL-33 related genes in the heart and in the abdominal aorta in KD mouse was designed by using the public database of Ingenuity Pathway Analysis (Fig. 1B). Further, IL-33 quantitation in the serum of LCWE and PBS injected mice was performed by ELISA. There was no difference between LCWE and PBS injected mice IL-33 levels (Fig. 1C), indicating that or systemic IL-33 is not a finding in this model or this cytokine can only be found in the serum in another time point than 14 days after LCWE injection.

Development of coronary artery (CA) lesions and abdominal aorta aneurysms (AAA) in LCWE-induced KD vasculitis mouse model is dependent on IL-33

In order to access the potential involvement of IL-33 in LCWE-induced KD vasculitis, WT mice were treated with either Goat IgG isotype or anti-IL-33 Ab at days 0, 2 and 7 and the hearts harvested at day 14 post LCWE (500 µL) injection. Compared to LCWE-injected control mice treated with Goat IgG isotype, anti-IL-33 Ab treatment significant reduced development of coronary arteritis (Fig. 2A and B). In addition to reducing coronary arteritis, anti-IL-33 Ab treatment attenuates AAA formation as showed by inflammatory histology and measured by average aortic diameter (Fig. 2C and D). We next investigated if IL-33 was expressed locally in the abdominal aorta in the LCWE-induced vasculitis mice by immunofluorescence. As expected, IL-33 was highly expressed in the AAA lesions of the LCWE-injected mice (Fig. 2E). We then hypothesize that macrophages could be the source of IL-33 in the AAA. Co-localization with IL-33 and macrophages (F4/80) showed no IL-33-positive macrophages in the LCWE-injected mice (Fig. 2E). These data indicate that IL-33 has a role in the development of CA lesions and abdominal aorta aneurysms (AAA) in LCWE-induced KD vasculitis mouse model, however, which cells are producing this cytokine still remains unknown.

ST2 production in the serum and ST2 expression in the abdominal aorta showed no difference between PBS or LCWE-induced KD vasculitis mouse

We next performed a sST2 quantitation in the serum of LCWE and PBS injected mice by ELISA to observe if the increasing in IL-33 was followed by an increase in its receptor decoy. Like IL-33, no difference was found between LCWE and PBS injected mice sST2 levels (Fig. 3A). We further investigated if ST2 was expressed

locally in the abdominal aorta in the LCWE-induced vasculitis mice by immunofluorescence. ST2 expression was increased in the AAA lesions of both PBS and LCWE-injected mice (Fig. 3B). Altogether, these results suggest that IL-33 participation is independent of ST2 increasing in this LCWE-induced KD vasculitis mouse model.

DISCUSSION

Kawasaki disease (KD), a systemic inflammatory disease of unknown etiology, is the leading cause of acquired cardiac disease among children in the US.[3,18,19] If untreated, coronary artery aneurysm will develop in approximately 25% of children and can lead to ischemic heart disease, myocardial infarction, and even death.[2,11] However, the etiology and mechanisms leading to vessel inflammation, coronary artery (CA) lesions, and aneurysms remain largely unknown. In this sense, the *Lactobacillus casei* cell-wall extract (LCWE) mouse model of KD vasculitis is of large importance to study the mechanisms underlying the lesions presented by patients suffering from KD symptoms. In the present study, we demonstrate for the first time that the LCWE-induced coronary arteritis, aortitis, myocarditis, and abdominal aorta dilatation and aneurysms (AAA) in mice were reduced by the neutralization of IL-33. We also observed an increased expression of IL-33 in the abdominal aorta (AA) tissue of LCWE mice compared to PBS mice, however, no IL-33-positive macrophages were found in the AA, suggesting another type of infiltrating cells are responsible for IL-33 increased production in this model. It is been shown that several immune cells are recruited to the CA and AA during KD inflammation development such as dendritic cells (DCs),[20] monocytes/macrophages,[9,20] neutrophils,[21] $CD3^+$ T cells[20] and $CD8^+$ T cells.[17] A mechanism by which KD pathology can be developed in the LCWE model is a sequence of events starting by activation of macrophages and DCs[10] with consequent production of inflammatory cytokines, including IL-1β.[7] IL-1β in turn, acts on stromal cells in the site of inflammation development leading to an additional release of pro-inflammatory cytokines and chemokines that promote an increased influx of inflammatory cells.[8,17] Together, these mediators and cells contribute to the inflammatory response that induces the development of CA lesions and AAA in the acute phase of the LCWE model of KD.

IL-33 is a member of IL-1 family that plays a role in innate and adaptive immunity.[12,22] IL-33 is released during stress conditions or cell death mediated by infectious agents

and can induce inflammatory responses in several diseases. For instance, IL-33 is overexpressed in the inflamed arteries of patients with Giant-cell arteritis (GCA) and this overexpression was correlated with the number of inflammatory parameters suggesting a participation of IL-33 as a pro-inflammatory cytokine.[23] In this regard, although IL-33 production was not increased in the serum, here we demonstrated an increased *IL33* gene expression by RNA sequencing in both heart and AA of LCWE stimulated mice. These results confirm that IL-33 is somehow involved in the LCWE model of KD vasculitis.

IL-33 signaling occurs through ligation to its receptor ST2L.[12,24] The *ST2* gene encodes two isoforms of ST2 protein: ST2L, a transmembrane form, and sST2, a secreted form that can serve as a decoy receptor of IL-33.[12,13] IL-33 signaling through ST2 induces the interaction with IL‑1 receptor accessory protein (IL‑1RAcP) and recruits MYD88, IRAK1, IRAK4 and TRAF6, thus leading to activation of mitogen‑activated protein kinases (MAPKs) and nuclear factor κB (NFκB).[12] ST2L is expressed in different cell types such as $CD8^+$ T cells,[25] NK cells,[26] cardiomyocytes,[27] macrophages,[28] smooth muscle cells,[29] endothelial cells,[29] among others. The role of IL-33-ST2 pathway it is been demonstrated in cardiovascular diseases. sST2 was increased in serum of patients 1 day after myocardial infarction,[27] and IL-33/ST2 pathway is associated with coronary artery disease in a Chinese population.[30] We found that sST2 production was not increased in the serum of mice stimulated with LCWE compared to PBS mice. In addition, ST2L is expressed in both PBS and LCWE injected mice in the AA. Thus, IL-33 is acting by its ligation with ST2, however increased expression of ST2 is not required in this mouse model of KD vasculitis. Our current studies identified IL-33 as playing an important role in coronary artery lesions and abdominal aorta aneurysms development and thus place this cytokine as a target for therapy in Kawasaki disease. Furthermore, the LCWE-induced KD vasculitis is an important tool for providing novel mechanistic clues and therapeutic approaches for Kawasaki Disease.

ACKNOWLEDGEMENTS

We thank Debbie Pamela Moreira and Malcolm Lane for their technical support.

Funding Sources: Supported by grant from the National Institutes of Health 1R01HL139766-01 to M.N.R and Brazilian Federal Agency for Support and Evaluation of Graduate Education (CAPES) - PDSE - Process: 88881.133324/2016-01 for the scholarship granted to TTC.

Disclosures: None.

ETHICS STATEMENT

All animal experiments were performed according to the guidelines and approved protocol (IACUC Protocol #5093) of the Cedars-Sinai Medical Center Institutional Animal Care and Use Committee. Cedars-Sinai Medical Center is fully accredited by the Association for Assessment and Accreditation of Laboratory Animal Care (AAALAC International) and abides by all applicable laws governing the use of laboratory animals. Laboratory animals are maintained in accordance with the applicable portions of the Animal Welfare Act and the guidelines prescribed in the DHHS publication, Guide for the Care and Use of Laboratory Animals.

REFERENCES

1. Kawasaki T, Kosaki F, Okawa S, Shigematsu I, Yanagawa H. A new infantile acute febrile mucocutaneous lymph node syndrome (mlns) prevailing in japan. *Pediatrics*. 1974; 54:271–276.

2. Chen S, Lee Y, Crother TR, Fishbein M, Zhang W, Yilmaz A, Shimada K, Schulte DJ, Lehman TJA, Shah PK, Arditi M. Marked Acceleration of Atherosclerosis After Lactobacillus casei-Induced Coronary Arteritis in a Mouse Model of Kawasaki Disease. *Arterioscler Thromb Vasc Biol*. 2012; 32:60-71.

3. Newburger JW, Takahashi M, Gerber MA, et al. Diagnosis, treatment, and long-term management of kawasaki disease: A statement for health professionals from the committee on rheumatic fever, endocarditis and kawasaki disease, council on cardiovascular disease in the young, american heart association. *Circulation*. 2004; 110:2747–2771.

4. Wallace CA, French JW, Kahn SJ, Sherry DD. Initial Intravenous Gammaglobulin Treatment Failure in Kawasaki Disease. *Pediatrics*. 2000; 105(6):1-4.

5. Wakita D, Kurashima Y, Crother TR, Noval Rivas M, Lee Y, Chen S, Fury W, Bai Y, Wagner S, Li D, Lehman T, Fishbein MC, Hoffmann H, Shah PK, Shimada K,

Arditi M. Role of Interleukin-1 Signaling in a Mouse Model of Kawasaki Disease-Associated Abdominal Aortic Aneurysm. *Arterioscler Thromb Vasc Biol*. 2016; 36:886–897.

6. Gupta-Malhotra M, Gruber D, Abraham SS, Roman MJ, Zabriskie JB, Hudgins LC, Flynn PA, Levine DM, Okorie U, Baday A, Schiller MS, Maturi J, Meehan D, Dyme J, Parker TS, Wittkowski KM et al. Atherosclerosis in survivors of Kawasaki disease. *J Pediatr*. 2009; 155:572-577.

7. Lee Y, Schulte DJ, Shimada K, Chen S, Crother TR, Chiba N, Fishbein MC, Lehman TJ, Arditi M. Interleukin-1β is crucial for the induction of coronary artery inflammation in a mouse model of kawasaki disease. *Circulation*. 2012; 125:1542–1550.

8. Lee Y, Wakita D, Dagvadorj J, Shimada K, Chen S, Huang G, Lehman TJA, Fishbein MC, Hoffman HM, Crother TR, Arditi M. Il-1 signaling is critically required in stromal cells in kawasaki disease vasculitis mouse model: Role of both il-1α and il-1β. *Arterioscler Thromb Vasc Biol*. 2015; 115:306475.

9. Lehman TJ, Walker SM, Mahnovski V, McCurdy D. Coronary arteritis in mice following the systemic injection of group b lactobacillus casei cell walls in aqueous suspension. *Arthritis & Rheumatism*. 1985; 28:652–659.

10. Rosenkranz ME, Schulte DJ, Agle LMA, Wong MH, Zhang W, Ivashkiv L, Doherty TM, Fishbein MC, Lehman TJA, Michelsen KS, Arditi M. Tlr2 and myd88 contribute to lactobacillus casei extract-induced focal coronary arteritis in a mouse model of kawasaki disease. *Circulation*. 2005; 112:2966–2973.

11. Schulte DJ, Yilmaz A, Shimada K, Fishbein MC, Lowe EL, Chen S, Wong M, Doherty TM, Lehman T, Crother TR, Sorrentino R, Arditi M. Involvement of innate and adaptive immunity in a murine model of coronary arteritis mimicking kawasaki disease. *J Immunol*. 2009; 183:5311-5318.

12. Schmitz J, Owyang A, Oldham E, Song Y, Murphy E, McClanahan TK, Zurawski G, Moshrefi M, Qin J, Li X, Gorman DM, Bazan JF, Kastelein RA. IL-33, an interleukin-1-like cytokine that signals via the IL-1 receptor-related protein ST2 and induces T helper type 2-associated cytokines. *Immunity*. 2005; 23:479-490.

13. Trajkovic V, Sweet MJ, Xu D. T1/ST2—an IL-1 receptor-like modulator of immune responses. *Cytokine Growth Factor Rev*. 2004; 15:87-95.

14. Weinberg EO, Shimpo M, Hurwitz S, Tominaga S, Rouleau JL, Lee RT. Identification of serum soluble ST2 receptor as a novel heart failure biomarker. *Circulation*. 2003; 107:721-726.

15. Shimpo M, Morrow DA, Weinberg EO, Sabatine MS, Murphy SA, Antman EM, Lee RT. Serum levels of the interleukin-1 receptor family member ST2 predict mortality and clinical outcome in acute myocardial infarction. *Circulation*. 2004; 109:2186-2190.

16. Chen JM, Yin JM, Du ZD, Hao J, Yan HM. Qing Re Liang Xue Decoction Alleviates Hypercoagulability in Kawasaki Disease. *Evid Based Complement Alternat Med*. 2015:864597.

17. Noval Rivas M, Lee Y, Wakita D, Chiba N, Dagvadorj J, Shimada K, Chen S, Fishbein MC, Lehman TJ, Crother TR, Arditi M. CD8+ T Cells Contribute to the Development of Coronary Arteritis in the Lactobacillus casei Cell Wall Extract-Induced Murine Model of Kawasaki Disease. *Arthritis Rheumatol*. 2017; 69(2):410-421.

18. Burns JC. Kawasaki disease update. Indian J Pediatr. 2009; 76:71–76.

19. Burns JC, Glodé MP. Kawasaki syndrome. *Lancet*. 2004; 364:533–544.

20. Yilmaz A, Rowley A, Schulte DJ, Doherty TM, Schröder NWJ, Fishbein MC, Kalelkar M, Cicha I, Schubert K, Daniel WG, Garlichs CD, Arditi M. Activated myeloid dendritic cells accumulate and co-localize with cd3+ t cells in coronary artery lesions in patients with kawasaki disease. *Exp Mol Pathol*. 2007; 83:93–103.

21. Takeshita S, Nakatani K, Kawase H, Seki S, Yamamoto M, Sekine, I, Yoshioka S. The role of bacterial lipopolysaccharide-bound neutrophils in the pathogenesis of Kawasaki disease. *J Infect Dis*. 1999; 179:508-512.

22. Liew FY, Girard JP, Turnquist HR. Interleukin-33 in health and disease. *Nat Rev Immunol*. 2016; 16(11):676-689.

23. Ciccia F, Alessandro R, Rizzo A, Raimondo S, Giardina A, Raiata F, Boiardi L, Cavazza A, Guggino G, De Leo G, Salvarani C, Triolo G. IL-33 is overexpressed in the inflamed arteries of patients with giant cell arteritis. *Ann Rheum Dis*. 2013 Feb;72(2):258-64.

24. Liu X, Hammel M, He Y, Tainer JA, Jeng US, Zhang L, Wang S, Wang X. Structural insights into the interaction of IL‐33 with its receptors. *Proc Natl Acad Sci USA*. 2013; 110:14918-14923.

25. Bonilla WV, Fröhlich A, Senn K, Kallert S, Fernandez M, Johnson S, Kreutzfeldt M, Hegazy AN, Schrick C, Fallon PG, Klemenz R, Nakae S, Adler H, Merkler D, Löhning M, Pinschewer DD. The alarmin interleukin‐33 drives protective antiviral $CD8^+$T cell responses. *Science*. 2012; 335:984-989.

26. Gao X, Wang X, Yang Q, Zhao X, Wen W, Li G, Lu J, Qin W, Qi Y, Xie F, Jiang J, Wu C, Zhang X, Chen X, Turnquist H et al. Tumoral expression of IL‐33 inhibits tumor growth and modifies the tumor microenvironment through $CD8^+$ T and NK cells. *J Immunol*. 2015; 194:438-445.

27. Weinberg EO, Shimpo M, De Keulenaer GW, MacGillivray C, Tominaga S, Solomon SD, Rouleau JL, Lee RT. Expression and regulation of ST2, an interleukin-1 receptor family member, in cardiomyocytes and myocardial infarction. *Circulation*. 2002; 106(23):2961-2966.

28. Kurowska‐Stolarska M, Stolarski B, Kewin P, Murphy G, Corrigan CJ, Ying S, Pitman N, Mirchandani A, Rana B, van Rooijen N, Shepherd M, McSharry C, McInnes IB, Xu D, Liew FY. IL‐33 amplifies the polarization of alternatively activated macrophages that contribute to airway inflammation. *J Immunol*. 2009; 183:6469-6477.

29. Miller AM, Xu D, Asquith DL, Denby L, Li Y, Sattar N, Baker AH, McInnes IB, Liew FY. IL-33 reduces the development of atherosclerosis. *J Exp Med*. 2008; 205(2):339-346.

30. Tu X, Nie S, Liao Y, Zhang H, Fan Q, Xu C, Bai Y, Wang F, Ren X, Tang T, Xia N, Li S, Huang Y, Liu J, Yang Q et al. The IL-33-ST2L pathway is associated with coronary artery disease in a Chinese Han population. *Am J Hum Genet*. 2013; 93(4):652-660.

HIGHLIGHTS

- IL-33 is highly expressed in the abdominal aorta in the LCWE-induced KD vasculitis;
- Macrophages are not the source of IL-33 in the abdominal aorta in the LCWE-induced KD vasculitis;
- IL-33 neutralization reduces coronary artery lesions and abdominal aorta aneurysms in the LCWE-induced KD vasculitis;
- ST2 is not required to LCWE-induced KD vasculitis.

FIGURES AND LEGENDS

A

B

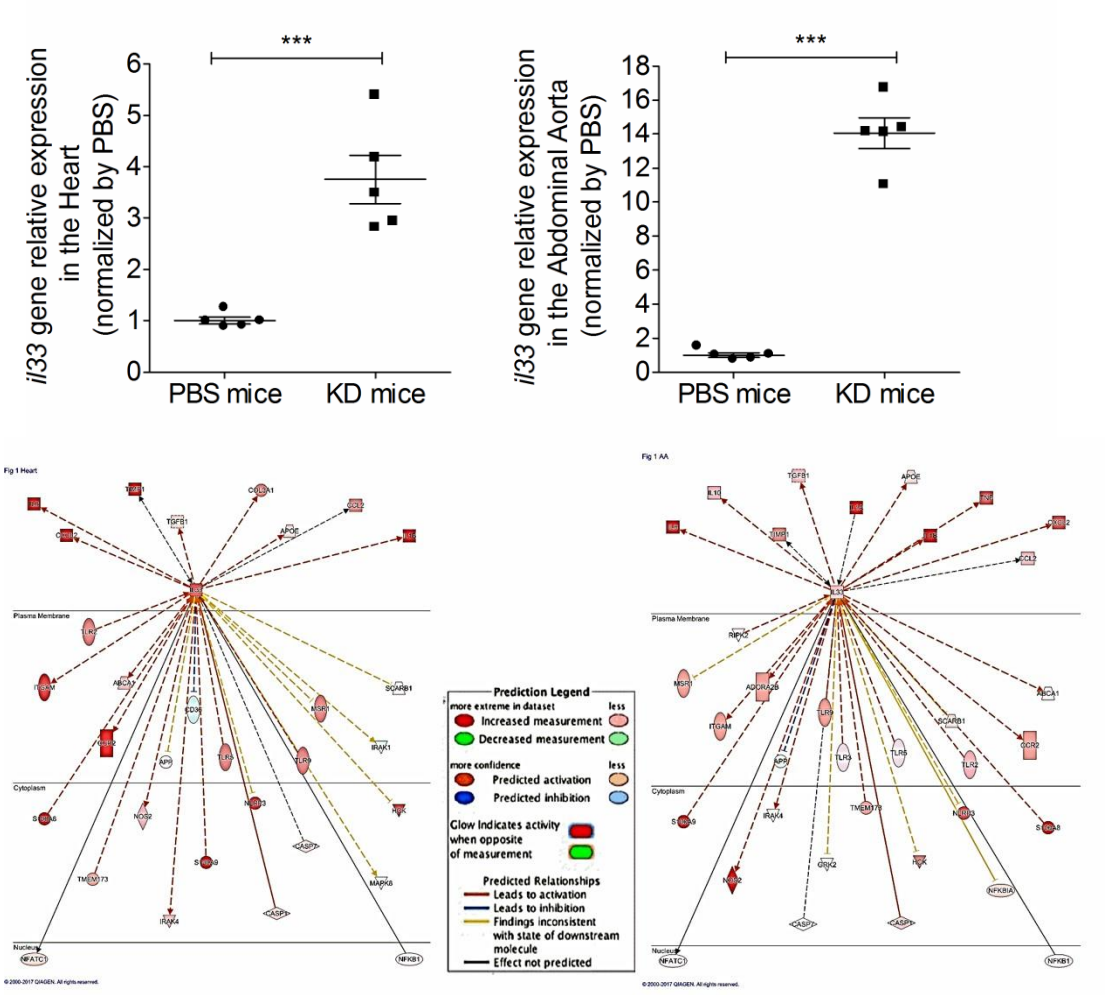

C

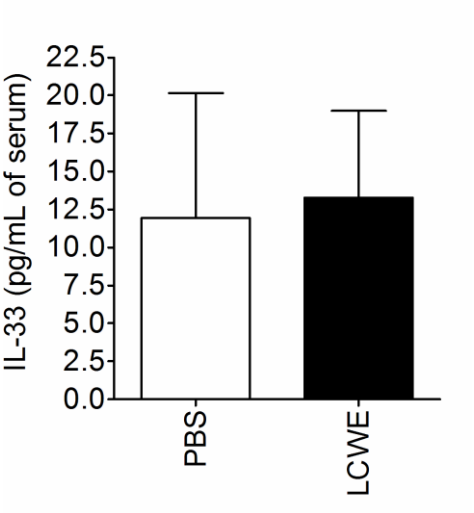

Figure 1. IL-33 gene expression and pathway interaction network in the heart and abdominal aorta, and production in serum of LCWE injected mice

The serum, heart and abdominal aortas were collected from LCWE-injected male mice at Day 14 and gene expression profiles were analyzed by RNA sequencing. The gene expression profiles were obtained from the public database of Ingenuity Pathway Analysis. (**A**) IL 33 gene relative expression in the heart and abdominal aorta in KD mouse *versus* PBS mouse. Data were analyzed by One-way ANOVA with Tukey's post-test. (***; $p<0.001$) (**B**) Pathway interaction map of IL-33 related genes in the heart and in the abdominal aorta in KD mouse (n=5). (**C**) IL-33 quantitation in the serum of KD mouse *versus* PBS mouse.

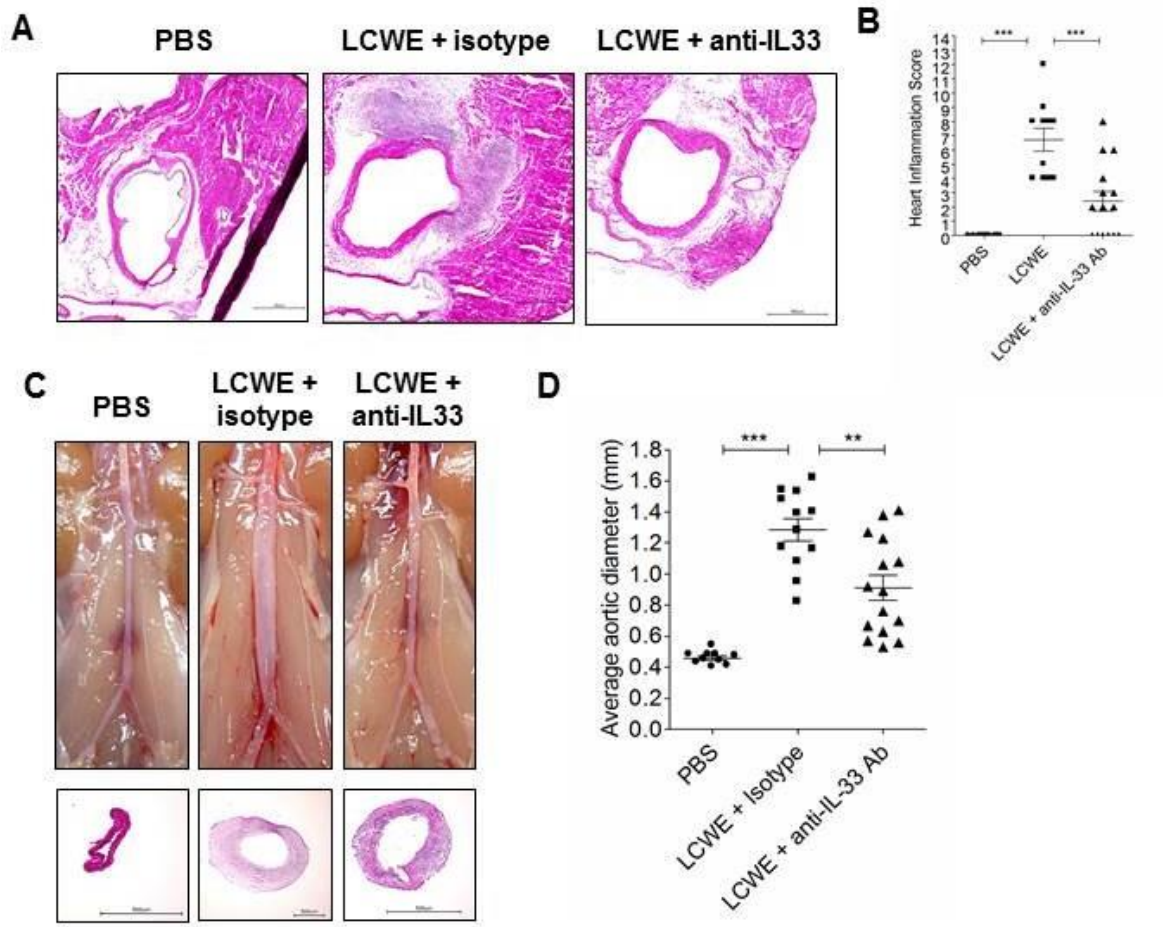
A
PBS
LCWE + isotype
LCWE + anti-IL33
B
Heart Inflammation Score
***
***
PBS
LCWE
LCWE + anti-IL-33 Ab
C
PBS
LCWE + isotype
LCWE + anti-IL33
D
Average aortic diameter (mm)
***
**
PBS
LCWE + Isotype
LCWE + anti-IL-33 Ab

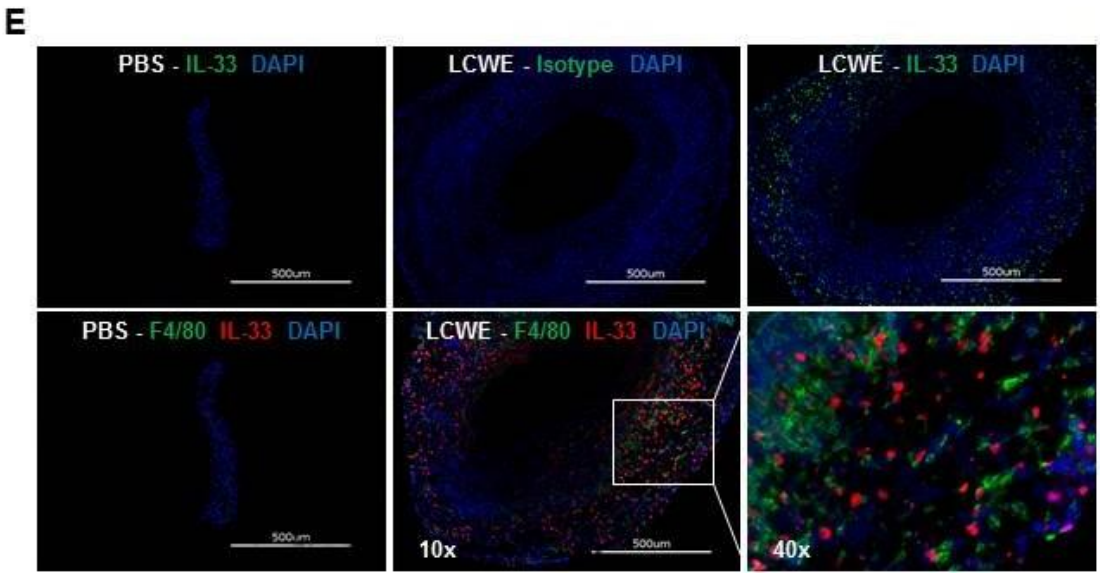
E
PBS - IL-33 DAPI
LCWE - Isotype DAPI
LCWE - IL-33 DAPI
PBS - F4/80 IL-33 DAPI
LCWE - F4/80 IL-33 DAPI
10x
40x
500um

Figure 2. IL-33 is required in development of LCWE-induced vasculitis and abdominal aortic aneurysm and is not produced by macrophages in the abdominal aorta

(**A–C**) Male mice were injected with LCWE, sacrificed at Day 14, and heart and aortic cryosections were obtained. (**A**) Heart cryosections were stained with H&E. (**B**) Heart inflammation score. Data were analyzed by One-way ANOVA with Tukey's post-test. (***; $p<0.001$) (**C**) Representative gross photographs of abdominal aorta and aortic cryosections stained with H&E. (**D**) Average aorta diameter. Data were analyzed by One-way ANOVA with Tukey's post-test. (**; $p<0.01$, ***; $p<0.001$) (**E**) The abdominal aorta sections of PBS or LCWE-injected mice were stained with IL-33 (Green) or co-stained with IL-33 (Red), anti-F4/80 (Green) and DAPI.

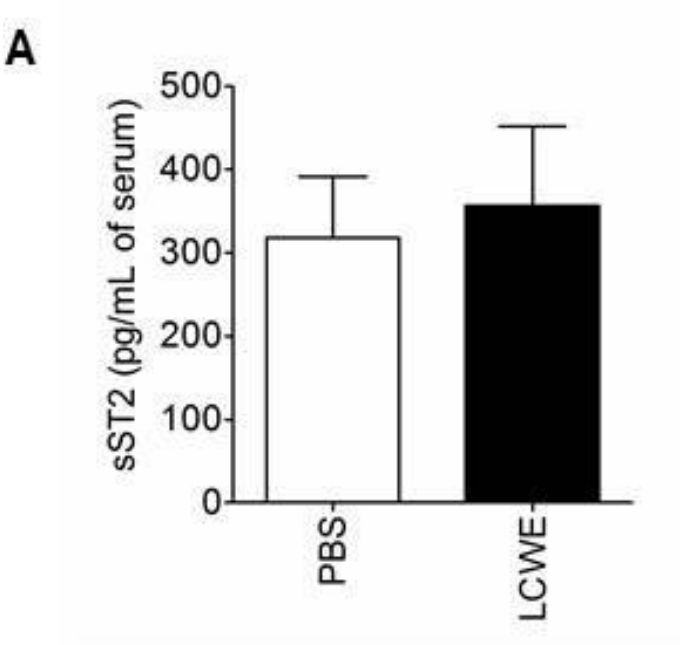
A
sST2 (pg/mL of serum)
500
400
300
200
100
0
PBS
LCWE

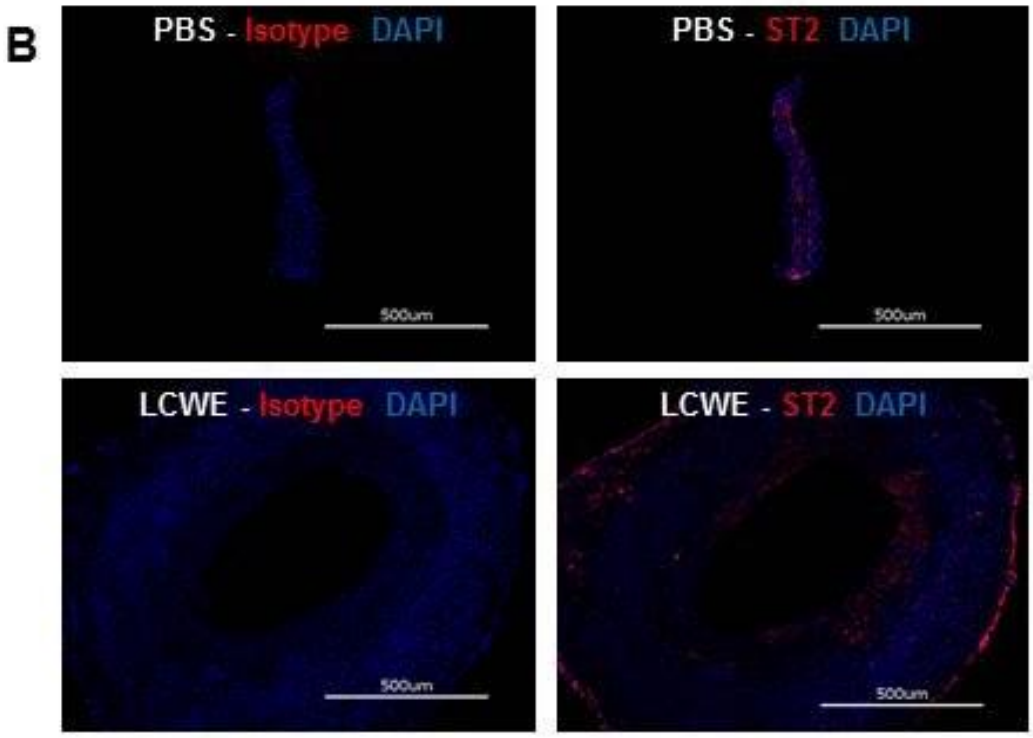
B
PBS - Isotype DAPI
500um
PBS - ST2 DAPI
500um
LCWE - Isotype DAPI
500um
LCWE - ST2 DAPI
500um

Figure 3. ST2 is not increased in the serum or abdominal aorta of LCWE injected mice

The serum and abdominal aortas were collected from LCWE-injected male mice at Day 14. (**A**) sST2 quantitation in the serum of KD mouse *versus* PBS mouse. (**B**) The abdominal aorta sections of PBS or LCWE-injected mice were stained with ST2 (Red) and DAPI.

4 CONCLUSÃO

Neste estudo foi demonstrado que as citocinas TNFα, IL-1β and IL-10 apresentam um papel importante na hiperalgesia induzida pelo Fator Estimulador de Colônias de Granulócitos (G-CSF). Além disso, foi observado que a ativação do fator de transcrição NFκB é uma ferramenta chave na dor induzida pelo G-CSF. Por meio da utilização de inibidores específicos para cada alvo do estudo, animais deficientes e também de um flavonoide, foi possível ainda observar que a hiperalgesia induzida pelo G-CSF pode ser controlada por drogas que possuem efeito sobre a produção das citocinas pró-inflamatórias TNFα e IL-1β. Assim, este trabalho demonstra um avanço no entendimento da hiperalgesia decorrente da terapia com o G-CSF e propõe que o uso de terapias biológicas ou o uso de flavonoides, como a rutina, bem como a combinação destes com AINEs ou opióides em doses abaixo da dose terapêutica são estratégias terapêuticas concebíveis para o controle da dor apresentada na clínica por pacientes em tratamento com o G-CSF.

Ademais, foi demonstrado neste estudo que a citocina IL-33 participa na formação de arterite coronária e aneurisma da aorta abdominal em modelo murino da Doença de Kawasaki induzido pelo Extrato da Parede Celular de *Lactobacillus casei* (LCWE). Dessa forma, este conhecimento mostra um avanço no entendimento dos mecanismos envolvidos na Doença de Kawasaki e também indica que a inibição da IL-33 pode ser um tratamento adjuvante para crianças acometidas pela Doença de Kawasaki.

REFERÊNCIAS

ABBAS, A. K.; LICHTMAN, A. H.; PILLAI, S. **Imunologia celular e molecular**. 7 ed. Rio de Janeiro: Elsevier, 2011, 592 p.

ALI, S. et al. U. IL-1 receptor accessory protein is essential for IL-33-induced activation of T lymphocytes and mast cells. **Proc. Natl Acad. Sci. USA**, v. 104, n. 47, p. 18660–18665, 2007.

ALLAKHVERDI, Z. et al. Cutting edge: the ST2 ligand IL-33 potently activates and drives maturation of human mast cells. **J. Immunol.**, v. 179, p. 2051–2054, 2007.

CALLEROS, L. et al. Low cell cholesterol levels increase NFkappaB activity through a p38 MAPK-dependent mechanism. **Cell. Signal.**, v. 18, n. 12, p. 2292-2301, 2006.

CARVALHO, T. T. et al. Granulocyte-colony stimulating factor (G-CSF) induces mechanical hyperalgesia via spinal activation of MAP kinases and PI3K in mice. **Pharmacol Biochem Behav.**, v. 98, n. 2, p. 188–95, 2011.

CAYROL, C. & GIRARD, J. P. The IL-1-like cytokine IL-33 is inactivated after maturation by caspase-1. **PNAS**, v. 106, n. 22, p. 9021–9026, 2009.

CHACKERIAN, A. A. et al. A. IL-1 receptor accessory protein and ST2 comprise the IL-33 receptor complex. **J. Immunol.**, v. 179, p. 2551–255, 2007.

CHEN, S. et al. Marked Acceleration of Atherosclerosis After Lactobacillus casei–Induced Coronary Arteritis in a Mouse Model of Kawasaki Disease. **Arterioscler. Thromb. Vasc. Biol.**, v. 32, p. e60-e71, 2012.

CUNHA, T.M. et al. An electronic pressure-meter nociception paw test for mice. **Braz. J. Med. Biol. Res**., v. 37, p. 401-407, 2004.

DEVOR, M. Unexplained peculiarities of the dorsal root ganglion. **Pain**, Suppl. 6. p.S27-35, 1999.

FEIN, A. **Nociceptores: As células que sentem dor.** Petrov, P.; Francischi, J. N.; Ferreira, S. H. et al. tradutores. Ribeirão Preto – SP: Dor On Line, 2011.

FERREIRA, S. H. et al. Dor Inflamatória. In: ALVES NETO, O. & cols. **Dor – Princípios e Prática**, Primeira Edição, Editora Artmed, 2009, p. 265-279.

GAZZINELLI, R.T. In the absence of endogenous IL-10, mice acutely infected with *Toxoplasma gondii* succumb to a lethal immune response dependent on CD4+ T cells and accompanied by overproduction of IL-12, IFN-[gamma] and TNF-[alpha]. **J. Immunol.**, v. 157, p. 798-805, 1996.

GILDAWIE, K. R. et al. Protective Effects of Foods Containing Flavonoids on Age-Related Cognitive Decline. **Curr. Nutr. Rep**., v. 7, 39-48, 2018.

GUO, H.; CALLAWAY, J. B. & TING, J. P. Y. Inflammasomes: mechanism of action, role in disease, and therapeutics. **Nat. Med.**, v. 21, n. 7, p. 667-687, 2015.

GUPTA-MALHOTRA, M. et al. Atherosclerosis in survivors of Kawasaki disease. **J. Pediatr.**, v. 155, p. 572–577, 2009.

HARDY, J. D.; WOLFF, H. G.; GOODELL, H. Experimental evidence on the nature of cutaneous hyperalgesia. **J. Clin. Invest**., v. 29, p. 115-140, 1950.

HOGGATT, J. & PELUS, L. M. New G-CSF agonists for neutropenia therapy. **Expert. Opin. Investig. Drugs**, v. 23, p. 21-35, 2014.

HOSSEINZADEH, H. & NASSIRI-ASL, M. Review of the protective effects of rutin on the metabolic function as an important dietary flavonoid. **J. Endocrinol. Invest**., v. 37, p. 783-788, 2014.

IASP - International Association for the Study of Pain. **IASP Taxonomy**. 2012. Disponível em:<http://www.iasp-pain.org/Content/NavigationMenu/GeneralResourceLinks/PainDefinitions/default.htm#Pain>. Acesso em: 04 de julho de 2018.

KAMALAKKANNAN, N. & PRINCE, P.S. Antihyperglycaemic and antioxidant effect of rutin, a polyphenolic flavonoid, in streptozotocin-induced diabetic wistar rats. **Basic Clin. Pharmacol. Toxicol**., v. 98, p. 97-103, 2006a.

KAMALAKKANNAN, N. & STANELY MAINZEN PRINCE, P. Rutin improves the antioxidant status in streptozotocin-induced diabetic rat tissues. **Mol. Cell. Biochem**., v. 293, p. 211-219, 2006b.

KODA, T.; KURODA, Y.; IMAI, H. Rutin supplementation in the diet has protective effects against toxicant-induced hippocampal injury by suppression of microglial activation and pro-inflammatory cytokines: protective effect of rutin against toxicant-induced hippocampal injury. **Cell. Mol. Neurobiol**., v. 29, p. 523-531, 2009.

KUMAR, S. & PANDEY, A. K. Chemistry and biological activities of flavonoids: an overview. **Scientif. World J**., v. 2013, 162750, 2013.

KUMAR, V.; ABBAS, A.; ASTER, J. Inflamação e Reparo. In:_____. **Robbins & Cotran, patologia: bases patológicas das doenças**. 9 ed. Rio de Janeiro: Elsevier, 2016, 71-113.

LEHMAN, T. et al. Coronary arteritis in mice following the systemic injection of group B *Lactobacillus casei* cell walls in aqueous suspension. **Arthritis Rheum.**, v. 28, p. 652– 659, 1985.

LI, Q.; VERMA, I.M. NF-κB Regulation in the Immune System. **Nat. Rev. Immunol**., v. 2, p. 725-734, 2002.

LIEW, F. Y.; GIRARD, J. P.; TURNQUIST, H. R. Interleukin-33 in health and disease. **Nat. Rev. Immunol**., v. 16, p. 676-689, 2016.

LISK, C. Nrf2 activation: a potential strategy for the prevention of acute mountain sickness. **Free Radic. Biol. Med**., v. 63, p. 264-273, 2013.

LOU, H. et al. Naringenin protects against 6-OHDA-induced neurotoxicity via activation of the Nrf2/ARE signaling pathway. **Neuropharmacol.**, v. 79, p. 380-388, 2014.

MADOURI, F. et al. Caspase-1 activation by NLRP3 inflammasome dampens IL-33-dependent house dust mite-induced allergic lung inflammation. **J. Mol. Cell Biol.**, v. 7, n. 4, p. 351–365, 2015.

MASCARAQUE, C. et al. Rutin has intestinal antiinflammatory effects in the CD4þ CD62Lþ T cell transfer model of colitis. **Pharmacol. Res**., v. 90, p. 48-57, 2014.

NEUPOGEN® [Filgrastim] Package Insert Kirin-Amgen, Thousand Oaks, CA, 2013.

NEWBURGER, J. W. et al. The treatment of Kawasaki syndrome with intravenous gamma globulin. **N. Engl. J. Med.**, v. 315, p. 341–347, 1986.

O'GARRA, A. et al. Strategies for use of IL-10 or its antagonists in human disease. **Immunol. Rev**., v. 223, p. 114-131, 2008.

PEDRIALI, C. A. **Síntese química de derivados hidrossolúveis da rutina: determinação de suas propriedades físico-químicas e avaliação de suas atividades antioxidantes**. 2005. 127 f. Dissertacão (Mestrado) – Faculdade de Ciências Farmacêuticas. Universidade de São Paulo, São Paulo, 2005.

RANG, H. P.; BEVAN, S.; DRAY, A. Chemical activation of nociceptive peripheral neurones. **Br. Med. Bull**., v. 47, p. 534-548, 1991.

ROSENKRANZ, M. E. et al. TLR2 and MyD88 contribute to Lactobacillus casei extract-induced focal coronary arteritis in a mouse model of Kawasaki disease. **Circulation**, v. 112, p. 2966-2973, 2005.

SCHMITZ, J. et al. IL-33, an interleukin-1-like cytokine that signals via the IL-1 receptor-related protein ST2 and induces T helper type 2-associated cytokines. **Immunity**, v. 23, p. 479-490, 2005.

SCHULTE, D. J. et al. Involvement of innate and adaptive immunity in a murine model of coronary arteritis mimicking Kawasaki disease. **J. Immunol.**, v. 183, p. 5311–5318, 2009.

SELLON, R. K. et al. Resident enteric bacteria are necessary for development of spontaneous colitis and immune system activation in interleukin-10-deficient mice. **Infect. Immun**., v. 66, p. 5224-5231, 1998.

SZABO, G. & PETRASEK, J. Inflammasome activation and function in liver disease. **Nat. Rev. Gastroenterol. Hepatol.**, v. 12, p. 387-400, 2015.

TIAN, R. et al. Rutin ameliorates diabetic neuropathy by lowering plasma glucose and decreasing oxidative stress via Nrf2 signaling pathway in rats. **Eur. J. Pharm**., v. 771, p. 84-92, 2016.

TRAJKOVIC, V.; SWEET, M. J. & XU, D. T1/ST2—an IL-1 receptor-like modulator of immune responses. **Cytokine & Growth Factor Reviews**, v. 15, p. 87–95, 2004.

UGUSMAN, A. et al. Role of Rutin on Nitric Oxide Synthesis in Human Umbilical Vein Endothelial Cells. **Scientific World J**., v. 2014, 169370, 2014.

VERRI, W. A., Jr. et al. IL-33 mediates antigen-induced cutaneous and articular hypernociception in mice. **Proc. Natl. Acad. Sci. U S A**, v. 105, n. 7, p. 2723–2728, 2008.

VERRI, W.A., Jr. et al. Flavonoids as Anti-Inflammatory and Analgesic Drugs: Mechanisms of Action and Perspectives in the Development of Pharmaceutical Forms. In: Atta-ur-Rahman (Ed.). **Studies in Natural Products Chemistry**, Elsevier, Amsterdam, 2012, pp. 297-322.

VON FREY, M. Untersuchunger über die Sinnesfunctionen der menschlichen Haut. Bandes der Abhandlungen der mathematischphysischen Classe der Königl. **Sächsischen Gesellschaft der Wissenschaften**, v. 23, p. 175-266, 1896.

WALLACE, C. A. et al. Initial Intravenous Gammaglobulin Treatment Failure in Kawasaki Disease. **Pediatrics**, v. 105, n. 6, p. 1-4, 2000.

WEINBERG, E. O. et al. Expression and regulation of ST2, an interleukin-1 receptor family member, in cardiomyocytes and myocardial infarction. **Circulation**, v. 106, p. 2961–2966, 2002.

WELTE, K. et al. Recombinant human granulocyte colony stimulating factor. Effects on hematopoiesis in normal and cyclophosphamide-treated primates. **J. Exp. Med.**, v. 165, p. 941-948, 1987.

WELTE, K. G-CSF: filgrastim, lenograstim and biosimilars. **Expert. Opin. Biol. Ther**., v. 14, p. 983-993, 2014.

XU, D. et al. Selective expression of a stable cell surface molecule on type 2 but not type 1 helper T cells. **J. Exp. Med.**, v. 187, p. 787–794, 1998.

YAO, L. H. et al. Flavonoids in Food and Their Health Benefits. **Plant Foods Hum. Nutr**., v. 59, p. 113-122, 2004.

ZARPELON, A. C. et al. IL-33/ST2 signalling contributes to carrageenin-induced innate inflammation and inflammatory pain: role of cytokines, endothelin-1 and prostaglandin E2. **Brit. J. Pharmacol.**, v. 169, p. 90–101, 2013.

ZARPELON, A. C. et al. Spinal cord oligodendrocyte-derived alarmin IL-33 mediates neuropathic pain. **FASEB J**., v. 30, n. 1, p. 54-65, 2016.